



# European Scalable Offshore Renewable Energy Source (EU-SCORES)

## D6.3 'European High resolution Resource Assessments'

Delivery Date	03/06/2024
Dissemination Level	PU
Status	DELIVERED
Version	FINAL
Keywords	Hindcast, resource assessment, Europe, wave energy, wind energy, solar energy

## Disclaimer

This deliverable reflects only the author's views, and the Agency is not responsible for any use that may be made of the information contained therein.

## Document Information

<b>Grant Agreement Number</b>	101036457
<b>Project Acronym</b>	EU-SCORES
<b>Work Package</b>	6
<b>Related Task(s)</b>	Task 6.1
<b>Deliverable</b>	D 6.3
<b>Title</b>	European High resolution Resource Assessments
<b>Author(s)</b>	Matias Alday Gonzalez Harish Baki George Lavidas
<b>File name</b>	D6.3_EU-SCORES_FINAL

## Revision History

<b>Revision</b>	<b>Date</b>	<b>Description</b>	<b>Reviewer</b>
01	27/02/2024	TUD revision	George Lavidas
02	20/03/2024	TUD revision	Matias Alday-Gonzalez Harish Baki
03	25/03/2024	TUD revision	George Lavidas
04	27/05/2024	Consortium revision	All partners
05	01/06/2024	Final	George Lavidas Matias Alday-Gonzalez Harish Baki



# Contents

Disclaimer	2
Document Information	2
Revision History	2
Contents	3
Figures	5
Tables	8
Executive summary	9
1 High resolution wave dataset	11
2 Wave Energy Resource Assessment, the ECHOWAVE dataset	12
2.1 Wave climate characterization	13
2.1.1 Mean wave characteristics for the 32 years dataset ECHOWAVE	13
2.1.2 Mean seasonal conditions	17
2.1.3 Wave Extreme Value Analysis	22
2.1.4 Operation time windows	31
2.2 Wave energy resource characterization	37
2.2.1 32-year mean energy flux estimation	38
2.2.2 32-year mean seasonal energy flux	39
3 High-resolution wind resource dataset	42
4 Wind resource assessment	43
4.1 Wind climate characteristics	43
4.1.1 Overall-interannual wind characteristics for 31 years	44
4.1.2 Annual-seasonal wind characteristics	47
4.1.3 Wind extremes analysis	49
4.2 Wind power density climate characteristics	51
4.2.1 Overall-interannual climate characteristics for 31 years	51
4.2.2 Annual-seasonal wind characteristics	53
5 High-resolution solar resource dataset	55
6 Solar resource assessment	57
6.1 Surface air temperature climate characteristics	57
6.1.1 Overall-interannual characteristics for 31 years	57
6.1.2 Annual-seasonal characteristics	59
	3



6.1.3	Heat extremes analysis	60
6.2	Surface solar radiation flux climate characteristics	62
6.2.1	Overall-interannual characteristics for 31 years	62
6.2.2	Annual-seasonal characteristics	63
6.3	Surface wind climate characteristics	65
6.3.1	Overall-interannual characteristics for 31 years	65
6.3.2	Annual-seasonal characteristics	67
Annex A: Seasonal mean wave conditions at specific locations		69
Annex B: Seasonal mean wave conditions at specific locations		75



## Figures

Figure 1: (a) Multi-grid nesting scheme adapted from Alday, et al. (2023). (b) Detail of N_ATL-8M and EU_ATL-2M.....	12
Figure 2: Significant wave height 32-years mean. (a) Iberian Peninsula, Bay of Biscay(b) Ireland, UK and The North Sea. Using the EU_ATL-2M active nodes which have 500 maximum depth as limiter.....	14
Figure 3: Peak period 32-years mean. (a) Iberian Peninsula (b) Ireland, UK and The North Sea. Using the EU_ATL-2M active nodes which have 500 maximum depth as limiter.....	15
Figure 4: (a) $H_s$ and (b) $T_p$ yearly mean values compared to the 32-years mean.....	16
Figure 5: $H_s$ 32-years seasonal mean for the Iberian Peninsula and The Bay of Biscay. Using the EU_ATL-2M active nodes which have 500 maximum depth as limiter.....	18
Figure 6: $H_s$ 32-years seasonal mean for Ireland, UK and The North Sea. ....	19
Figure 7: $T_p$ 32-years seasonal mean for Portugal and The Bay of Biscay.....	20
Figure 8: $T_p$ 32-years seasonal mean for Ireland, UK and The North Sea.....	21
Figure 9: $H_s$ 32-years (1990 to 2021) 95 <sup>th</sup> percentile (a) and 99 <sup>th</sup> percentile (b). Portugal and Bay of Biscay.....	22
Figure 10: $H_s$ 32-years (1990 to 2021) 95 <sup>th</sup> percentile (a) and 99 <sup>th</sup> percentile (b). Ireland, UK The North Sea.....	23
Figure 11: Weibull probability distribution fit correlation ( $F_x, F_m$ ) for (a) Portugal and Bay of Biscay, and (b) Ireland, UK and The North Sea.....	25
Figure 12: Expected extreme significant wave height return value ( $H_R$ ) for 10, 25, 50, 75, and 100 years return periods. Portugal and Bay of Biscay.....	27
Figure 13: Upper and lower confidence bounds from the 90% confidence interval (for each $H_R$ return value in Figure 12). Portugal and Bay of Biscay.....	28
Figure 14: Expected extreme significant wave height return value ( $H_R$ ) for 10, 25, 50, 75, and 100 years return periods. Ireland, UK and The North Sea.....	29
Figure 15: Upper and lower confidence bounds from the 90% confidence interval (for each $H_R$ return value in Figure 14). Ireland UK and The North Sea.....	30
Figure 16: Return value $H_R$ and 90% confidence interval bounds.....	31
Figure 17: (a) Wave height Probability of exceedance from Weibull best fit and from modelled time series. (b) wave height density probability distribution from modelled time series and Weibull fit. ...	32
Figure 18: Mean duration of periods where $H_s$ is $< H_{ac}$ .....	33
Figure 19: : (a) Yearly probability of occurrence of continuous time windows with $H_s < H_{ac}$ . (b) Yearly estimated number of events with time windows of duration $\tau_i$ with $H_s < H_{ac}$ .....	34
Figure 20: Estimated yearly $\tau_{ac}$ , mean duration of periods with $H_s < H_{ac}=2$ m. ....	35
Figure 21: Estimated yearly prob. of occurrence $Q$ of $H_s < H_{ac}=2$ m for continuous time windows of 6, 9 and 12 hrs (top, mid and bottom panels respectively). (a) Portugal and Bay of Biscay, (b) Ireland, UK and North Sea.....	36
Figure 22: 32-year pWave average for (a) Portugal and Bay of Biscay, and (b) Ireland, UK and The North Sea.....	38
Figure 23: Yearly mean pWave compared to the 32-year average (1990-2021).....	39
Figure 24: $H_s$ 32-years pWave seasonal mean for Portugal and The Bay of Biscay.....	40
Figure 25: $H_s$ 32-years pWave seasonal mean for Ireland, UK and The North Sea. ....	41
Figure 26: Spatial illustration of 100 m wind speed from CERRA reanalysis, averaged over 31 years, during 1990 to 2021. The red dashed boxes represent regions of interest for further analysis, at Iberia, Ireland, and BeNeLux (combination of Belgium, Netherlands, and Luxemburg countries) locations. ....	43
Figure 27: Left panel: Surface plots of Weibull scale parameter of 100 m wind speed, estimated during the whole analysis period (1990-2020), over the Iberia region. Right panel: Time-series of 100 m wind Weibull scale parameter computed during each year, at points P1, P2, and P3, shown in the left panel. Horizontal dashed lines represent the overall statistics at the respective points.....	45
Figure 28: Same as Figure 27, but for the Ireland region.....	45
Figure 29: Same as Figure 27, but for the BeNeLux region. ....	45
Figure 30: Left panel: Surface plots of Weibull shape parameter of 100 m wind speed, estimated during the whole analysis period (1990-2020), over the Iberia region. Right panel: Time-series of 100	



m wind Weibull shape parameter computed during each year, at points P1, P2, and P3, shown in the left panel. Horizontal dashed lines represent the overall statistics at the respective points.....	46
Figure 31: Same as Figure 30, but for the Ireland region.....	46
Figure 32: Same as Figure 30, but for the BeNeLux region.....	47
Figure 33: Time-series of 100 m wind Weibull scale parameter computed during each month, at points P1, P2, and P3, over the Iberia region. Horizontal dashed lines represent the overall statistics at the respective points.....	48
Figure 34: Same as Figure 33, but for the Ireland region.....	48
Figure 35: Same as Figure 33, but for the Ireland region.....	49
Figure 36: Left panel: Surface plots of 99p of 100 m wind speed, estimated during the whole analysis period (1990-2020), over the Iberia region. Right panel: Time-series of 99p of 100 m wind speed computed during each year, at points P1, P2, and P3, shown in the left panel. Horizontal dashed lines represent the overall statistics at the respective points.....	50
Figure 37: Same as Figure 36, but for the Ireland region.....	50
Figure 38: Same as Figure 36, but for the BeNeLux region.....	50
Figure 39: Left panel: Surface plots of mean 100 m wind power density, estimated during the whole analysis period (1990-2020), over the Iberia region. Right panel: Time-series of mean 100 m wind power density computed during each year, at points P1, P2, and P3, shown in the left panel. Horizontal dashed lines represent the overall statistics at the respective points.....	52
Figure 40: Same as Figure 39, but for the Ireland region.....	52
Figure 41: Same as Figure 39, but for the Ireland region.....	52
Figure 42: Time-series of 100 m wind power density computed during each month, at points P1, P2, and P3, over the Iberia region. Horizontal dashed lines represent the overall statistics at the respective points.....	54
Figure 43: Same as Figure 42, but for the Ireland region.....	54
Figure 44: Same as Figure 42, but for the BeNeLux region.....	54
Figure 45: Spatial illustration of 10 m wind speed from CERRA reanalysis, averaged over 31 years, during 1990 to 2021. The red dashed boxes represent regions of interest for further analysis, at Iberia, Ireland, and BeNeLux (combination of Belgium, Netherlands, and Luxemburg countries) locations.....	56
Figure 46: Spatial illustration of 2 m air temperature from CERRA reanalysis, averaged over 31 years, during 1990 to 2021. The red dashed boxes represent regions of interest for further analysis, at Iberia, Ireland, and BeNeLux (combination of Belgium, Netherlands, and Luxemburg countries) locations.....	56
Figure 47: Spatial illustration of downward shortwave radiation flux at the surface from CERRA reanalysis, averaged over 31 years, during 1990 to 2021. The red dashed boxes represent regions of interest for further analysis, at Iberia, Ireland, and BeNeLux (combination of Belgium, Netherlands, and Luxemburg countries) locations.....	57
Figure 48: Left panel: Surface plots of mean 2m temperature, estimated during the whole analysis period (1990-2020), over the Iberia region. Right panel: Time-series of 2 m temperature mean computed during each year, at points P1, P2, and P3, shown in the left panel. Horizontal dashed lines represent the overall statistics at the respective points.....	58
Figure 49: Same as Figure 48, but for the Ireland region.....	58
Figure 50: Same as Figure 48, but for the BeNeLux region.....	59
Figure 51: Time-series of 2 m temperature mean computed during each month, at points P1, P2, and P3, over the Iberia region. Horizontal dashed lines represent the overall statistics at the respective points.....	60
Figure 52: Same as Figure 51, but for the Ireland region.....	60
Figure 53: Same as Figure 54, but for the Ireland region.....	60
Figure 54: Left panel: Surface plots of 99p of 2 m temperature, estimated during the whole analysis period (1990-2020), over the Iberia region. Right panel: Time-series of 99p of 2m temperature computed during each year, at points P1, P2, and P3, shown in the left panel. Horizontal dashed lines represent the overall statistics at the respective points.....	61
Figure 55: Same as Figure 54, but for the Ireland region.....	62
Figure 56: Same as Figure 54, but for the BeNeLux region.....	62
Figure 57: Left panel: Surface plots of mean SWDOWN, estimated during the whole analysis period (1990-2020), over the Iberia region. Right panel: Time-series of SWDOWN mean computed during	



each year, at points P1, P2, and P3, shown in the left panel. Horizontal dashed lines represent the overall statistics at the respective points. ....	63
Figure 58: Same as Figure 57, but for the Ireland region. ....	63
Figure 59: Same as Figure 57, but for the BeNeLux region. ....	63
Figure 60: Time-series of SWDOWN computed during each month, at points P1, P2, and P3, over the Iberia region. Horizontal dashed lines represent the overall statistics at the respective points. ....	64
Figure 61: Same as Figure 60, but for the Ireland region. ....	64
Figure 62: Same as Figure 60, but for the BeNeLux region. ....	65
Figure 63: Left panel: Surface plots of Weibull scale parameter of 10 m wind speed, estimated during the whole analysis period (1990-2020), over the Iberia region. Right panel: Time-series of 100 m wind Weibull scale parameter computed during each year, at points P1, P2, and P3, shown in the left panel. Horizontal dashed lines represent the overall statistics at the respective points. ....	66
Figure 64: Same as Figure 63, but for Ireland region. ....	66
Figure 65: Same as Figure 48, but for BeNeLux region. ....	67
Figure 66: Time-series of 10 m wind Weibull scale parameter computed during each month, at points P1, P2, and P3, over the Iberia region. Horizontal dashed lines represent the overall statistics at the respective points. ....	68
Figure 67: Same as Figure 66, but for the Ireland region. ....	68
Figure 68: Same as Figure 51, but for the BeNeLux region. ....	68
Figure 69: (a) $H_s$ and (b) $T_p$ yearly mean seasonal values compared to the 32-years mean. Location: Portugal. ....	69
Figure 70: (a) $H_s$ and (b) $T_p$ yearly mean seasonal values compared to the 32-years mean. Location: Brittany (France). ....	70
Figure 71: (a) $H_s$ and (b) $T_p$ yearly mean seasonal values compared to the 32-years mean. Location: Ireland. ....	71
Figure 72: (a) $H_s$ and (b) $T_p$ yearly mean seasonal values compared to the 32-years mean. Location: Scotland. ....	72
Figure 73: (a) $H_s$ and (b) $T_p$ yearly mean seasonal values compared to the 32-years mean. Location: North Sea. ....	73
Figure 74: (a) $H_s$ and (b) $T_p$ yearly mean seasonal values compared to the 32-years mean. Location: Scotland. ....	74
Figure 75: Seasonal 32-year mean (dashed black lines) and yearly seasonal mean in (a) Portugal and (b) Brittany (France). ....	75
Figure 76: Seasonal 32-year mean (dashed black lines) and yearly seasonal mean in (a) Ireland and (b) Scotland. ....	76
Figure 77: Seasonal 32-year mean (dashed black lines) and yearly seasonal mean in Dutch waters (North Sea). ....	77



## Tables

Table 1: Model grids details.....	12
Table 2: Constans for the standard deviation of the return value. ....	26





## Executive summary

Renewable energy projects require long-term climate information, and offshore renewable energies in particular are in need of higher fidelity information as both power production, reliability and survivability rely on them. Existing open source datasets are too coarse, and often do not have the suitable physics-based solutions to resolve high fidelity areas.

The deliverable offers an in-depth resource assessment for wind-wave-solar renewable energy resources along the European Atlantic region. The duration of information covers 1990-2021 (including 2021), resulting in 32 years. This deliverable uses state-of-the-art high-resolution data for wind and solar, and introduces the European Coasts High-resolution Ocean WAVES (ECHOWAVE) hindcast, a new open source database for wave conditions with superior accuracy. ECHOWAVE covers North Atlantic European waters within the coastal shelf, from intermediate to shallow water relative depths and is specially adjusted to improve the representation of sea states within the area of interest. This translates as a reduction of the uncertainties in the estimation of some of the most important wave parameters for wave energy applications.

There is a clear overall difference in the mean significant wave height ( $H_s$ ) between several regions. The 32-years mean off the coasts of Portugal is of about 2.4 m, slightly higher than 2.6 m on the North-West coast of Spain and Brittany (France). A higher wave heights' mean is found along the Atlantic coasts of Ireland and the UK. The mean  $H_s$  in Ireland is  $\approx 3.2$  m at distances from the coast  $> 25$  km (in intermediate to deep waters  $> 80$  m). Significantly smaller values are observed along the southern coasts of the North Sea, with mean  $H_s \approx 1.4$  m at distances ranging from 25 to 30 km offshore (depths of about 25 m). The 32-years  $T_p$  mean peak wave period along the coasts of Portugal and Western Spain is 11 s. Similar values are found in the southern end of the Bay of Biscay and only slightly shorter mean peak periods of  $\approx 10.8$  s are observed along the coasts of western Brittany. Values of the  $H_s$  yearly mean can have a variability of  $\pm 0.3$  to  $\pm 0.5$  m with respect to the 32 years mean, in average, along the North Atlantic European coasts (Portugal, Brittany, Ireland, and Scotland). Smaller oscillations of about  $\pm 0.2$  m are observed in the North Sea when comparing yearly wave heights mean with the 32-years bulk mean. For the peak periods, these oscillations are in general  $< \pm 0.4$  s for all locations. ECHOWAVE allows to confidently evaluate the extreme conditions in the European Atlantic coastlines. The extreme return wave of 100 year period is close to 12-15 m off the Portuguese coastlines, 15-18 m in the Spanish Atlantic coastlines. Highest values are obtained off the coast of Ireland and Scotland with values 20-25 m.

The wind resource assessment based on a high-resolution dataset from 1990-2020, wind speed magnitudes range from 2 m/s to 10 m/s. More specifically for regions of interest Iberia coast, Ireland coast, and BeNeLux (Belgium, Netherlands, and Luxemburg) coasts the mean wind speeds are  $\approx 6$  m/s, 10 m/s, and 8 m/s, over the 31 years. In terms of temperature decrease is observed as latitude increases.



However, temperatures in Ireland and Netherlands coasts are relatively warmer compared to the areas on the same latitude, which is attributed to the Gulf Stream. Over the interested regions, the mean temperatures are seen to be around 15 oC (Iberia) and 10 oC (Ireland and BeNeLux). The annual mean downward shortwave radiation flux at the surface is persistent throughout the 31 year dataset, in Iberia it is 200 W/m<sup>2</sup>, 125 W/m<sup>2</sup> Ireland, and 100 W/m<sup>2</sup> (BeNeLux).



# 1 High resolution wave dataset

The wave resource characterization and wave energy flux analysis considered in the present document, is carried out using the 32-years high resolution hindcast specially develop for this purpose. This wave dataset, which covers from 1990 to 2021, is described in-depth within report D6.6. Here, a brief description included to provide some context.

The high resolution spectral wave model has been implemented, adjusted and validated for North Atlantic European waters using the WAVEWATCH III (WW3) modelling framework ( The WAVEWATCH III® Development Group, 2019). The main aim of this implementation, is to generate a database adequate for the assessment of the available wave resource within intermediate to shallow water conditions. This includes properly capturing the transformation processes of the wave field in coastal environments, mainly, wave-current interactions, depth induced refraction, dissipation due to bottom friction. To develop this high quality wave dataset, special attention was paid to the nesting scheme, spatial and spectral resolution, forcing fields included, and the physical parameterizations' adjustments. In particular, to improve the modelled sea states characterization, within the European North Atlantic waters, a series of adjustments were applied to the wind-wave growth and swell dissipation parameterizations (Ardhuin, et al., 2010). These adjustments follow the analysis proposed in Alday et al. (Alday, Accensi, Ardhuin, & Dodet, 2021).

The model uses a multi-grid system with a 2-way nesting scheme, which means that higher rank grids, in this case with higher resolution too, feed spectral information back to the lower rank grids (Chawla, et al., 2013; Tolman, 2008). Three regular grids have been defined with increasing resolution: The base grid N\_ATL-15M with a spatial resolution of  $0.25^\circ$ , an intermediate grid for European waters (N\_ATL-8M) with  $0.125^\circ$  resolution, and a coastal grid (EU\_ATL-2M) with high spatial resolution of  $0.03^\circ$  (see Figure 1). Details of the spatial resolution and extension of each grid are presented in Table 1.



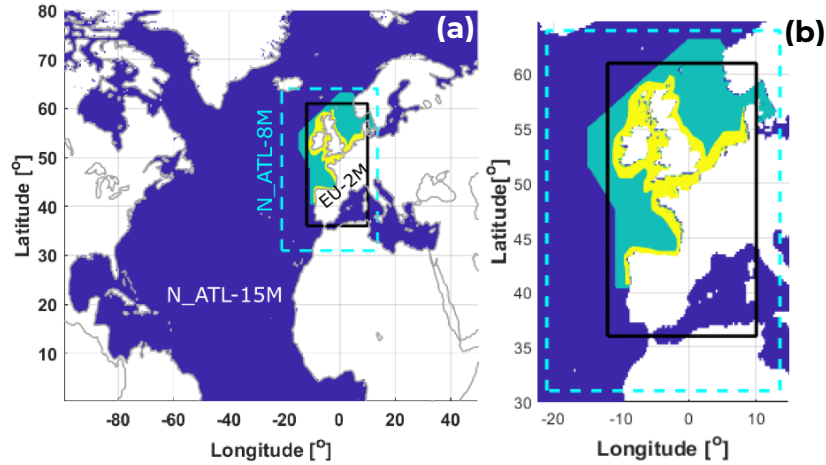


**Figure 1: (a) Multi-grid nesting scheme adapted from Alday, et al. (2023). (b) Detail of N\_ATL-8M and EU\_ATL-2M.**

Obs.: In blue, active nodes from N\_ATL-15M. In cyan dashed lines the limits of N\_ATL-8M, with its active nodes in green. Black lines show the limits of EU\_ATL-2M, its active grid nodes in yellow. Computations are only performed on active grid nodes.

**Table 1: Model grids details.**

Grid Name	Grid Rank	Longitude		Latitude		Spatial resolution	
		[°]		[°]			
		Min	Max	Min	Max	[°]	[m]
N_ATL-15M	1	-99.5	50.0	0.25	80.0	0.25	18125,0
N_ATL-8M	2	-21.0	64.0	31.0	64.0	0.125	9062,5
EU_ATL-2M	3	-12.0	10.0	36.0	61.0	0.03	2175,0

Obs.: Spatial resolution in m estimated for dx considering 1° as 72.5 km (at 50° latitude). Resolution in dy should be estimated using 1° = 111 km approx.

## 2 Wave Energy Resource Assessment, the ECHOWAVE dataset

In the present section, the wave climate and wave energy flux (pWave) characterizations are included. All computations are done using the modelled wave data from the **EU\_ATL-2M** high-resolution grid, which covers North Atlantic European waters within the coastal shelf, from intermediate to shallow water relative depths (Figure 1, Table 1).

One of the main advantages of the high resolution hindcast developed for the EU-SCORES project, is that it is specially adjusted to improve the representation of sea states within the area of interest. This translates as a reduction of the uncertainties in the estimation of some of the most important wave parameters for wave energy

applications. Additionally, the high resolution of the **E**uropean **C**oasts **H**igh resolution **O**cean **W**AVEs hindcast, known from now on as ECHOWAVE, allows to better capture spatial variability of the wave field down to ~3 km offshore and minimum depths of about 20 m. This means that most areas of interest for the development of wave energy (or floating wind) projects, within the European North Atlantic, are covered by the high resolution domain. Which is unique and superior to existing wave datasets

The following statistical parameters are used to characterized the wave climate and the wave energy flux: The mean (Equation 1), the coefficient of variation (Equation 2), and percentiles 95 and 99 ( $P_{99}$ ,  $P_{95}$ ):

**Equation 1** 
$$MEAN(X) = \mu = \frac{1}{N} \sum_{i=1}^N X_i$$

**Equation 2** 
$$CoV = \frac{\sigma}{\mu}$$

**Equation 3** 
$$STD(X) = \sigma = \sqrt{\frac{1}{N} \sum_{i=1}^N (X_i - \mu)^2}$$

In Equation 1 to Equation 3, X is the analysed variable and N the total amount of analysed data. More specific formulations (outside  $P_{99}$  and  $P_{95}$ ) are employed for the analysis of extreme wave conditions, and the estimation of operation time windows, these are described in sections 2.1.3 and 2.1.4 respectively.

The wave climate characterization is presented in section 2.1, then the wave energy resource is analysed in section 2.2. Given the size of the high resolution fields output from the wave model, the analysis is divided in 2 zones: Portugal-Biscay and North of Europe. The latter includes the UK, North sea and the English Channel (La Manche).

## 2.1 Wave climate characterization

Characterization of the wave conditions within the modelled domain is done in terms of the significant wave height ( $H_s$ ) and the peak period ( $T_p$ ). These 2 wave parameters are selected since they are widely used in many wave energy applications, from estimation of the wave energy flux to the construction of power matrices from wave energy converters.

Most of the wave heights' characteristics described in this section should be considered representative reference value. In general within intermediate to shallow water depth (for example <30m) the local wave field characteristics are highly dependent on the local bathymetry. This implies potential changes in the scales of a few kilometres.

### 2.1.1 Mean wave characteristics for the 32 years dataset ECHOWAVE

First, an overview of the  $H_s$  and  $T_p$  is presented with the 32-years mean, which provides a general description of the expected values of these parameters within the analysed area.



There is a clear overall difference in the mean  $H_s$  between Portugal and the Bay of Biscay, the UK Atlantic coasts and the North Sea. The 32-years mean off the coasts of Portugal is of about 2.4 m, slightly higher than 2.6 m on the North-West coast of Spain and Brittany (France), and typically  $< 2$  m within the Bay of Biscay at depths around 30 to 40 m (Figure 2.a). A higher wave heights' mean is found along the Atlantic coasts of Ireland and the UK. The mean  $H_s$  in Ireland is typically  $\sim 3.2$  m at distances from the coast  $> 25$  km (in intermediate to deep waters  $> 80$  m), similar values are found in The Hebrides Islands. Significantly smaller values are observed along the southern coasts of the North Sea (Figure 2.b), with mean  $H_s$  of about 1.4 m at distances ranging from 25 to 30 km offshore (depths of about 25 m).

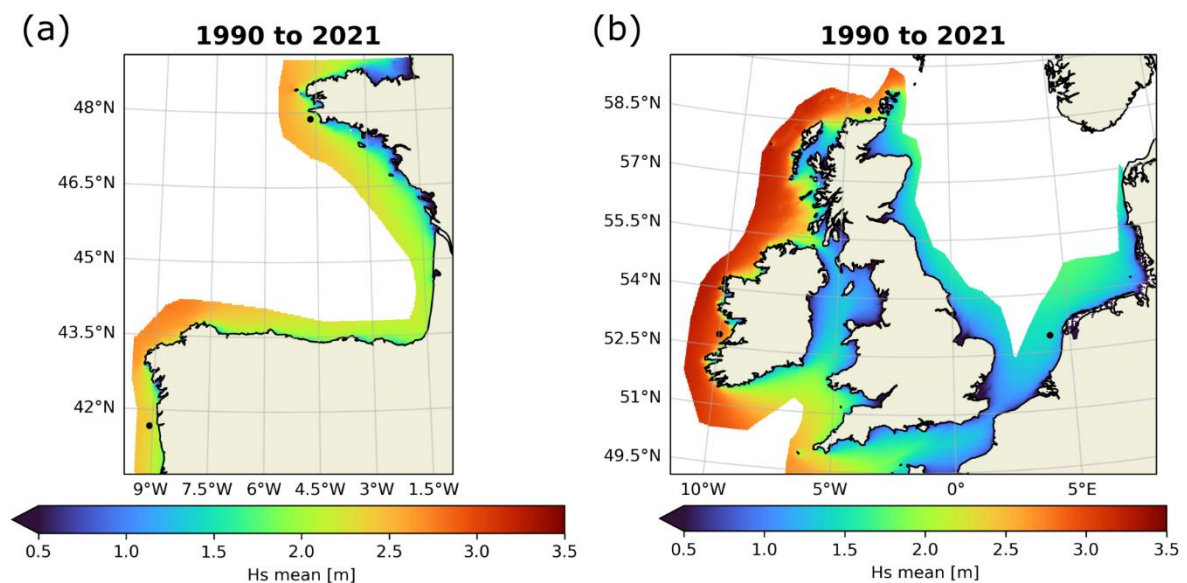


**Figure 2: Significant wave height 32-years mean. (a) Iberian Peninsula, Bay of Biscay (b) Ireland, UK and The North Sea. Using the EU\_ATL-2M active nodes which have 500 maximum depth as limiter.**

*Obs.: black circles show the position of the locations detailed in Figure 4.*

In terms of the overall mean peak period, similar results are found on the western coasts of Europe, directly exposed to the storms and radiated swells from the North Atlantic. The 32-years  $T_p$  mean along the coasts of Portugal (and west coast of Spain) is 11 s. Similar values are found in the southern end of the Bay of Biscay and only slightly shorter mean peak periods of  $\sim 10.8$  s are observed along the coasts of western Brittany (Figure 3.a).

In fact this latter value is also found along the western coasts of Ireland and Scotland (Figure 3.b). Shorter peak periods are more common in those areas where the local winds are the main drivers of the sea states as it is the case of the Irish Sea and The North Sea (Figure 3.b). An overall mean  $T_p$  of 7 s is characteristic within the southern coasts of the North Sea (e.g.; along the Dutch coast), with shorter values around 6 s found closer towards the English Channel.



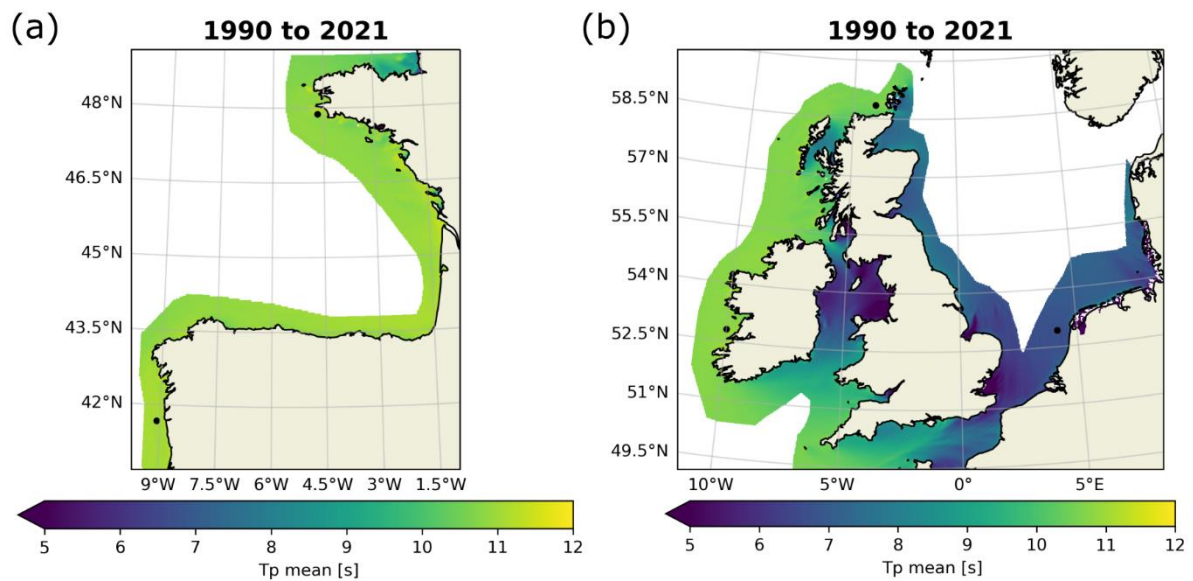


**Figure 3: Peak period 32-years mean. (a) Iberian Peninsula (b) Ireland, UK and The North Sea. Using the EU\_ATL-2M active nodes which have 500 maximum depth as limiter.**

*Obs.: black circles show the position of the locations detailed in Figure 4.*

These “bulk”  $H_s$  and  $T_p$  mean values provide a good description of the expected average wave conditions and its spatial variability. Nevertheless, it is still interesting to have an idea of the differences between yearly mean wave field conditions. In Figure 4 the time series of yearly mean  $H_s$  and  $T_p$  is presented for 5 selected locations in Portugal, Brittany, Ireland, Scotland and The North Sea. The specific position of these locations is detailed in the maps from Figure 2 and Figure 3.

Values of the  $H_s$  yearly mean can have a variability of  $\pm 0.3$  to  $\pm 0.5$  m with respect to the 32 years mean, in average, along the North Atlantic European coasts (Portugal, Brittany, Ireland, and Scotland). Smaller oscillations of about  $\pm 0.2$  m are observed in the North Sea when comparing yearly wave heights mean with the 32-years bulk mean. For the peak periods, these oscillations are in general  $< \pm 0.4$  s for all locations.

The occurrence of yearly mean  $H_s$  values particularly larger or smaller than the 32-years wave heights average can be observed in Figure 4.a. Those specific “high” or “low” energy years do not necessarily coincide for all 5 locations, but there are some apparent trends that could be related to atmospheric oscillations. For example in 1996 the mean  $H_s$  for the location selected at Portugal (off the coast of Viana do Castelo) is close to the total average, while in all the other 4 locations 1996 might be considered a “low energy” year. Then, something similar is observed for 2010. 2002 is clearly a “high energy” year for Portugal and Brittany, where one of the largest yearly mean  $H_s$  values are found for these locations. On the other hand, the same year can be considered as “low energy” for Scotland. Again, a similar pattern is observed for 2014.



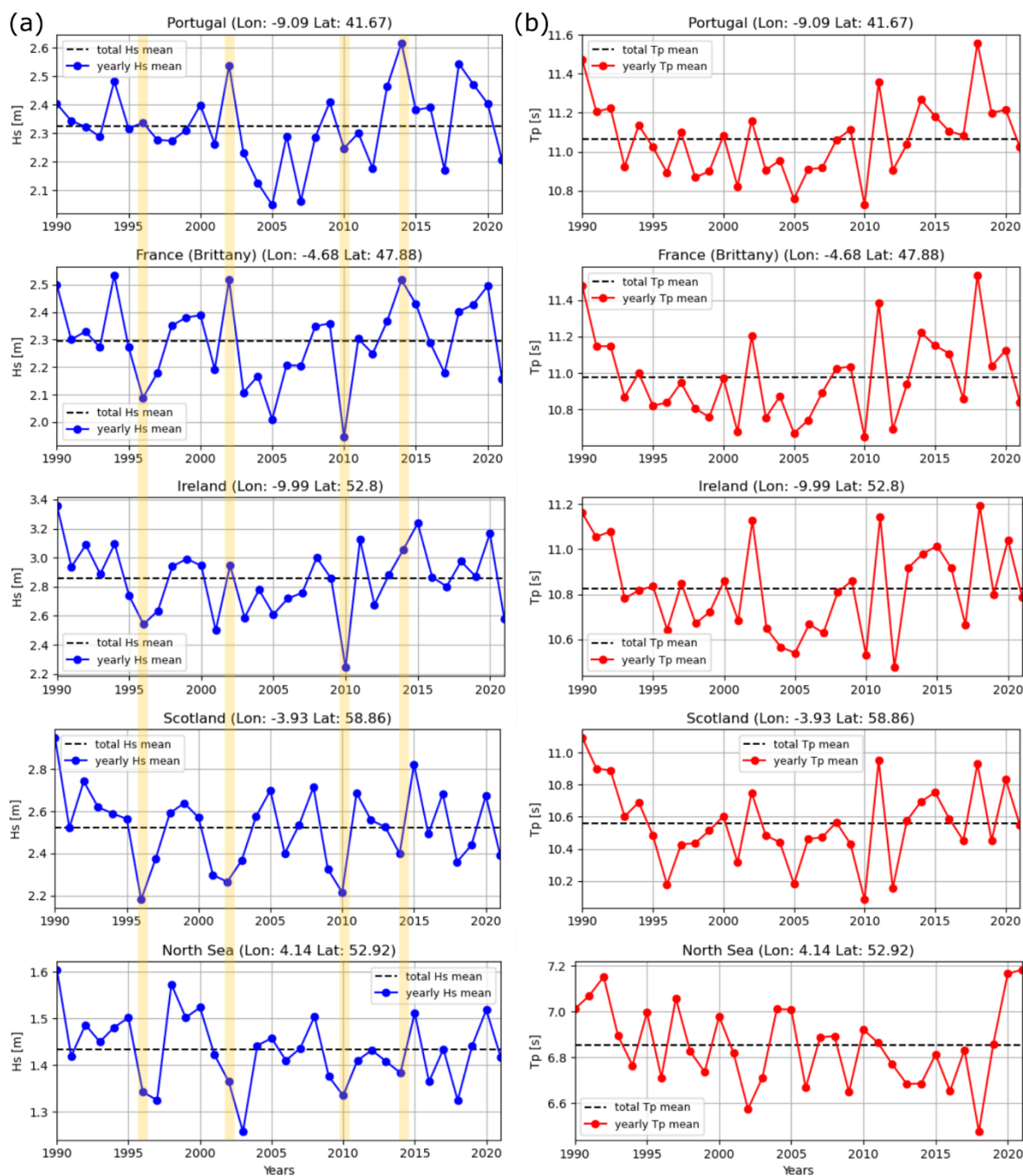


**Figure 4: (a)  $H_s$  and (b)  $T_p$  yearly mean values compared to the 32-years mean.**

Obs.: Locations showed in maps from Figure 2 and Figure 3. Yellow rectangles in (a) highlight years 1996, 2002, 2010 and 2014. Dashed black lines show the 32-years mean of  $H_s$  or  $T_p$  at each location.





## 2.1.2 Mean seasonal conditions

The seasonal analysis provides further insights on the variability of the wave field characteristics throughout the year. This is done by estimating the mean  $H_s$  and  $T_p$  values for winter (DJF), spring (MAM), summer (JJA), and autumn (SON) months. As presented in section 2.1.1, the analysis is done first for the average per season using the 32 years dataset. All wave height mean values provided for general areas, should be considered as a reference and not an absolute value since the wave height conditions will change locally depending on the interactions between wave fields and the bathymetric features (or/and wave-current interactions). Analog to the information provided in Figure 4, the detail of the mean seasonal conditions per year, for  $H_s$  and  $T_p$ , are presented in Annex A, for the same specified locations included in Figure 4.

At the coasts of Portugal and the Bay of Biscay the higher mean  $H_s$  values are found during the winter months (DJF). Along the Portuguese coast, the DJF mean goes from ~3.3 m in deep waters till depths of approximately 40 m, and decreases to ~2.5 m in shallower areas closer to the shore. At the North-West coast of Spain and Brittany in France, the DJF wave height mean is of about 3.6 m in deep waters. These values decrease in shallower areas as the wave fields interact with the sea bottom and refraction becomes important, for example in Brittany, at 40 m depth the mean  $H_s$  is closer to 2.6 m, similar to the DJF mean along the Bay of Biscay at 50 to 40 m depth (see Figure 5, top left panel).

Similar and “milder” sea state conditions are found during spring (MAM) and autumn (SON) months. In this case, along the coast of Portugal, the MAM and SON  $H_s$  mean is of about ~2.4 m in deep waters down to 40 m depth, reducing to about 2 in shallower areas closer to the coast (this depends on the local bathymetric features). Similar values are found in deep waters off the coast of Brittany in France, and in general reducing to ~1.8 m for depth in the range of 80 to 60 m. Along most of the Bay of Biscay the MAM and SON bulk  $H_s$  mean ranges from 1.7 to 1.8 m at depth from 60 to 40 m depth. (Figure 5, top and bottom right panels).



1990 to 2021

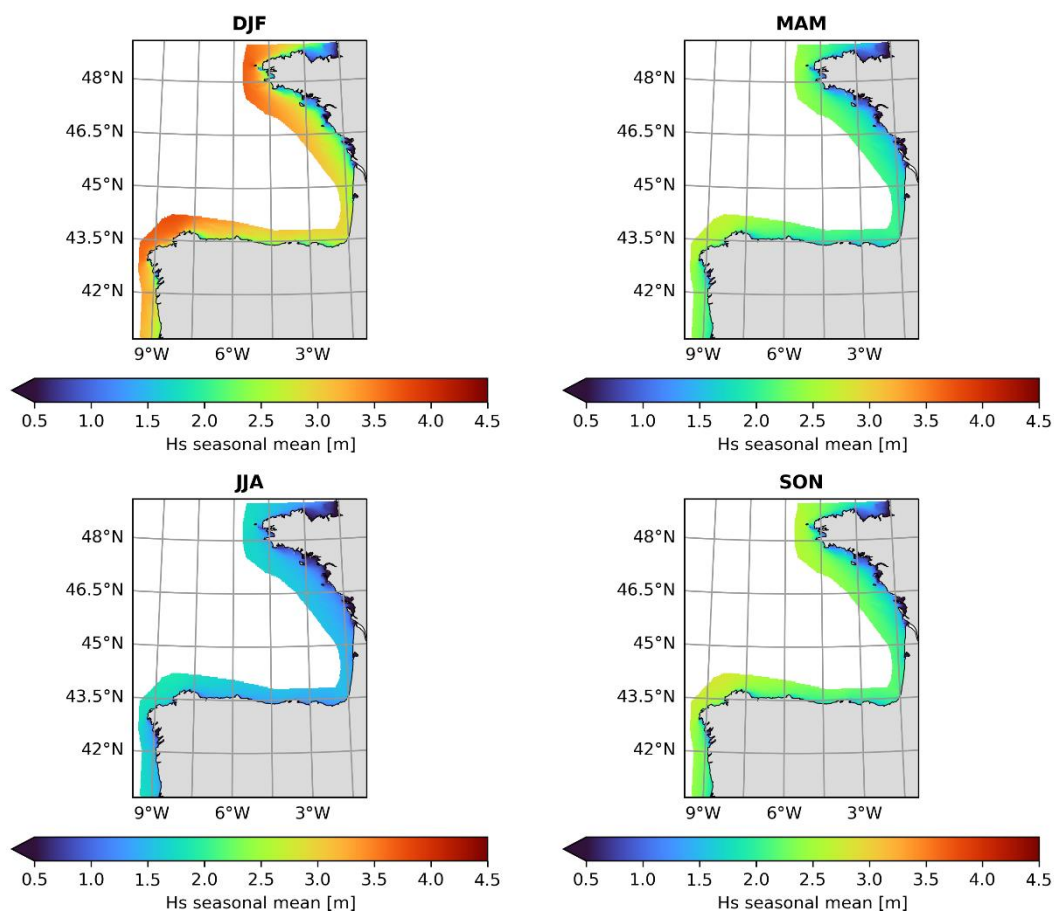


**Figure 5:  $H_s$  32-years seasonal mean for the Iberian Peninsula and The Bay of Biscay. Using the EU\_ATL-2M active nodes which have 500 maximum depth as limiter.**

The lowest wave heights mean is found for summer months (JJA). Mean  $H_s$  values of ~1.7 m are observed off the coast of Portugal in deep waters, decreasing to 1.6 or 1.5 m at depth of ~40 m. Similar mean values are found in deep waters along the North-West coast of Spain and Brittany. Along most of the Bay of Biscay the JJA mean  $H_s$  ranges between 1.4 to 1.3 m at depths ranging from 40 to 60 m. (Figure 5, bottom left panel).

As expected, a similar behaviour to what is observed at Portugal and the Bay of Biscay, is found along the western coasts of Ireland and the UK, also exposed to the North Atlantic storms and swells travelling from far away. This implies higher wave heights during winter, smaller ones during autumn and spring, and the smallest  $H_s$  mean during summer. On the other hand, a slightly different pattern can be seen within the North Sea (Figure 6).

The DJF  $H_s$  mean is typically ~4.5 m between Ireland and The Hebrides at depths close to 150 m, and in average decreasing towards the coast to mean values < 3.5 m at depths of about 60 m (Figure 6, top left panel). Then, the wave heights mean decreases during MAM and SON, although the mean for SON is slightly higher than the one for MAM. The SON  $H_s$  mean is close to 3.3 m between Ireland and The



Hebrides (3.0 m during MAM) at depths of 150 m. In average this mean decreases to 2.5 m for depths in the range of 60 to 80 m (similar during MAM; Figure 6, top and bottom right panels). Finally, during summer month (JJA) the mean  $H_s$  is close to 2 m at depths of 150 m between Ireland and The Hebrides, and in average decreasing to 1.7 or 1.8 m at depths of 60 to 80 m (Figure 6, bottom left panel).

At the North Sea, the highest mean  $H_s$  values are also found during winter (DJF), followed by SON, then MAM, and finally the smallest mean values are obtained for summer (JJA). In general along the Dutch and German coast the DJF mean is in the range of 1.8 to 2.0 m within depths of 25 to 35 m (Figure 6, top left panel). This values are progressively smaller towards the Belgian coast (~1.5 m). These values range between 1.4 to 1.7 m during SON for the Dutch and German coast (depths between 25 to 35 m) and 1.1. to 1.3 m within Belgian waters. For MAM the wave heights mean ranges between 1.2 to 1.4 m, and reducing to about 1 m within Belgian waters. Finally, JJA the 32-years mean a long the Dutch and German coasts ranges from 1.0 to 1.2 m (in average) within depths of 25 to 35 m, and ranges approximately between 0.7 to 0.8 m off the Belgian coast.

**1990 to 2021**

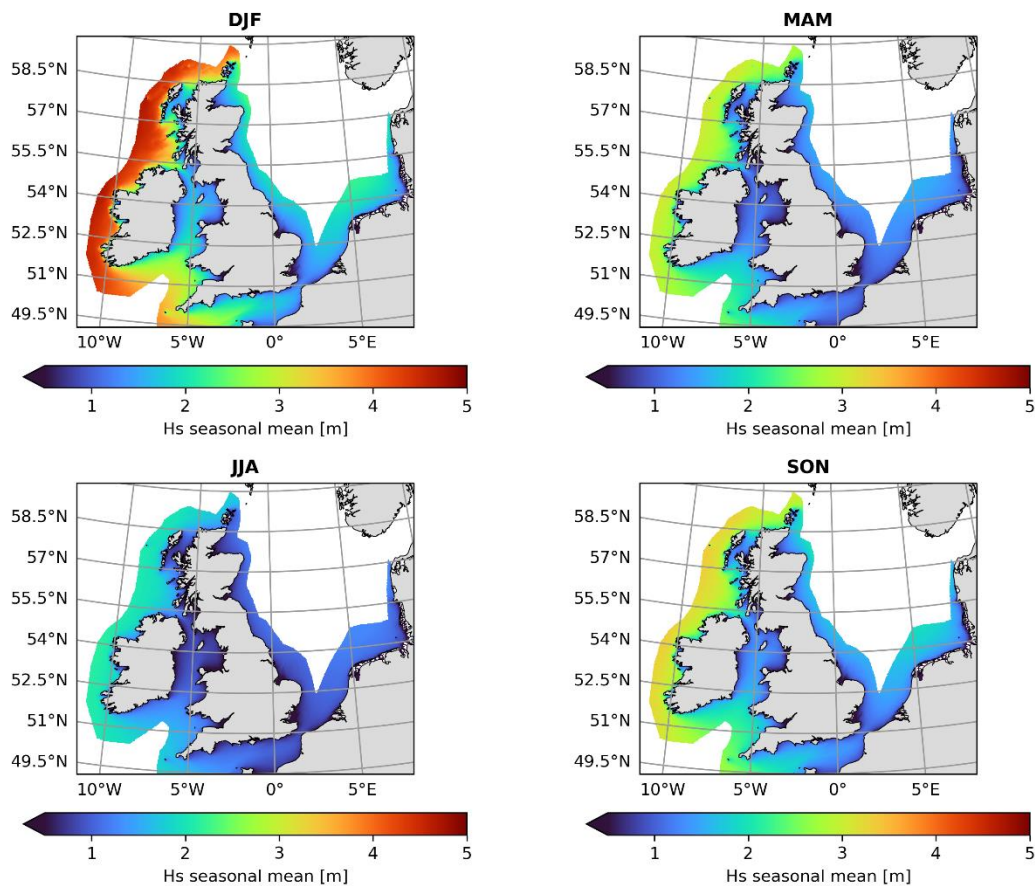


**Figure 6:  $H_s$  32-years seasonal mean for Ireland, UK and The North Sea.**



As for the mean seasonal wave heights, the mean peak periods at Portugal and the Bay of Biscay have their highest values (longer waves) during DJF, with similar shorter mean periods during MAM and SON, and the smallest mean values during JJA (Figure 7). The mean DJF  $T_p$  along Portugal is typically  $\sim 12.9$  s reaching about 13.1 s close to the shore. Smaller values are found at Brittany, the North-West coast of Spain and the Bay of Biscay, with mean  $T_p$  values of  $\sim 12.5$  s going up to  $\sim 12.8$  s (or higher) close to the shore (distances  $< 10$  km; Figure 7 top left panel). During SON and MAM, the mean peak periods along Portugal are on average 11.25 s increasing towards the coast up to 11.5 s, these values decrease to  $\sim 11$  s at Brittany, the North-West coast of Spain and the Bay of Biscay, also reaching 11.5 s closer to the shore (Figure 7 top and bottom right panel).

Finally, the mean  $T_p$  estimates for JJA range between 9 and 9.2 s along Portugal, with a slight increase towards the coast (distances  $< 10$  km offshore) reaching 9.3 s average. On the North-West coast of Spain the JJA mean ranges from 8.9 to 9.2 s, with mean values between 9.1 to 9.4 s in Western Brittany and the Bay of Biscay (Figure 7, bottom right panel).

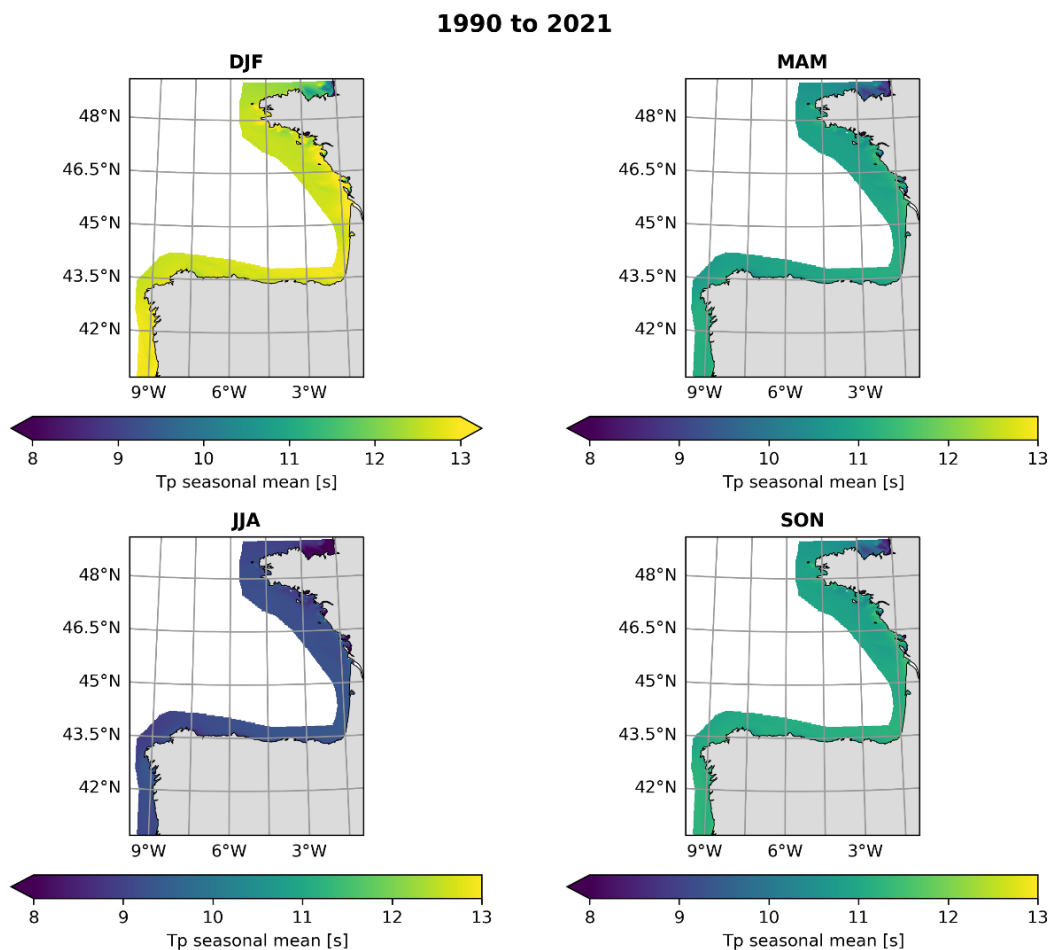


**Figure 7:  $T_p$  32-years seasonal mean for Portugal and The Bay of Biscay.**



Results for the seasonal mean peak periods in Ireland, the UK and the North Sea are presented in Figure 8. Along the western coasts of Ireland and The Hebrides, the DJF  $T_p$  mean typically ranges between 12.3 and 12.5 s. Higher values can be found closer to the shore reaching 13 s. At the North Sea more spatial variability is observed, with DJF mean peak periods of 6.9 to 8 s along the Dutch and German coasts and 6.5 to 7 s more common on the Belgian coast. (Figure 8, top left panel).

Very similar results are found for MAM and SON within the Atlantic coasts of the UK, and the North Sea. For these seasons, the mean  $T_p$  along the Irish and The Hebrides western coasts ranges from 10.7 to ~11 s, with some higher increases up to 11.5 s close to the shore. More homogeneous values are estimated along the Dutch and German coasts with mean values ranging from ~6.6 to ~7.0 s, and mean periods ranging from 6.2 to 6.8 s along the Belgian coast and closer to the English Channel. (Figure 8, top and bottom right panels)

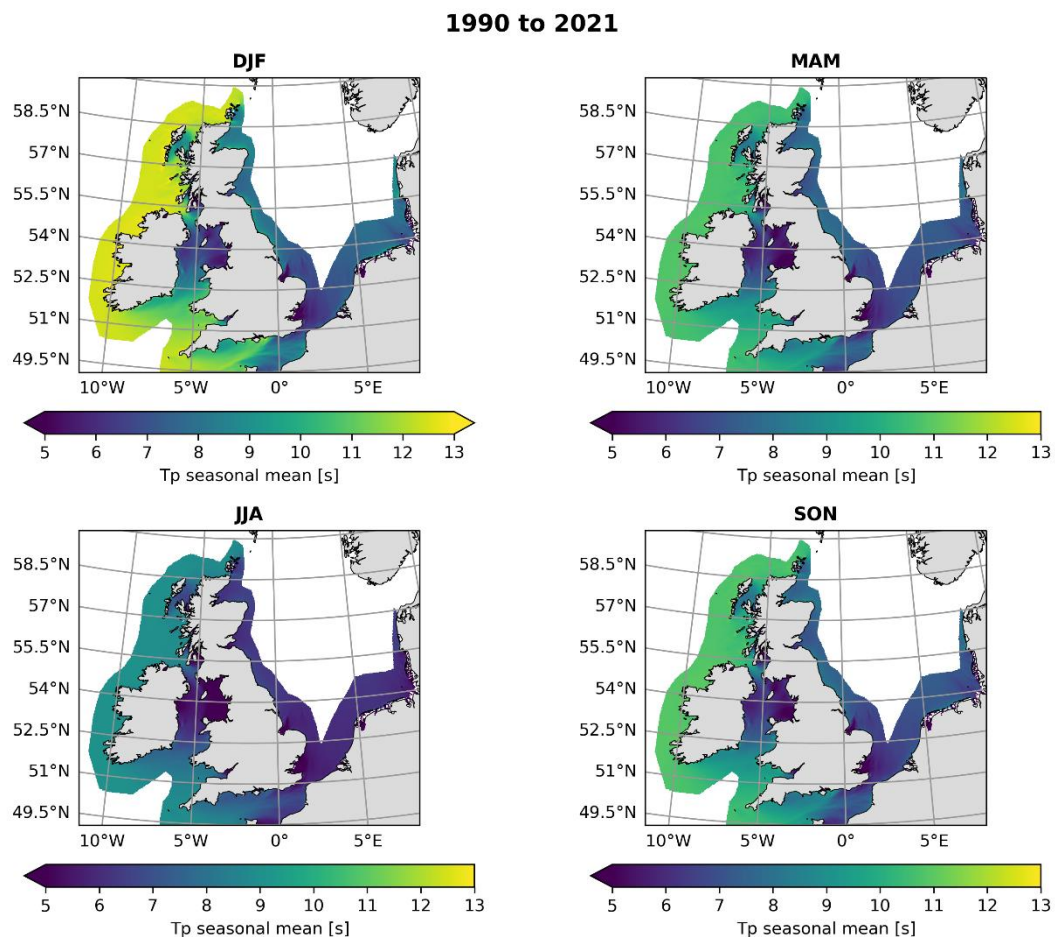


**Figure 8:  $T_p$  32-years seasonal mean for Ireland, UK and The North Sea.**



### 2.1.3 Wave Extreme Value Analysis

The extreme wave analysis is aimed to characterize first the highest wave heights ( $H_s$ ) obtained within the 32-years hindcast. Then, using a probabilistic fit over a set of  $H_s$  selected with a peaks over threshold (POT) analysis, the expected extreme wave height values are estimated for different return periods.

#### 2.1.3.1 Estimation of the highest wave heights

Characterization of highest wave heights obtained in the 32-years' time window, is done with the 95<sup>th</sup> and 99<sup>th</sup> percentiles (p95 and p99). These parameters give the wave height values that are exceeded, during severe storm conditions, 5% (p95) and 1% (p99) of the time. Particularly, p99 gives a good idea of the maximum wave heights obtained at each location for the 32-years dataset. Wave height percentiles p95 and p99 estimated for Portugal and the Bay of Biscay are presented in Figure 9. The same results for Ireland, the UK and The North Sea in Figure 10.

Offshore Portugal the wave heights' p95 and p99 are ~4.5 m and ~6.7 m respectively. These values decrease down to ~4 m in the case of p95 and ~5 m for p99 for depths typically <40 m. As seen before for the mean wave conditions, the highest  $H_s$  are found along the North-East coast of Spain and western Brittany in France. Along the North-East coast of Spain the  $H_s$  p95 is in average 5.3 m in deep waters and goes down to 4.6 m closer to the coast (depths <60 m). The p99 is about 7.3 m in deep waters and decreasing to ~6.6 m close to the coast. In Western Brittany the p95 and p99 are respectively ~5.5 m and ~7.5 m for depths > 120 m. At depths of 60 to 50 m the p95 wave heights range from 4.0 to 4.7 m and the p99 from ~6.5 to ~5.5 m (or less). Along the Bay of Biscay the  $H_s$  p95 is ~5 m for depth >80 m and the p99 is of the order of 7 m for the same depths (these values are smaller at the southern end of the bay), See Figure 9.

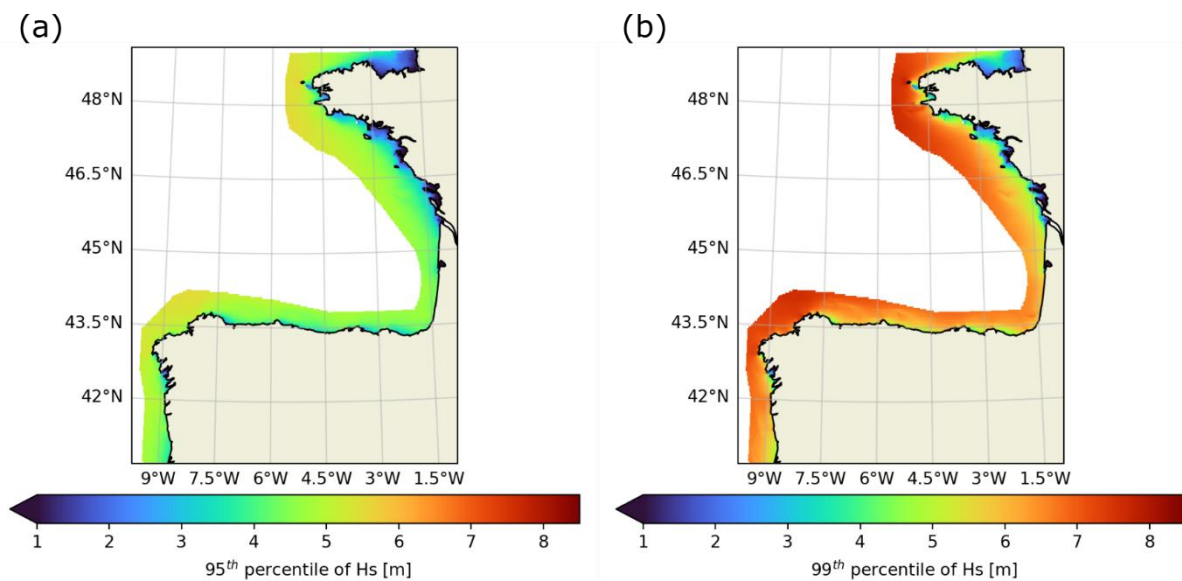


**Figure 9:  $H_s$  32-years (1990 to 2021) 95<sup>th</sup> percentile (a) and 99<sup>th</sup> percentile (b). Portugal and Bay of Biscay.**



Along the western coasts of Ireland the  $H_s$  p95 and p99 is typically ~6.7 m and 8.9 m respectively. In shallower depths (between 80 to 60 m) these values drop to about ~6.0 m (p95) and ~8.0 m (p99). Similar results are observed along the western coasts of The Hebrides, with clear a decrease of the highest wave heights towards the North coast of Scotland and the Orkneys. There, the p95 is of about 6.3 m and p99 close to 8.7 m (at depths between 100 to 80 m).

Finally, in The North Sea, the wave heights' p95 along the Dutch coast ranges between ~2.5 to ~3.2 m between depths of approximately 25 to 35 m. The p99 in the same area ranges between ~3.3 to ~4.0 m. Following the behaviour already observed in the mean wave conditions characterization, the extreme wave heights are also smaller towards the Belgian coast. Here the p95 ranges between ~1.5 to ~2.5 m, and the p99 between ~2.2 to ~3.4 m (at depths between 20 to 30 m). (see Figure 70)

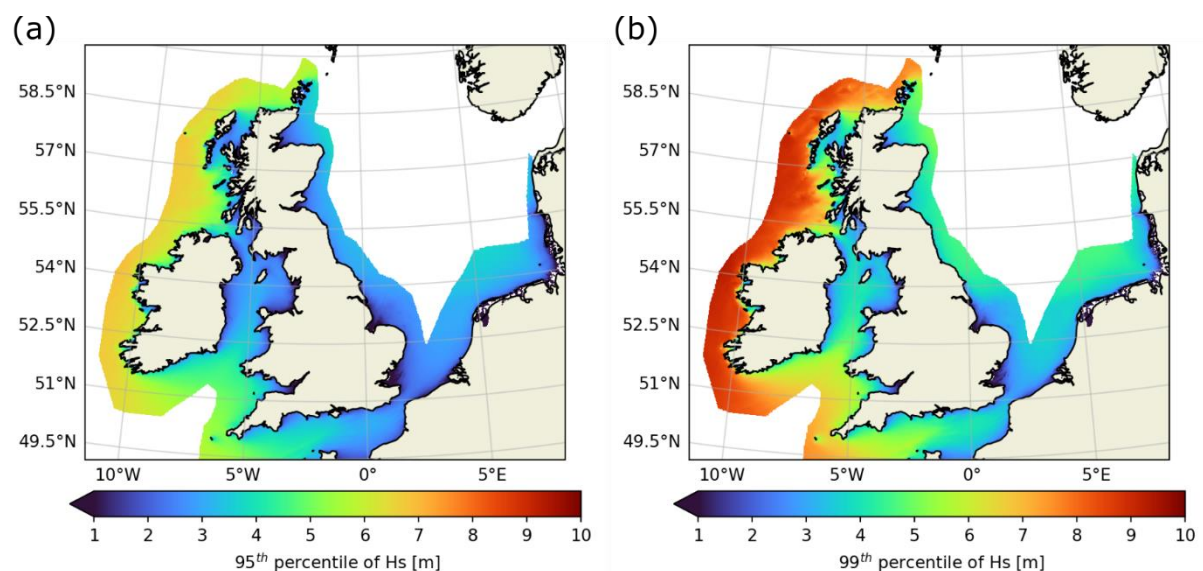


**Figure 10:  $H_s$  32-years (1990 to 2021) 95<sup>th</sup> percentile (a) and 99<sup>th</sup> percentile (b). Ireland, UK The North Sea.**

### 2.1.3.2 Estimation of expected extreme wave height for different return periods

The estimation of the expected extreme wave heights for different return periods is mainly aimed to provide reliable information for design conditions.

First, a selection of the storms considered “extreme events” is performed for each year of the wave hindcast. This selection is done based on the POT method applied to the time series of  $H_s$  at each grid node of the high resolution grid (EU\_ATL-2M). In this case, the  $H_s$  value corresponding to the p95 (Figure 9.a and Figure 10.a) is used as the threshold to consider an event as extreme. Thus, the threshold applied to each grid node depends on its local wave conditions. From each group of wave

heights corresponding to an extreme event, the maximum value (the peak) is selected. In this case, to ensure that each wave height “peak” corresponds to an independent (different) storm, a minimum time separation of 24 hours is imposed in the peaks selection.

With the selected  $H_s$  peaks from each identified extreme event, it is then required to apply a probabilistic fit of the wave heights samples. The selected cumulative probability distribution function is Weibull (Equation 4), typically used to analyse extreme wave heights data (Goda, 2000). The data fitting is done in two steps. A first guess of the shape ( $k$ ), scale ( $A$ ) and location ( $B$ ) parameters is done using the maximum like method implemented in the weibull\_min function from the scipy computation library package (Virtanen, et al., 2020) in Python (Van Rossum & Drake, 2009). Subsequently, this first guess of  $k$ ,  $A$  and  $B$  is used to start the iteration for the least squares fit between the extreme wave heights selection and the cumulative probability function, which gives the final set of Weibull parameters.

Finally, to verify the suitability of the Weibull distribution with the obtained distribution parameters, a the Pearson correlation index (CORR, Equation 5) is computed using the unbiased plotting probability of the wave heights selected (Equation 6), with the cumulative probability function. A minimum value of CORR of 0.95 was imposed to ensure that the distribution fit is well suited for the estimation of extreme wave heights related to a given return period. All locations with CORR <0.95 are not considered in the analysis (a few cases in very shallow waters , depth <15). This helps to reduce the potential over estimation of the extreme  $H_s$ .

**Equation 4** 
$$F(x) = 1 - \exp \left[ - \left( \frac{x-B}{A} \right)^k \right]$$

**Equation 5** 
$$CORR = r_{\hat{X}, \hat{Y}} = \frac{\sum_{i=1}^N (\hat{X}_i - \bar{\hat{X}})(\hat{Y}_i - \bar{\hat{Y}})}{\sqrt{\sum_{i=1}^N (\hat{X}_i - \bar{\hat{X}})^2} \sqrt{\sum_{i=1}^N (\hat{Y}_i - \bar{\hat{Y}})^2}}$$

**Equation 6** 
$$\hat{F}(m) = 1 - \frac{m-\alpha}{N_T+\beta}, m = 1, 2, \dots, N$$

were 
$$\alpha = 0.2 + 0.27/\sqrt{k} \text{ and } \beta = 0.2 + 0.23/\sqrt{k}^1$$

In Equation 3 (the Weibull cumulative probability function),  $x$  is the significant wave height,  $k$  is the shape parameter,  $A$  the scale parameter and  $B$  the location parameter. In Equation 5,  $\hat{X}$  is the Weibull cumulative probability and  $\hat{Y} = \hat{F}(m)-1$ , the unbiased plotting probability (Equation 6) of the  $H_s$  selected with the POT method. In Equation 6,  $m$  are each one of the  $N$  extreme  $H_s$  values sorted from minimum to maximum. In this case  $N_T=N$  because no “sub group” of extreme wave heights has been selected from the initial population defined with POT (otherwise,  $N < N_T$ ).

---

<sup>1</sup> Equation 6 and its parameters have been take from equation 11.14 and table 11.2 from Goda (2000).





The CORR results for the probability distribution fit at each grid node in EU\_ATL-2M is presented in Figure 11. In most areas the CORR values are >0.998, which implies that the selected  $k$ ,  $A$  and  $B$  parameters properly describe the extreme waves distribution at each location.

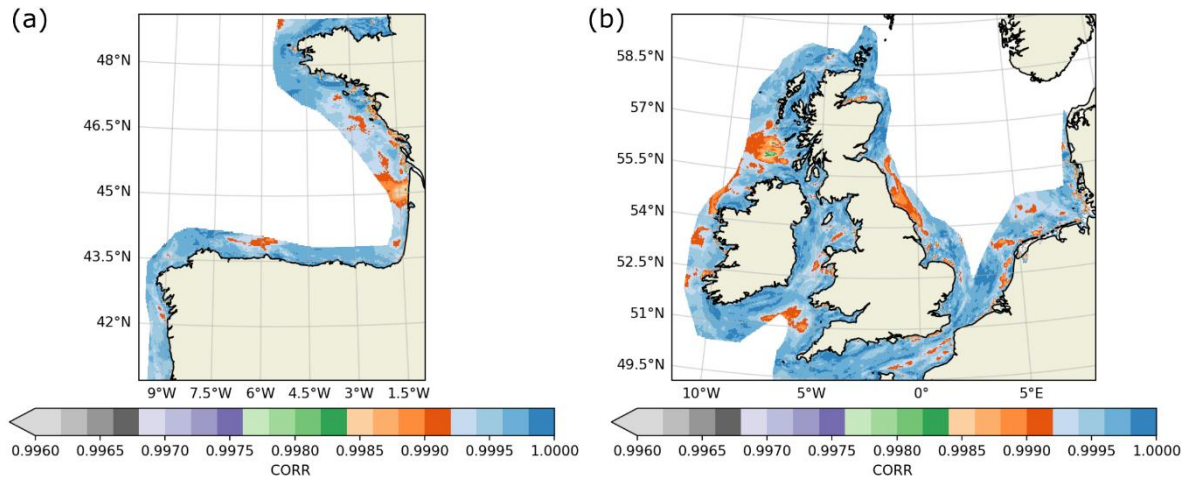


**Figure 11: Weibull probability distribution fit correlation ( $F(x)$ ,  $\hat{F}(m)$ ) for (a) Portugal and Bay of Biscay, and (b) Ireland, UK and The North Sea.**

With the probability distribution function defined, it is possible to estimate the expected extreme wave height ( $H_R$ ) for a storm of a certain return period  $R$  with the following expression:

**Equation 7** 
$$H_R = B + Ay_R$$

where  $B$  and  $A$  are the Weibull parameters obtained from the best fitting, and  $y_r$  is the so called reduced variable. For the Weibull distribution, this reduced variable has the following expression:

**Equation 8** 
$$y_R = [\ln(\lambda R)]^{1/k}$$

with 
$$\lambda = N/K$$

where  $k$  is the Weibull shape parameter,  $N$  the total amount of  $H_s$  values selected with the POT method and  $K$  is the total amount of analysed years.

One must consider the intrinsic variability of the return value  $H_R$  at every return period  $R$  considered. This variability range is largely related to the sampling method and the effects of the variability in the data population used to estimate the probability distribution fit. For practical cases, a normal distribution of the return value is assumed (Goda, 2000), which helps to define the upper and lower bounds. Thus, the 90% confidence interval is set as the range  $\pm 1.645$  times the standard deviation around the estimate of the return value ( $H_R$ ).

The standard deviation of  $H_r$  for each return period can be expressed with the following empirical formula:



**Equation 9** 
$$\sigma(H_R) = \sigma_z \sigma_x$$

where  $\sigma_x$  is the standard deviation of the extreme  $H_s$  sample, and  $\sigma_z$  is the standard deviation of the reduced variable (Equation 8) given by:

**Equation 10** 
$$\sigma_z = [1.0 + a(y_R - c + a \ln(v))^2]^{0.5} / \sqrt{N}$$

and where the constant  $a$  is computed as follows:

**Equation 11** 
$$a = a_1 \exp[a_2 N^{-1.3} + \kappa(-\ln(v))]$$

Then, the rest of the constants from Equation 10 and Equation 11 are interpolated between the tabulated values from Table 2 depending on the value of the Weibull shape parameter  $k$ .

**Table 2: Constans for the standard deviation of the return value.**

Weibull ( $k$ )	$a_1$	$a_2$	$\kappa$	$c$	$\alpha$
0.75	1.65	11.4	-0.63	0	1.15
1.0	1.92	11.4	0	0.3	0.90
1.4	2.05	11.4	0.69	0.4	0.72
2.0	2.24	11.4	1.34	0.5	0.54

Obs.: Adapted from Table 11.11 in Goda (2000).

Following this method, the extreme wave height values ( $H_R$ ) and the corresponding 90% confidence intervals, for return periods ( $R$ ) of 10, 25, 50, 75 and 100 years were computed. Results are presented from Figure 12 to Figure 15.

To provide an idea of the extreme wave height obtained, for the selected return periods in different areas, the  $H_R$  v/s  $R$  curves (and the 90% confidence interval bounds) at the same locations from Figure 4 are presented in Figure 16. Here the differences of the estimated return value are notorious, with  $H_R(100)$  close to 14 m off the coasts of Viana do Castelo in Portugal and ~18.5 m in Western Brittany (France). Then, higher values are obtained off the coast of Doonbeg (Ireland) and the Orkneys (Scotland) with  $H_R(100)$  of ~24.8 m and 21.0 m respectively. In contrast, but also expected, smaller extreme wave height values are found in the North Sea (Dutch waters), where the  $H_R$  for 100 years return period is close to 6.4 m.

Although outside the scopes of this study, it is important to highlight that, there is a difference between the significant wave heights and the maximum estimated wave height ( $H_{max}$ ) from the same sea state. In general, the ratio  $H_{max}/H_s$  is assumed to be close to ~1.8, which is a reasonable approximation (Holthuijsen, 2010; Goda, 2000). Nevertheless, in highly energetic locations (as the west coast of Ireland, or Portuguese waters) this ratio can be >2.4 during extreme events, and depending on the local distribution of waves (Oliveira, Neves, Fidalgo, & Esteves, 2018). In the



present section all the analysis of extreme wave heights has been done in terms of  $H_s$ , thus, the estimation of the  $H_{max}$ , for design purposes, should be carried out carefully depending on the analysed location.

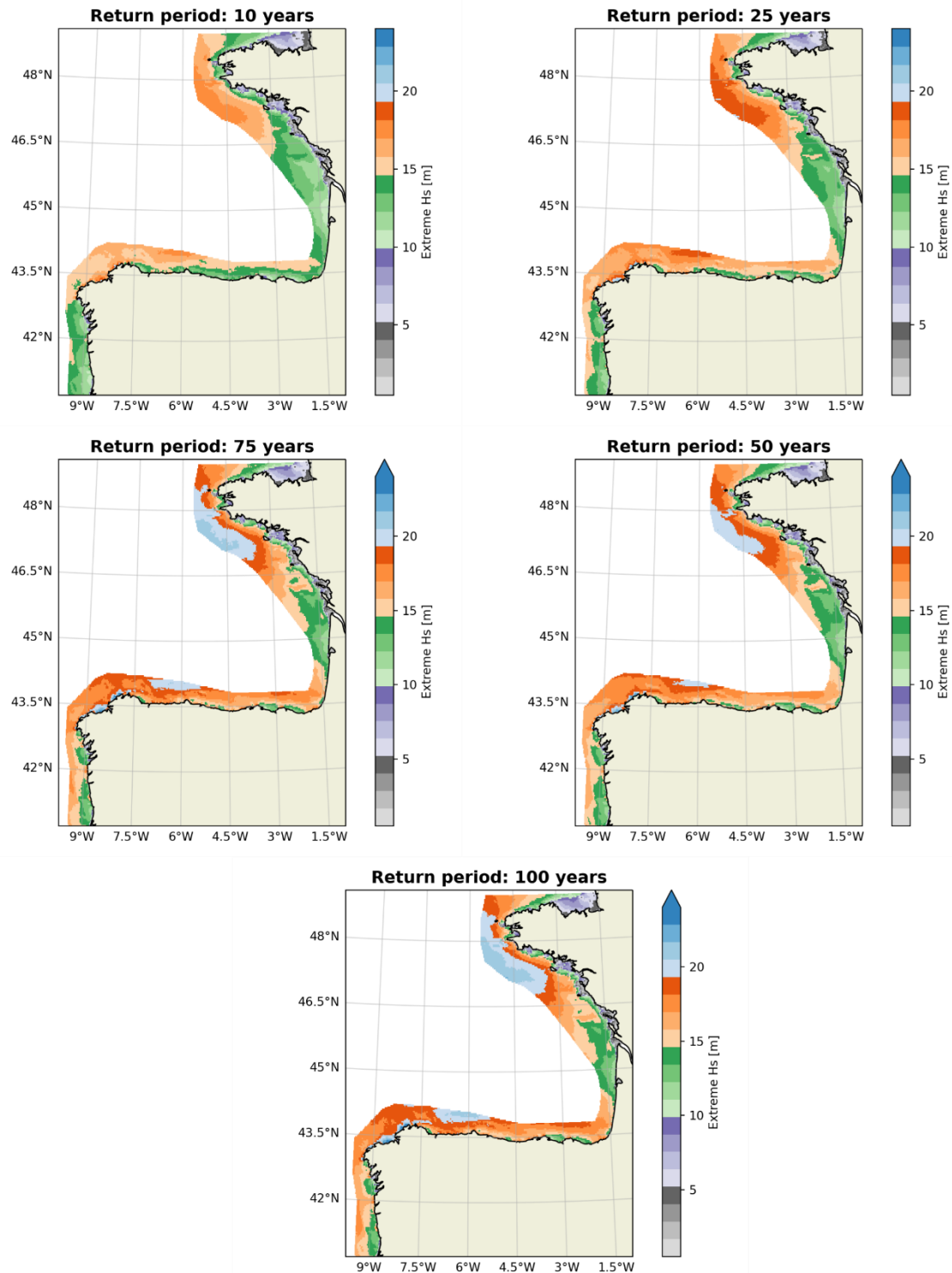


**Figure 12: Expected extreme significant wave height return value ( $H_R$ ) for 10, 25, 50, 75, and 100 years return periods. Portugal and Bay of Biscay.**



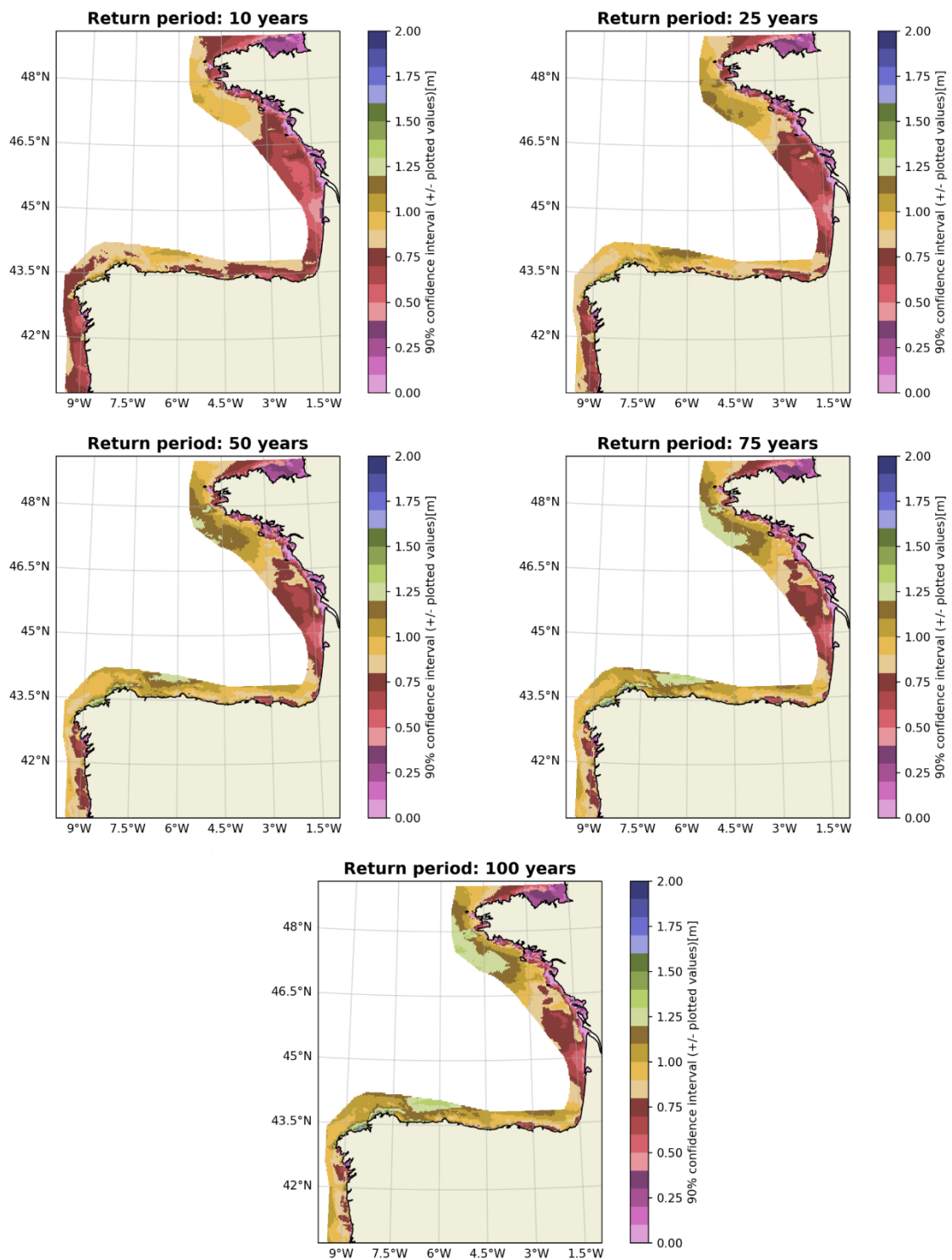


**Figure 13: Upper and lower confidence bounds from the 90% confidence interval (for each  $H_R$  return value in Figure 12). Portugal and Bay of Biscay.**



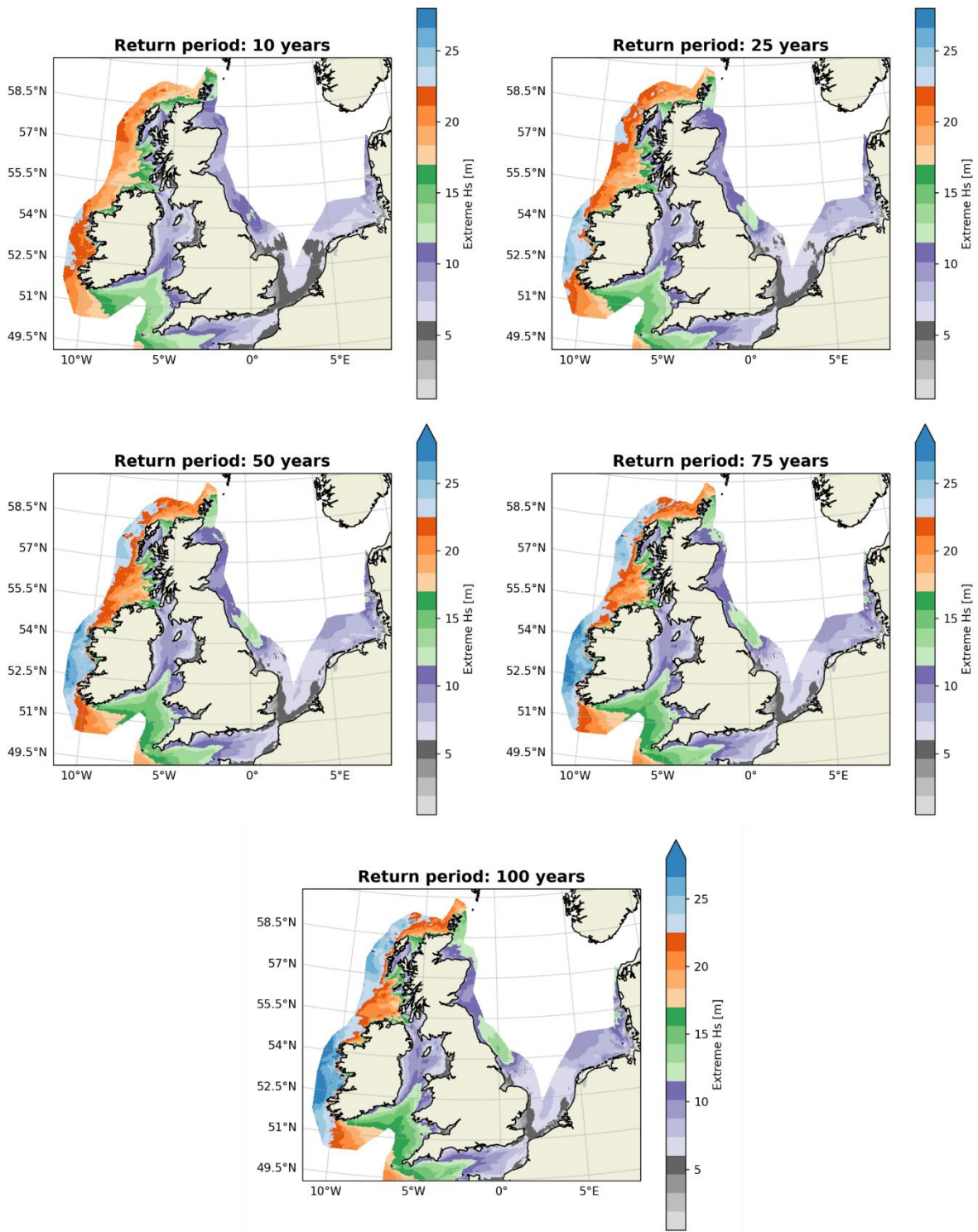


**Figure 14: Expected extreme significant wave height return value ( $H_R$ ) for 10, 25, 50, 75, and 100 years return periods. Ireland, UK and The North Sea.**



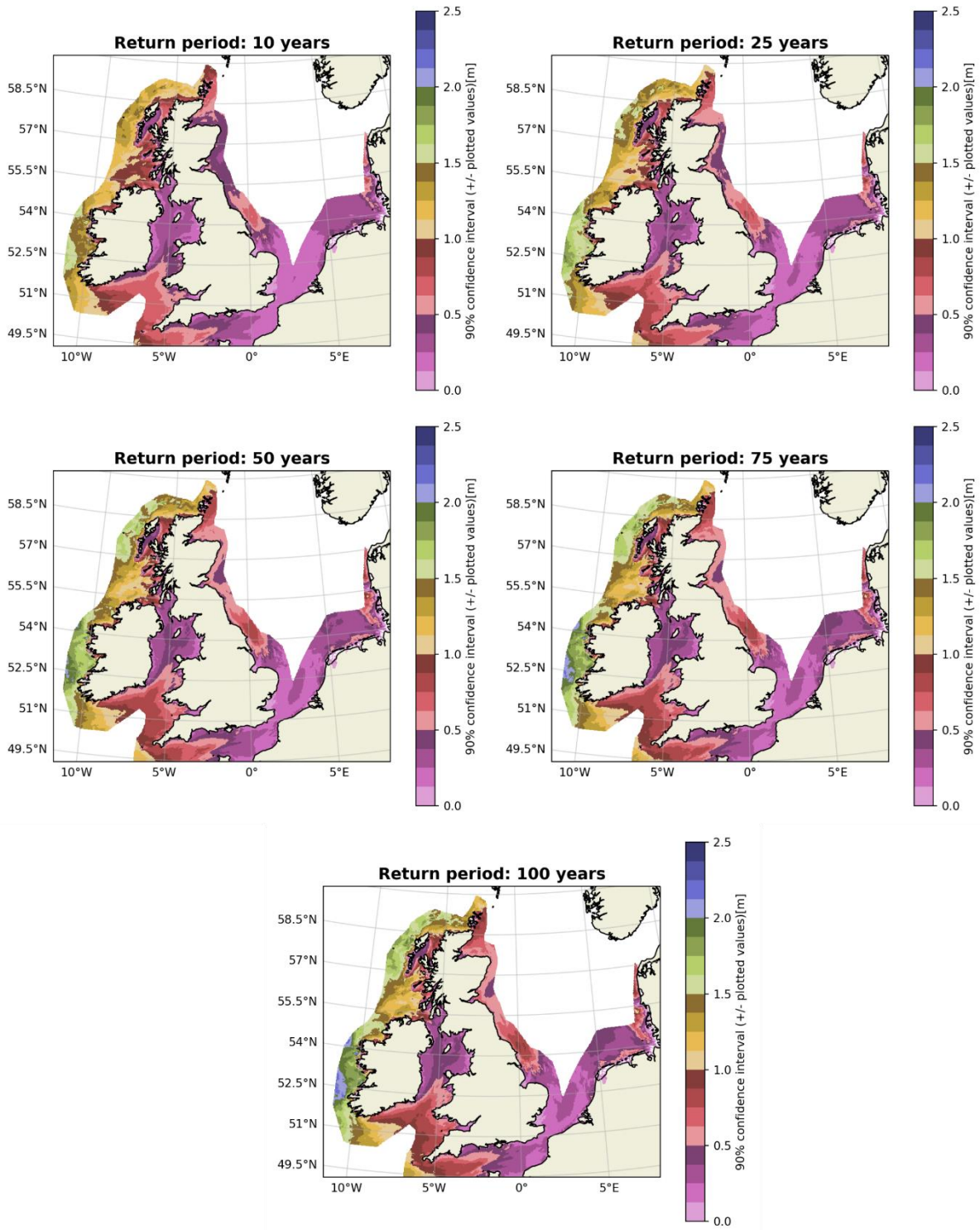


**Figure 15: Upper and lower confidence bounds from the 90% confidence interval (for each  $H_R$  return value in Figure 14). Ireland UK and The North Sea.**



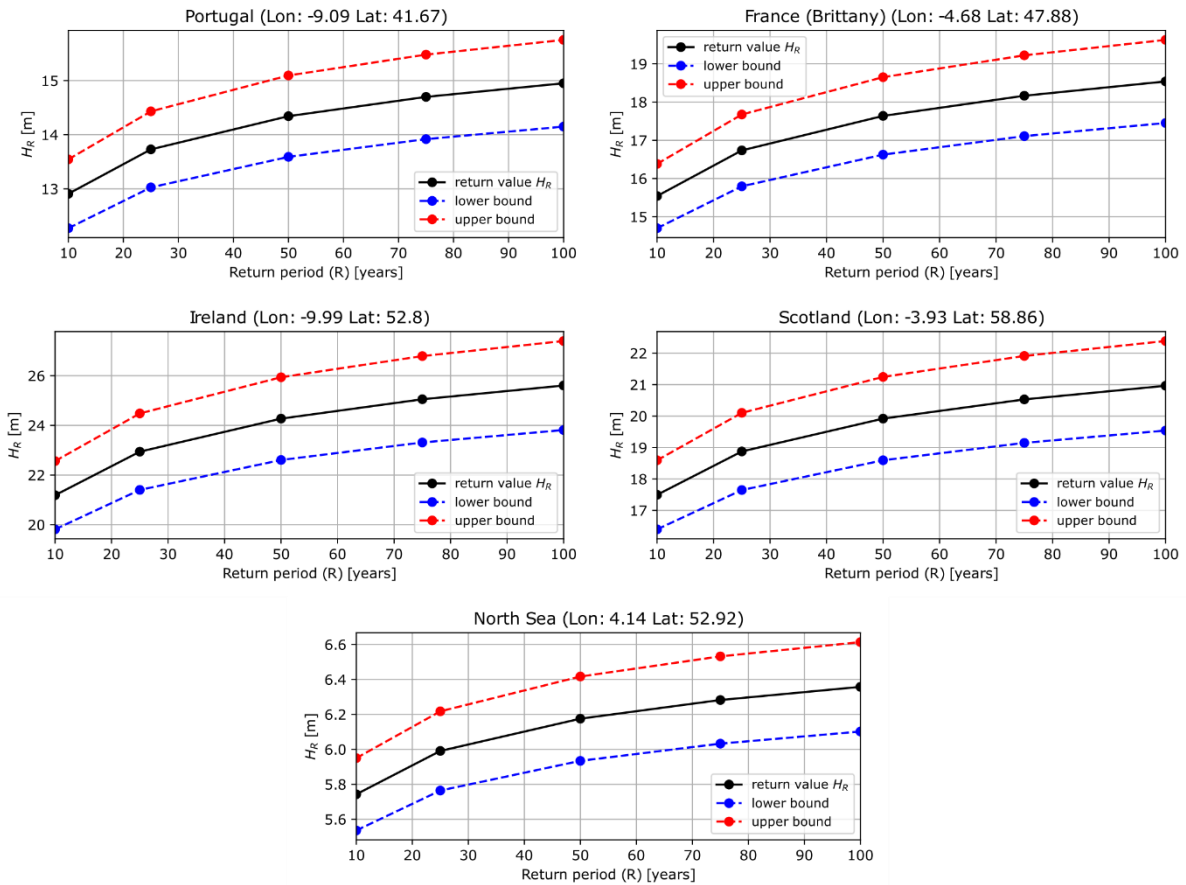


**Figure 16: Return value  $H_R$  and 90% confidence interval bounds.**

Obs.: Lower bound of the 90% confidence interval in blue. Upper bound of the 90% confidence interval in red.

## 2.1.4 Operation time windows

The study of the operation time windows or “weather windows”, is aimed to define the probability of having  $H_s$  smaller than a certain threshold  $H_{ac}$  continuously for a defined amount of hours  $T$ . Thus, the definition of the weather windows is expected to be of use to assess the time availability for access to deployment or maintenance at potential sites of interest.

The proposed analysis is based on the NMI method (Kuwashima & Hogben, 1986; Kato & Nobuoka, 1996) for estimating wave persistence statistics, which has been included in the EquiMar guidelines for analysing site accessibility (Stallard, Dhedin, Saviot, & Noguera, 2010). The followed steps are briefly explained here using a 30-year time series of  $H_s$  from a randomly selected point offshore Ireland (section 2.1.4.1). Then, the obtained results for the complete high resolution domain (EU\_ATL-2M grid) are presented in section 2.1.4.2.

### 2.1.4.1 Method

As done for the estimation of extreme waves, the first step is to find the best fit of a time series of  $H_s$  to a Weibull distribution using the same procedure described in



2.1.3.2. An initial estimation of the Weibull 3 parameters is done using the maximum likelihood method. Then, these parameters are used as the seed value for the least squared method which gives the final shape, location (or position) and scale parameters. To avoid confusion with the defined variables in previous sections, the Weibull probability of exceedance function is re-written as follows:

**Equation 12** 
$$P(H_s < H_{ac}) = \exp \left[ - \left( \frac{H_{ac} - x_0}{b} \right)^k \right]$$

Equation 12 describes then the probability of occurrence of  $H_s$  to be smaller than a certain threshold  $H_{ac}$ . Here,  $x_0$  is the location parameter,  $b$  the scale parameter, and  $k$  the shape parameter. An example of the probability function fitting results is presented in Figure 17.

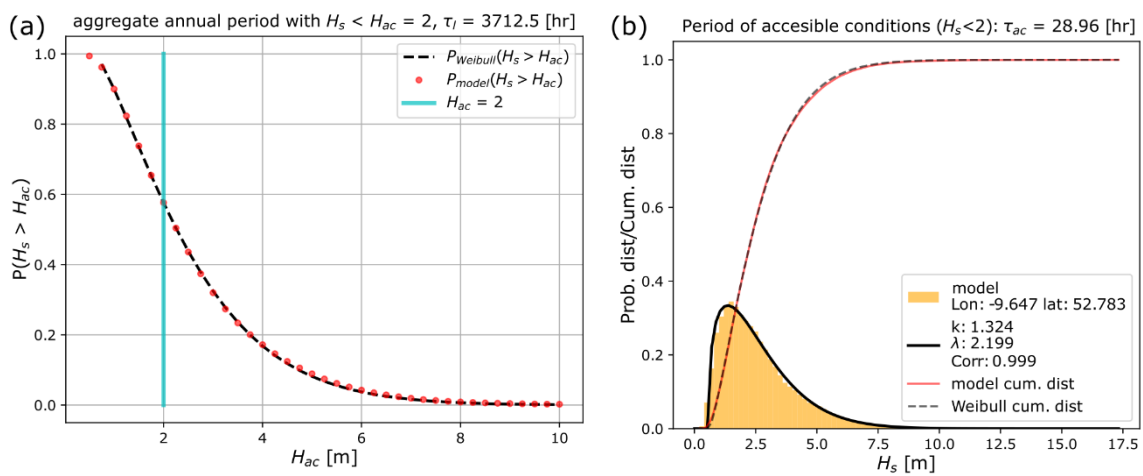


**Figure 17: (a) Wave height Probability of exceedance from Weibull best fit and from modelled time series. (b) wave height density probability distribution from modelled time series and Weibull fit.**

Obs.: Analysed period is from 1992 to 2021 (30 years). On (b) is possible to see the high correlation (CORR) between the modelled data distribution and the Weibull fit (black lines).

Considering the average number of hours per year as  $D = 8760$ , the aggregate annual period for which the significant wave height is smaller than a given threshold  $H_{ac}$  can be estimated as follows:

**Equation 13** 
$$\tau_l = D \cdot P(H_s < H_{ac})$$

$\tau_l$  includes all the individual “events”, with different durations, throughout the analysed period  $D$  (in this case a year), when  $H_s$  is  $< H_{ac}$ . As shown in Figure 17.a, for the analysed location,  $\tau_l = 3712.5$  hours for an “access” significant wave height  $H_{ac} = 2$  m.

The mean duration of these events during which the defined  $H_{ac}$  is not exceeded ( $\tau_{ac}$ ), is related to the Weibull distribution parameters:





**Equation 14** 
$$\tau_{ac} = \frac{1-P(H_s < H_{ac})}{P(H_s < H_{ac})} \frac{A}{[-\ln(P(H_s < H_{ac}))]^\beta}$$

with:

**Equation 15** 
$$A = 35/\sqrt{\gamma}$$

**Equation 16** 
$$\beta = 0.6\gamma^{0.287}$$

**Equation 17** 
$$\gamma = k + \frac{1.8x_o}{H-x_o}$$

**Equation 18** 
$$b\Gamma(1 + 1/k) + x_o$$

where  $x_o$ ,  $b$  and  $k$  are the Weibull coefficients.

An example of the behaviour of  $\tau_{ac}$  as a function of  $H_{ac}$ , for the analysed location, is presented in Figure 18. Notice that, at this site, the mean duration of a period where  $H_s$  is  $< H_{ac}=2$  m is  $\tau_{ac} = 28.96$  hours.

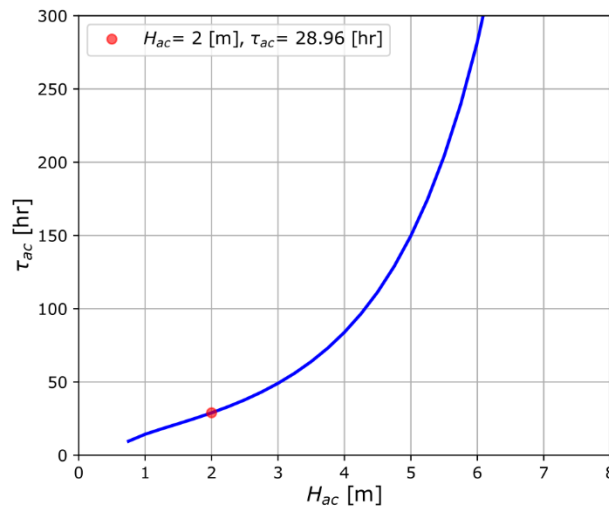


**Figure 18: Mean duration of periods where  $H_s$  is  $< H_{ac}$ .**

*Obs.: Analysed period is from 1992 to 2021 (30 years). Same location specified in Figure 17.*

Finally, it is also possible to define the distribution of the duration of “accessible time windows” in terms of the Weibull parameters obtained for each specific site (Kuwashima & Hogben, 1986). The probability to have wave conditions with  $H_s < H_{ac}$  that persist for a normalised duration  $X_i$  ( $Q(X_i > X_{ac})$ ) can be defined as:

**Equation 19** 
$$Q(X_i > X_{ac}) = \exp(-CX_i^\alpha)$$

where the parameters  $C$  and  $\alpha$  are obtained with the  $x_o$ ,  $b$  and  $k$  Weibull coefficients:

**Equation 20** 
$$C_{ac} = \left[ \Gamma\left(1 + \frac{1}{\alpha_{ac}}\right) \right]^{\alpha_{ac}} \quad (\Gamma \text{ is the Gamma function})$$



**Equation 21** 
$$\alpha_{ac} = 0.267\gamma \left(\frac{H_{ac}}{\bar{H}}\right)^{-0.4}$$

and with the normalized duration of an accessible period defined as:

**Equation 22** 
$$X_i = \tau_i / \tau_{ac}$$

Then, the number of occurrences of continuous time windows of duration  $\tau_i$  during which the wave height ( $H_s$ ) remains  $< H_{ac}$  is given by:

**Equation 23** 
$$N_i = \frac{Q(1-P)D}{\tau_i}$$

Finally, the cumulative probability to have  $H_s < H_{ac}$  for a duration  $\tau_i > \tau_{ac}$  can be expressed as follows:

**Equation 24** 
$$R_i = \frac{1}{D} \sum \tau_i N_i$$

An example of the results obtained with the explained steps is presented in Figure 19.a where the probability of occurrence of  $Q(X_i > X_{ac})$  is plotted as function of  $\tau_i = X_i \tau_{ac}$  for different  $H_{ac}$  values. Note that from this figure, it is possible to estimate the number of occurrences of continuous periods of duration  $\tau_i$  (within a year in this example) where the wave height ( $H_s$ ) remains  $< H_{ac}$ . This is possible using Equation 23 (Figure 19.b).

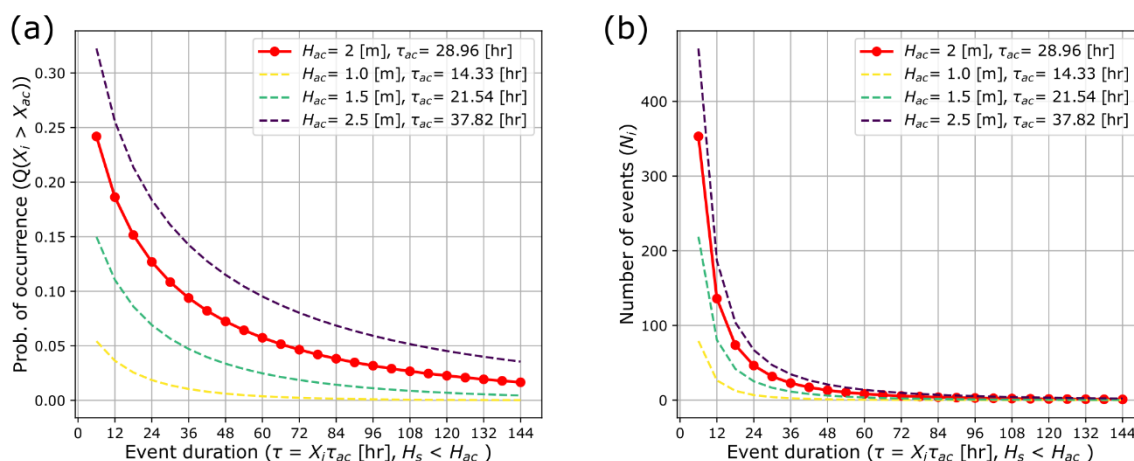


**Figure 19: (a) Yearly probability of occurrence of continuous time windows with  $H_s < H_{ac}$ . (b) Yearly estimated number of events with time windows of duration  $\tau_i$  with  $H_s < H_{ac}$ .**

Obs.: Analysed period is from 1992 to 2021 (30 years). Same location specified in Figure 17.

#### 2.1.4.2 Operation (weather) time windows general characteristics

The wave height threshold ( $H_{ac}$ ) to define the access time windows is directly related to the operation requirements on site, including vessel type and safety conditions. These requirements are exclusive of each particular project (e.g.; deployment, maintenance). Here, a general description of the operation windows



is given assuming a general  $H_{ac}$  threshold of 2 m for the complete analysed domain. All the analysis was done using 30 years of  $H_s$  for the probabilistic fit.

The yearly mean duration of periods where  $H_s < H_{ac}$  is presented in Figure 20. Then, the joint probability of occurrence  $Q$  of  $H_s < H_{ac}$  to persist for a continuous time  $\tau_i = X_i \tau_{ac}$  of 6, 9 and 12 hrs is presented in Figure 21.

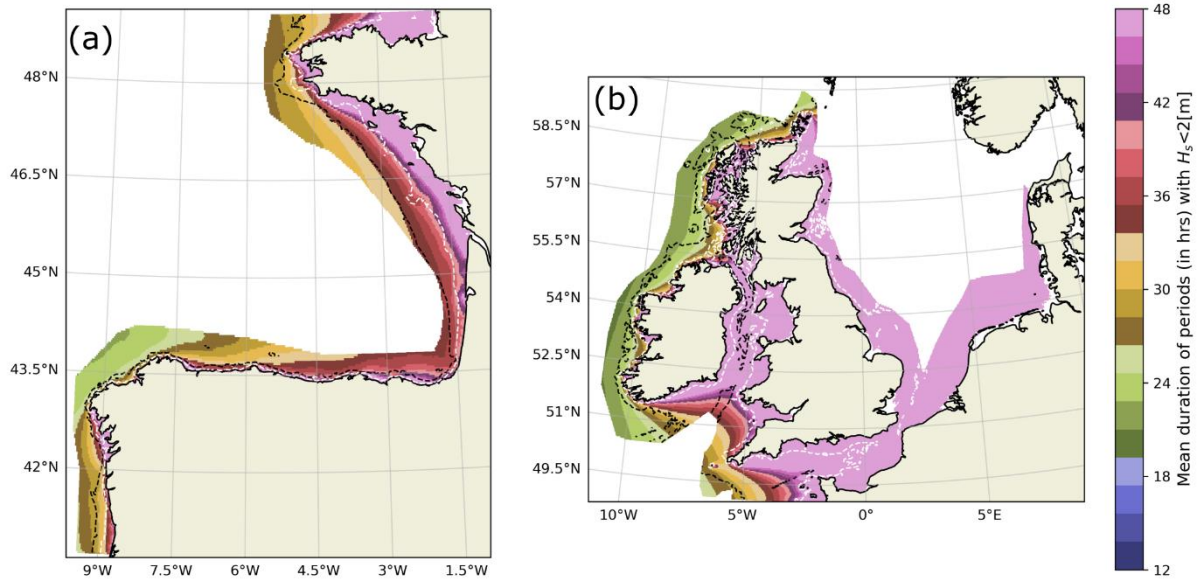


**Figure 20: Estimated yearly  $\tau_{ac}$ , mean duration of periods with  $H_s < H_{ac}=2$  m.**

Obs.: Dashed black lines show the 100 m depth contours, dashed white lines the 50 m depth contours. Colorbar shows  $\tau_{ac}$  in hours.



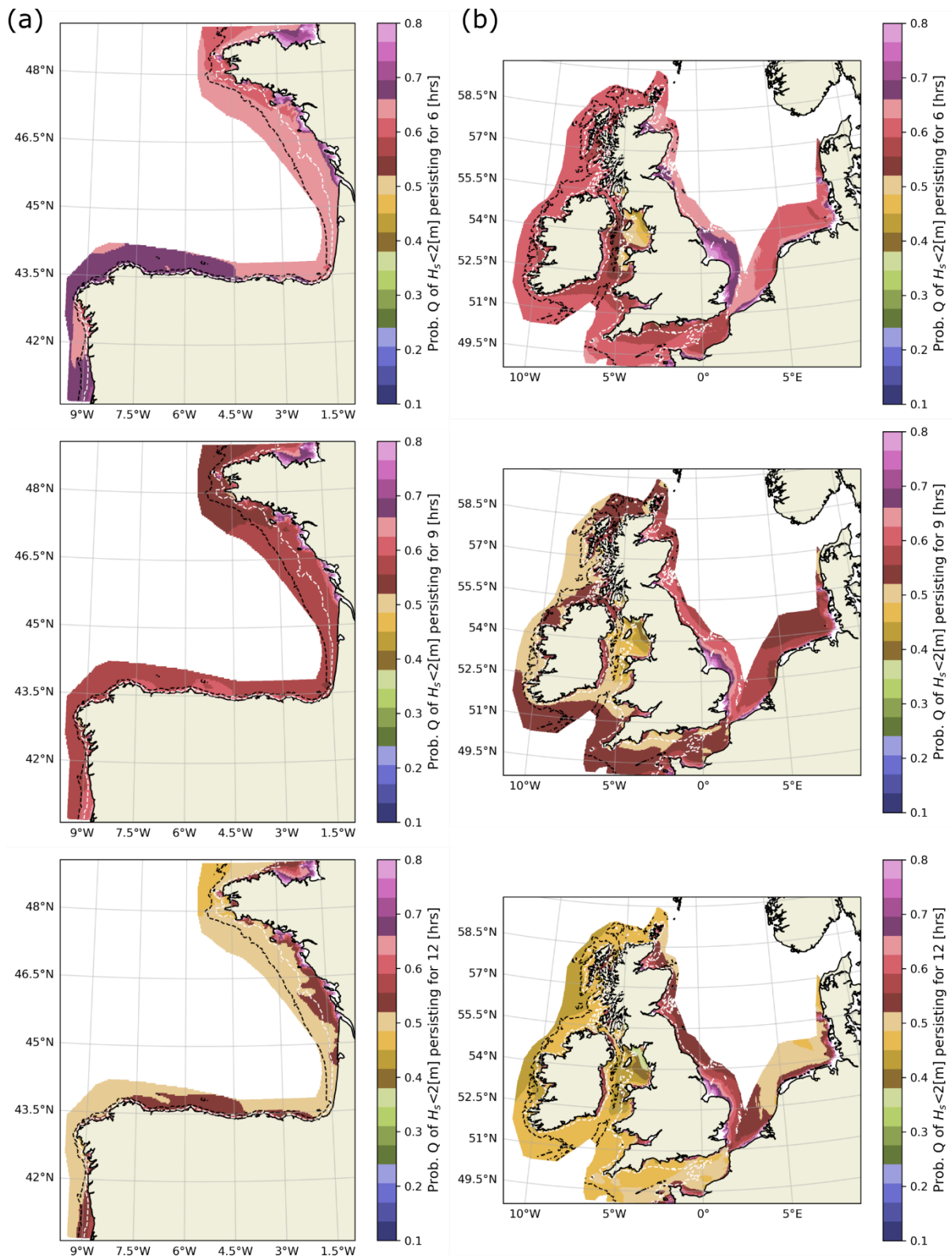


**Figure 21: Estimated yearly prob. of occurrence  $Q$  of  $H_s < H_{ac}=2$  m for continuous time windows of 6, 9 and 12 hrs (top, mid and bottom panels respectively). (a) Portugal and Bay of Biscay, (b) Ireland, UK and North Sea.**

*Obs.: Dashed black lines show the 100 m depth contours, dashed white lines the 50 m depth contours.*



## 2.2 Wave energy resource characterization

A complete statistical characterization of the sea states, in terms of  $H_s$  and  $T_p$  was developed in section 2.1. The use of a high resolution hindcast allows to better capture the spatial variability of the wave fields in intermediate to shallow waters, down to depths of 20 (to 15) m. The applied adjustments in physical parameterisations, to improve results in the North-East Atlantic area, have also shown to have a large impact on improving the accuracy of the simulations.

Extensive validation of the ECHOWAVE dataset with altimeter and buoy data showed a reduced and well constrained  $H_s$  and periods' bias ( $T_p$  and mean period  $T_{02}$ ) with high model-measurements correlations of these wave parameters. Logically, improved accuracy of the sea states representation is translated as improved accuracy in the estimation of the wave energy resource. Similar to the analysis performed in section 2.1, a characterization of the wave resource, in terms of the wave power density per meter (pWave), is presented in this section.

The high resolution grid used in this analysis covers (mostly) relative depth conditions considered intermediate waters, this implies that interactions between the wave fields and the local bathymetry are not negligible. For a given wave length (or period), as depth reduces, the celerity of a single wave also reduces, which in the end has an effect on the group celerity that is used in the estimation of the wave energy flux (pWave). Using the dispersion relation from the linear wave theory (Airy, 1845; Dean & Dalrymple, 1991), the wave length ( $L$ ) as a function of the local depth, is given by the following expression:

**Equation 25** 
$$L = \frac{g}{2\pi} T^2 \tanh\left(\frac{2\pi}{L} d\right)$$

where  $d$  is the local depth and  $g$  the acceleration of gravity (9.8 m/s<sup>2</sup>). If the expression of the wave energy flux is given by:

**Equation 26** 
$$F_w = pWave = C_g E_k = C_g \frac{1}{16} \rho_w g H^2$$

with  $E_w$  the wave kinetic energy,  $\rho_w$  the sea water density, here taken as 1026 kg/m<sup>3</sup>, and  $C_g$  the wave group celerity given by Equation 27.

**Equation 27** 
$$C_g = nC = \frac{1}{2} \left(1 + \frac{2kd}{\sinh(2kd)}\right) \frac{L}{T}$$

In the expression above,  $C=L/T$  is the wave celerity and  $k=L/(2\pi)$  the wave number.

Combining Equation 25 to Equation 27 the generalized expression for the wave energy flux (or power density), as a function of depth, can be written as follows:

**Equation 28** 
$$F_w = pWave = \frac{1}{2} \left(1 + \frac{2kd}{\sinh(2kd)}\right) \frac{g}{2\pi} T \tanh\left(\frac{2\pi}{L} d\right) \frac{1}{16} \rho_w g H^2$$

Here,  $T$  is replaced by the energy period  $T_e$  in s and  $H$  by the significant wave height  $H_s$  in m. With the wave energy period here estimated as  $0.9T_p$  (Lavidas & Vengatesan, 2018). Although this is a reasonable estimation of the energy period, it



is important to note that the conversion factor of  $T_p$  will depend on regional characteristics (Guillou, et al., 2020).

## 2.2.1 32-year mean energy flux estimation

A general characterization of the available wave resource along the Atlantic coasts of Europe is given with the 32-years pWave average (Figure 22). Notice that there is a clear difference between the mean kW/m observed along the coasts of Portugal and the Bay of Biscay (Figure 22.a), compared to the western coasts of Ireland or The North Sea (Figure 22.b). The latter area presents, comparatively, the lowest available power density, ranging from 9 to 13 kW/m along the Dutch coast for depths below ~35 m. A significantly larger mean pWave is found within Portuguese waters and the Bay of Biscay. Along Portugal, the mean power density for depths between 100 and 50 m ranges from 40 to 35 kW/m. Similar values are found along the Northern half of the Bay of Biscay. As can be seen in Figure 22.a, these levels typically decrease for depths <50 m (< 30 kW/m). Finally the higher (mean) resource availability is found along the western coasts of Ireland and Scotland, where the total mean pWave can be close to 70 kW/m (for depths between 50 to 100 m).

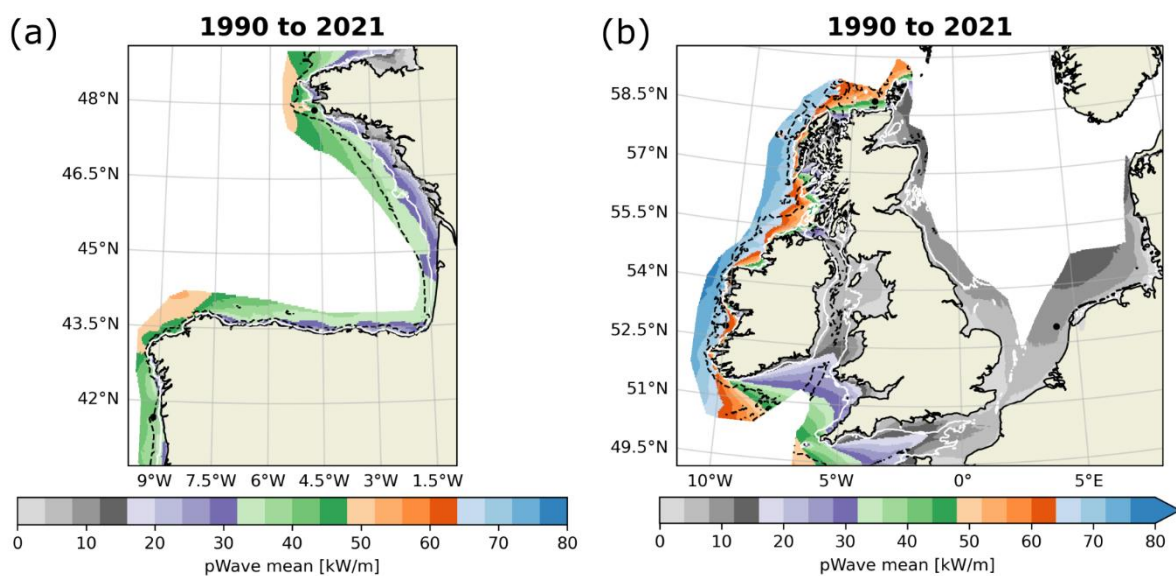


**Figure 22: 32-year pWave average for (a) Portugal and Bay of Biscay, and (b) Ireland, UK and The North Sea.**

*Obs.: Dashed black lines show the 100 m depth contours, continuous white lines the 50 m depth contours. Black circles correspond to the locations presented in Figure 23.*

Similar to the approach taken in section 2.1.1 with Figure 4, the yearly mean values of pWave are presented in Figure 23, providing further details on the estimated inter-year variability of the wave resource, at different locations. As already described in the wave climate characterization (section 2.1), high or low energy years (with respect to the global mean), do not necessarily coincide in all sites.



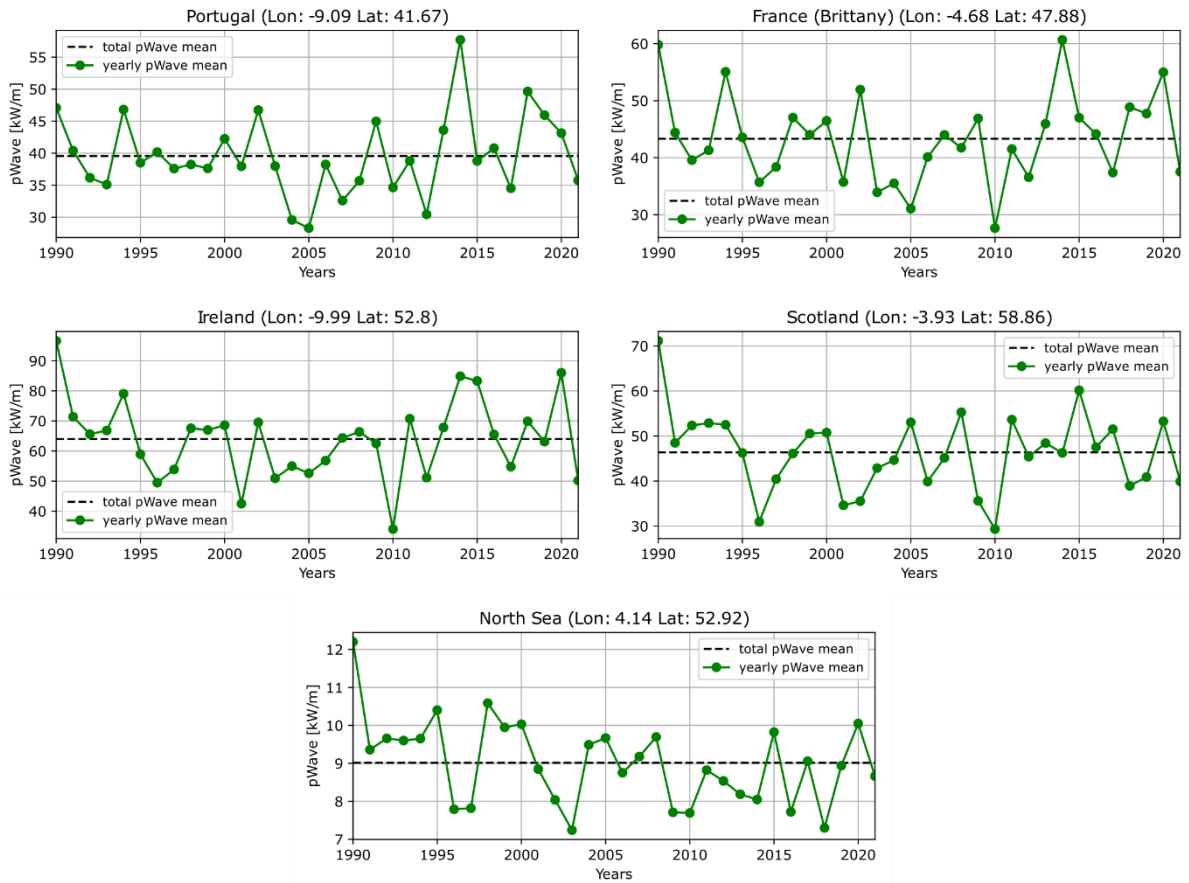


**Figure 23: Yearly mean pWave compared to the 32-year average (1990-2021).**

*Obs.: Analysed locations are indicated in Figure 23 and Figure 4.*

## 2.2.2 32-year mean seasonal energy flux

The mean values of the wave energy flux for each season (DJF, MAM, JJA, and SON), are presented in Figure 24 and Figure 25.

The mean pWave levels, along the coasts of Portugal and Western Brittany, during MAM and SON are similar to those of the overall yearly mean (Figure 24, top and bottom right panels), ranging between 30 to 40 kW/m for depths between 100 and 50 m. There is an important drop of the wave energy flux during summer months (JJA) with values typically <15 kW/m.

On the other hand, a large increase in the resource availability is observed during winter months (DJF). Levels of pWave range between ~70 to ~80 kW/m in Portuguese waters, and even reach ~100 kW/m in Western Brittany (both cases for depths between 100 to 50 m; Figure 24 top left panel).



## 1990 to 2021

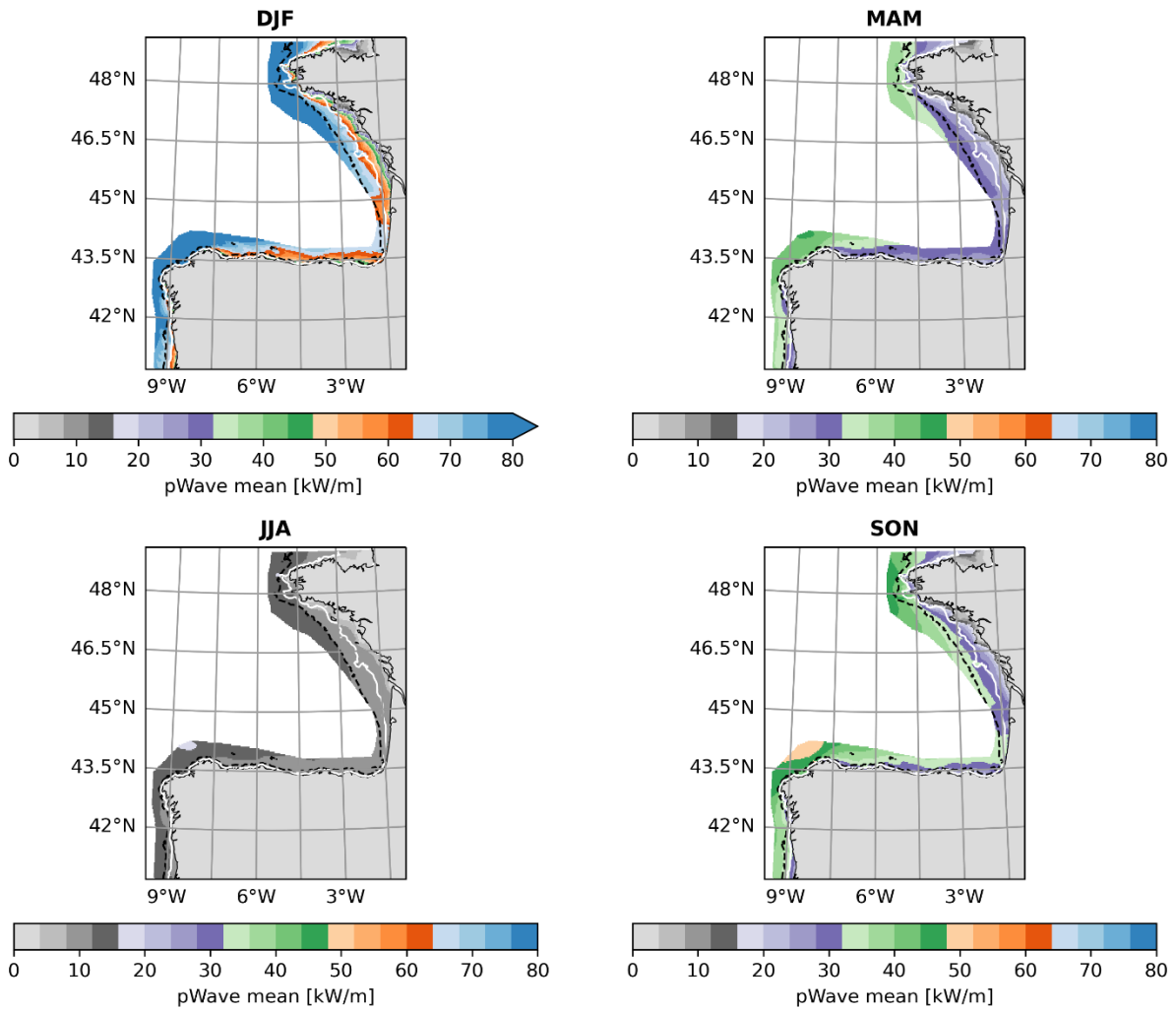


**Figure 24: H<sub>s</sub> 32-years pWave seasonal mean for Portugal and The Bay of Biscay.**

*Obs.: Dashed black lines show the 100 m depth contours, continuous white lines the 50 m depth contours*

Seasonality has similar effects along the North Atlantic coasts of Ireland and Scotland. Here, pWave values >120 kW/m along Ireland and The Hebrides, and ~100 kW/m off the coast of The Orkneys, are found during winter months (Figure 25, top left panel). The mean available resource is slightly higher during SON compared to MAM, ranging from 60 to 70 kW/m along Irish waters up to The Hebrides, and between 50 to 60 kW/m offshore The Orkneys. During summer months (JJA), these values drop to ~20 kW/m for Ireland and The Hebrides and to about ~15 kW/m close to The Orkneys.

Along Dutch waters, during winter months, the available pWave is estimated to range between 10 to 20 kW/m at depths > 25 m. These levels are of the order of 8 to 15 kW/m during MAM and SON, and drop below ~5 kW/m during summer months. The latter values are the lower ones from the analysed locations. For all seasons, the mean values are considerably lower towards Belgian waters.



1990 to 2021

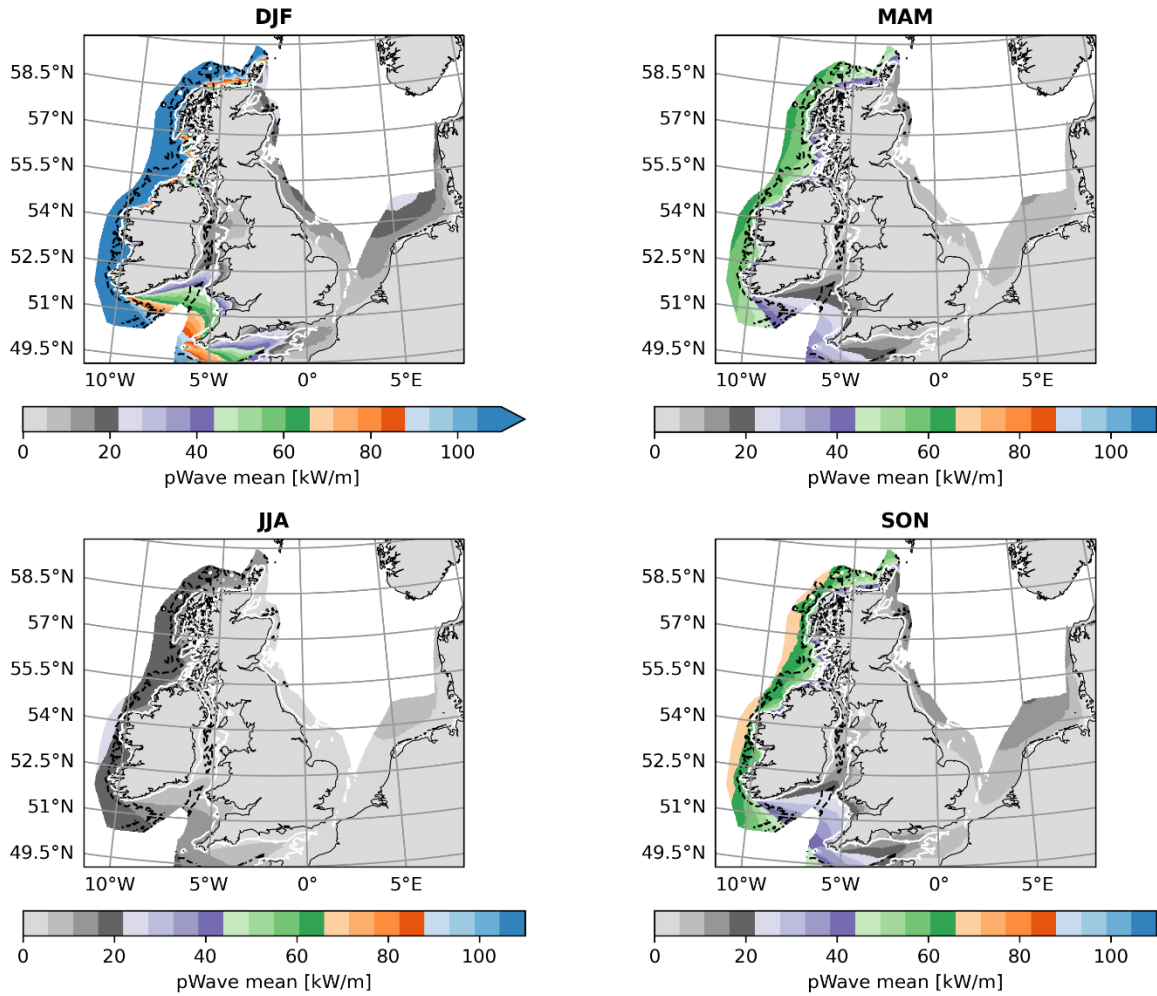


**Figure 25: H. 32-years pWave seasonal mean for Ireland, UK and The North Sea.**

*Obs.: Dashed black lines show the 100 m depth contours, .continuous white lines the 50 m depth contours*

The yearly seasonal means at a few selected locations (Portugal, Brittany, Ireland, Scotland, and The Netherlands) are included in Annex B.



### 3 High-resolution wind resource dataset

In the present document, the resource assessment analysis is carried out using the 31-year high-resolution reanalysis called Copernicus Regional Reanalysis for Europe (CERRA).

The Swedish Meteorological and Hydrological Institute (SMHI), in collaboration with the Norwegian Meteorological Institute (MET Norway) and Meteo-France, has developed a new reanalysis system for Europe called CERRA. This modernized system covers the period from the early 1980s to near real-time. It uses the Harmonie NWP system with ALADIN physics, Operational Interpolation (OI), and 3D-VAR for surface and upper-air analysis. CERRA provides a high-resolution pan-European reanalysis with a 5.5 km horizontal resolution and 106 vertical levels, covering Europe, Northern Africa, and Southeastern parts of Greenland.

The system is forced by the global ERA5 reanalysis and has an Ensemble Data Assimilation (EDA) system coupled with the deterministic CERRA system to regularly update the flow-dependent information in the background error covariance matrix (B-Matrix) used in the 3D-VAR deterministic system. The NWP system has a 3-hourly cycling interval and produces 30 h forecasts at 00 and 12z assimilation times, while six h forecasts are generated at the 03, 06, 09, 15, 18, and 21z assimilation times. On the other hand, the EDA system comprises ten ensemble members with an 11 km horizontal resolution and a 6-hour cycling interval. Unlike the ERA5 data, the CERRA provide analysis at every three hours. The CERRA dataset has been continuously updated and is available in the Copernicus Climate Data Store.

For the wind resource assessment, the CERRA 3-hourly wind speed data at 100 m level is used. For reference, Figure 26 illustrates the annual mean wind speed at 100 m level, averaged over 31 years from 1990 to 2020. The figure clearly illustrates the diversity in wind speed magnitude, ranging from 4 m/s to 12 m/s. Within this figure, the regions of interest are represented by red dashed rectangles, over the Iberia coast, Ireland coast, and BeNeLux (Belgium, Netherlands, and Luxemburg) coasts.



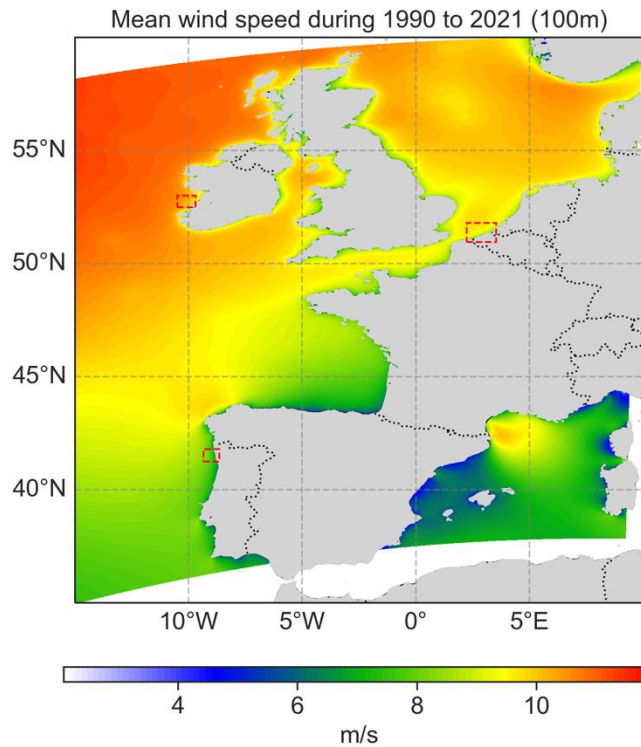


**Figure 26:** Spatial illustration of 100 m wind speed from CERRA reanalysis, averaged over 31 years, during 1990 to 2021. The red dashed boxes represent regions of interest for further analysis, at Iberia, Ireland, and BeNeLux (combination of Belgium, Netherlands, and Luxemburg countries) locations.

## 4 Wind resource assessment

### 4.1 Wind climate characteristics

The present section aims to provide climate characteristics of wind resources across three regions: Iberia, Ireland, and BeNeLux.

Unlike any other meteorological variable, wind speed merely follows a Gaussian distribution and has long tails. In cases with skewed data, the application of the Weibull distribution is more suitable, which is characterized by its slope and scale parameters, as shown in Equation 29.

**Equation 29**

$$f(v) = \frac{k}{c} \left(\frac{v}{c}\right)^{k-1} \exp\left[-\left(\frac{v}{c}\right)^k\right]$$

Here,  $k$  is the slope (shape) parameter, and  $c$  is the scale parameter. A slope parameter higher than 1 indicates a bell-shaped distribution, equal to 1 implies the exponential distribution and less than 1 indicates an exponent distribution. The scale parameter resonates with the expectation of wind speed (mean), while the slope parameter directly implies the variability in wind speed, such that a low slope parameter indicates higher variability and vice versa.

#### 4.1.1 Overall-interannual wind characteristics for 31 years

The statistical analysis of wind data plays a crucial role in wind energy resource assessment. In this context, the Weibull scale characteristics are computed over a period of 31 years (1990-2020) and every year, as shown in Figure 27 for the Iberia region, Figure 28 for the Ireland region, and Figure 29 for the BeNeLux region. The Weibull scale parameter is a statistical tool that characterizes the expectation of the wind speed probability distribution function. The left panel of each figure illustrates the overall Weibull scale parameter, while the right panel illustrates the Weibull scale parameter computed by grouping wind speed every year.

From the overall statistics, it is evident that the wind speed ranges between 7 m/s to 9.5 m/s for the Iberia region, 9.5 m/s to 12 m/s for the Ireland region, and 9.3 m/s to 11 m/s for the BeNeLux region. Among these three, the Iberia region exhibits a difference of 2 m/s in the scale parameter when moving from near shore to far shore, indicating that the spatial disparity is considerable in this region. On the other hand, the remaining regions exhibit a difference of 1 m/s when moving from near shore to far shore, indicating a marginal spatial disparity.

To quantitatively assess the spatial disparity, three random points P1, P2, and P3 are chosen from each region, and their overall statistics are presented as dashed lines in the right panel. The overall scale parameter values at P1, P2, and P3, are: 8.3 m/s, 9 m/s, and 9.2 m/s, respectively for Iberia; 11.8 m/s, 11.5 m/s, and 11.8 m/s, respectively for Ireland; and 10.75 m/s, 10.95 m/s, and 10.7 m/s, respectively for the BeNeLux regions. These values further strengthen the fact that the Iberia region has considerable spatial disparity, while the remaining two regions exhibit more or less homogeneity in spatial wind speed distribution.

From the yearly time-series plots, the scale parameter exhibits significant variability across different years. Interestingly, the variability trend is similar in the Ireland and BeNeLux regions, while vastly differed in the Iberia region. In the Iberia region, the parameter is seen to be lowest at 7.5 m/s during 2004 and 2012, while the highest value of 10.5 m/s is seen during 2013. On the contrary, the parameter is seen lowest during 2010, reaching 10 m/s over Ireland and 9.5 m/s over the BeNeLux. Across these two regions, the parameter is commonly highest during 1990, 2015, and 2020 years, while several years differently exhibit a maximum in both regions. This suggests that the large-scale climate teleconnections responsible for the wind maxima in the Ireland region are also responsible for the BeNeLux region, but the same cannot be inferred for the Iberia region.

Throughout the years, the scale parameter values consistently differ by 1 m/s among the three points in the Iberia region, while the difference is marginal at the remaining two regions. These observations provide valuable insights into the spatial and temporal variability of the Weibull scale parameter across different regions, which can aid in the design and implementation of wind energy systems.



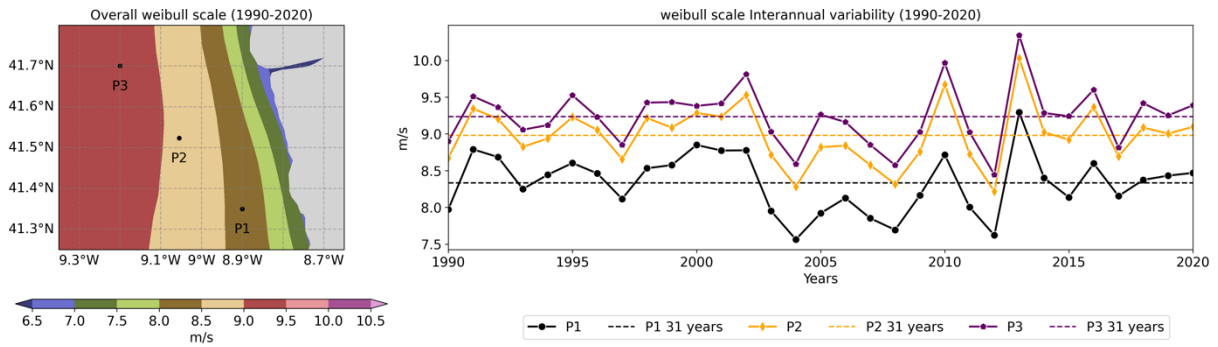


**Figure 27:** Left panel: Surface plots of Weibull scale parameter of 100 m wind speed, estimated during the whole analysis period (1990-2020), over the Iberia region. Right panel: Time-series of 100 m wind Weibull scale parameter computed during each year, at points P1, P2, and P3, shown in the left panel. Horizontal dashed lines represent the overall statistics at the respective points.

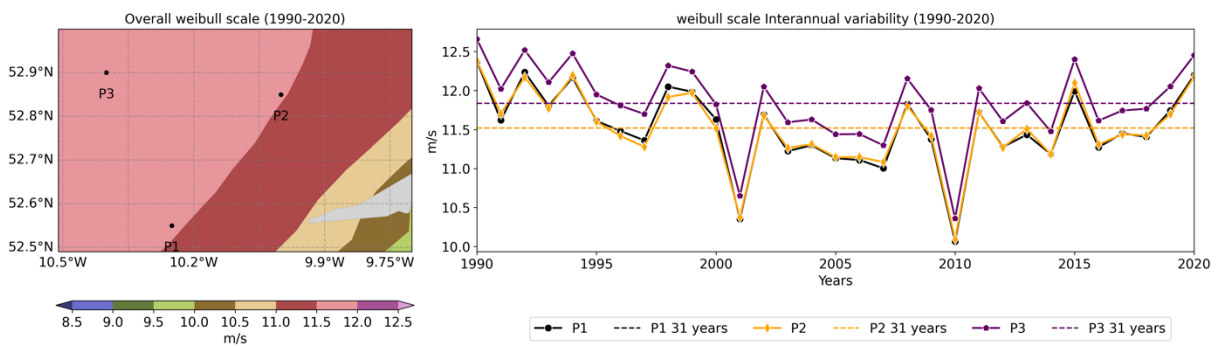


**Figure 28:** Same as Figure 27, but for the Ireland region.

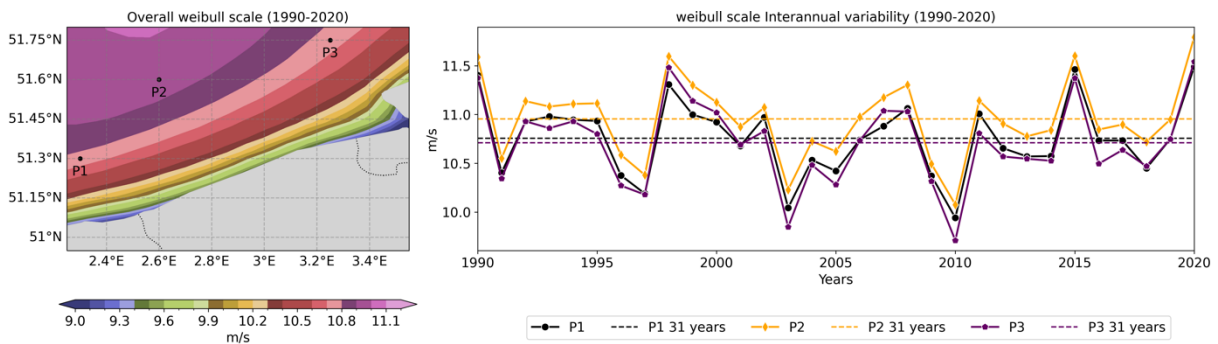


**Figure 29:** Same as Figure 27, but for the BeNeLux region.

The Weibull shape characteristics are computed over a period of 30 years (1990-2020) and every year, as shown in Figure 30 for the Iberia region, Figure 31 for the Ireland region, and Figure 32 for the BeNeLux region. The Weibull scale parameter is a statistical tool that characterizes the slope of the wind speed probability distribution function, which is inherently related to the variability within the data. The left panel of each figure illustrates the overall Weibull shape parameter, while the right panel illustrates the Weibull slope parameter computed by grouping wind speed every year.

From the overall statistics, it is evident that the Weibull shape ranges between 1.7 to 2 for the Iberia region, 2.1 to 2.3 for the Ireland region, and 2.1 to 2.3 for the



BeNeLux region. In the Iberia and Ireland coasts, the shape parameter also increases with proximity to the coast, similar to that of the scale parameter, which is interesting since the higher shape parameter indicates lesser variability, and more consistency. On the other hand, in the BeNeLux region, a small section of coast parallel shape parameter minima is observed, which is unusual. Among these three regions, Iberia exhibits a wider range of values, indicating a spatial disparity at here.

The overall scale parameter values at P1, P2, and P3, are: 1.84, 1.92, and 1.94, respectively for Iberia; 2.18, 2.2, and 2.2, respectively for Ireland; 2.16, 2.19, and 2.16, respectively for the BeNeLux regions. These values further strengthen the fact that the Iberia region has considerable spatial disparity, while the remaining two regions exhibit more or less homogeneity in spatial distribution.

From the yearly time-series plots, the shape parameter exhibits significant variability across different years, as well as different regions, unlike that of the scale parameter seen earlier. In the Iberia region, the parameter is seen to be lowest at 1.75 during 2011, while the highest value of 2.07 is seen during 2013. In the Ireland region, the parameter is seen to be lowest at 1.95 during 2007, while a highest value of 2.45 during 2012. On the contrary, in the BeNeLux region, the parameter is seen lowest of 1.95 during 1991, and a highest value of 2.32 during 2017.

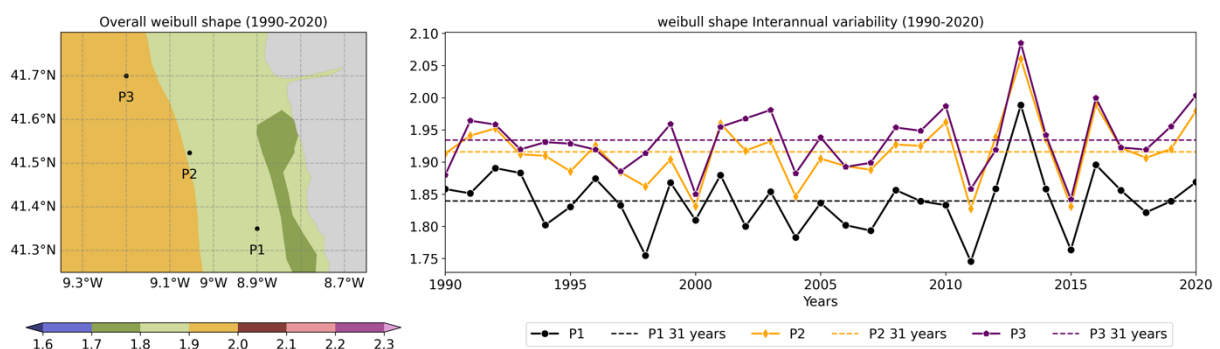


**Figure 30:** Left panel: Surface plots of Weibull shape parameter of 100 m wind speed, estimated during the whole analysis period (1990-2020), over the Iberia region. Right panel: Time-series of 100 m wind Weibull shape parameter computed during each year, at points P1, P2, and P3, shown in the left panel. Horizontal dashed lines represent the overall statistics at the respective points.

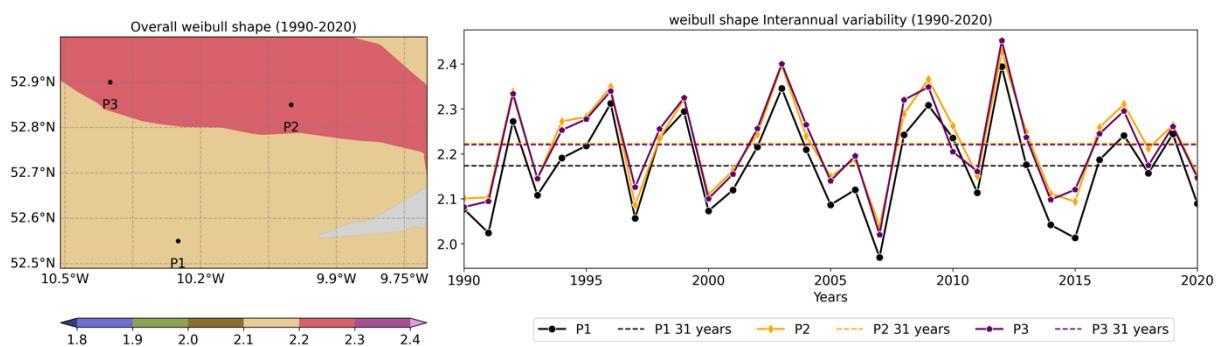


**Figure 31:** Same as Figure 30, but for the Ireland region.



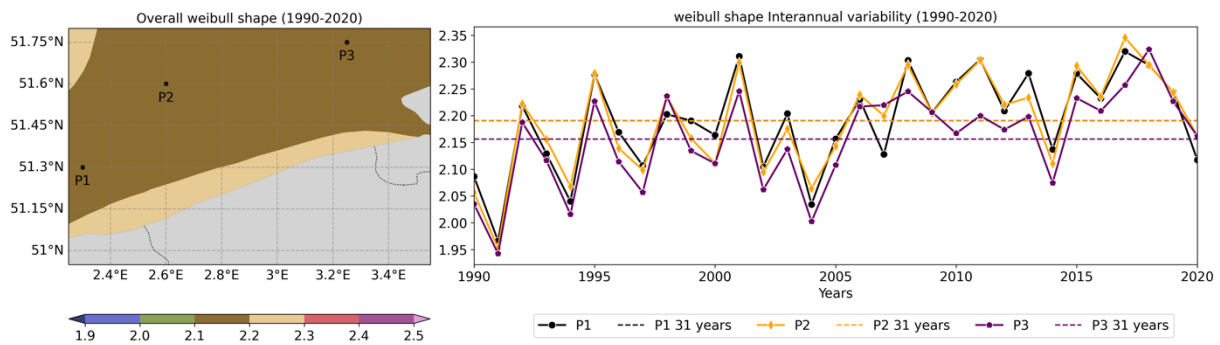


**Figure 32:** Same as Figure 30, but for the BeNeLux region.

## 4.1.2 Annual-seasonal wind characteristics

The Weibull scale statistics are computed across each month by grouping the wind speed during the respective month, extracted at the three points, and are presented in Figure 33 for the Iberia region, Figure 34 for the Ireland region, and Figure 35 for the BeNeLux region. Among the three regions, Iberia exhibits an entirely different annual variability across the months, such as a resource maximum seen during July and a subsequent minimum during September. This behavior is indeed attributed to the occurrence of Iberian Peninsula Coastal low-level Jets (IPCJ), a well-known coastal effect, during July. At this region, the scale parameter is seen highest during July (ranging between 8.9 m/s to 9.8 m/s among the three points) and least during September (ranging between 7.2 m/s to 8.2 m/s among the three points). Another interesting characteristic is that the scale parameter consistently differs by 1 m/s among the three points, indicating the significant spatial disparity.

On the contrary, the Ireland and BeNeLux regions exhibit a generic cyclic annual variability. In the Ireland region, the parameter is seen highest during January (ranging between 14 m/s to 14.5 m/s), gradually decreasing to the minimum during July (~9.5 m/s), and then increasing. A similar annual variability is observed in the BeNeLux region as well. The parameter is seen highest during January (ranging between 12.8 m/s to 13.2 m/s), gradually decreasing to the minimum during August (ranging between 8.9 m/s to 9.1 m/s), and then increasing.

Grouping the scale statistics seasonally as Winter (Dec, Jan, Feb), Spring (Mar, Apr, May), Summer (Jun, Jul, Aug), and Autumn (Sep, Oct, Nov) gives more insights regarding seasonal variability. In all regions, the scale parameter is seen highest during winter, which is mainly attributed to the European Windstorms, which are powerful extratropical cyclones associated with areas of low atmospheric pressure. They can occur throughout the year but are most frequent between October and March, with peak intensity in the winter months. On the contrary, the scale parameter is observed to be minimum during summer in the Ireland and BeNeLux regions, which has been the climatology over the North Sea. However, the Iberia region stands out as the outlier to have a maximum scale parameter during summer, which is again attributed to the occurrence of IPCJ.

One penciller observations is that the Ireland and BeNeLux regions have significantly higher scale parameters than overall mean during winter months, which is great for wind power production. However, the scale parameter drops much less than the overall mean during summer. Understanding such an annual variability is of paramount importance in designing wind farms. On the contrary, the Iberia region shows a consistent scale parameter throughout the months, except for the July and September, indicating the suitability for wind power production.

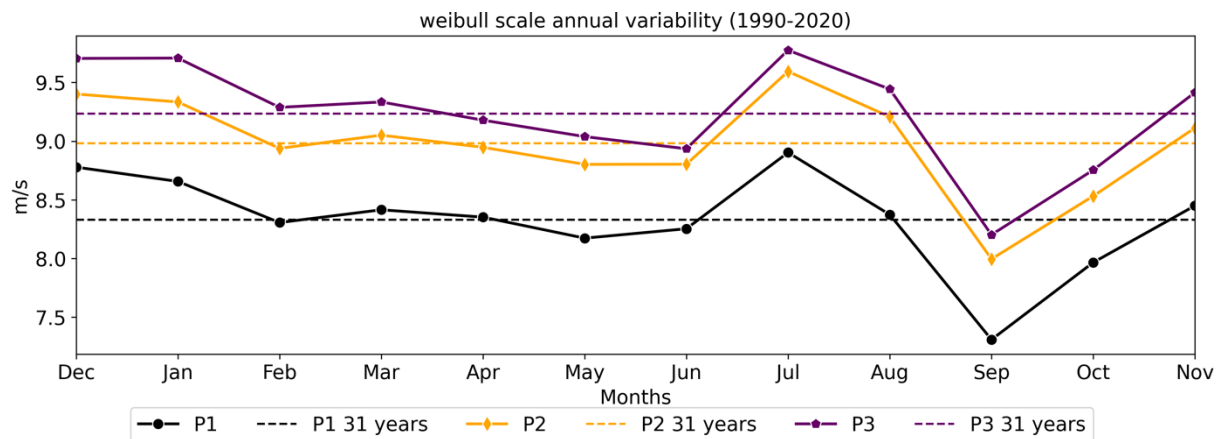


**Figure 33: Time-series of 100 m wind Weibull scale parameter computed during each month, at points P1, P2, and P3, over the Iberia region. Horizontal dashed lines represent the overall statistics at the respective points.**

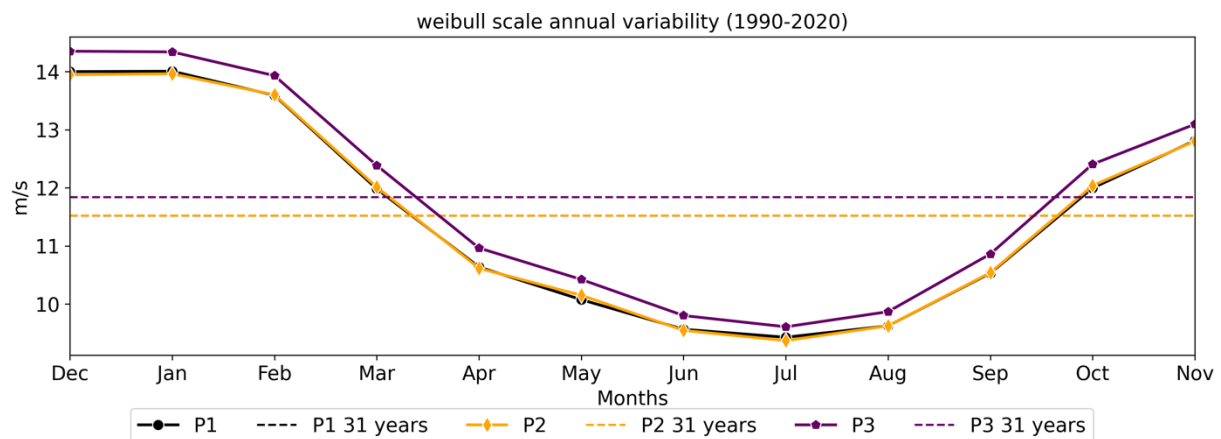


**Figure 34: Same as Figure 33, but for the Ireland region.**





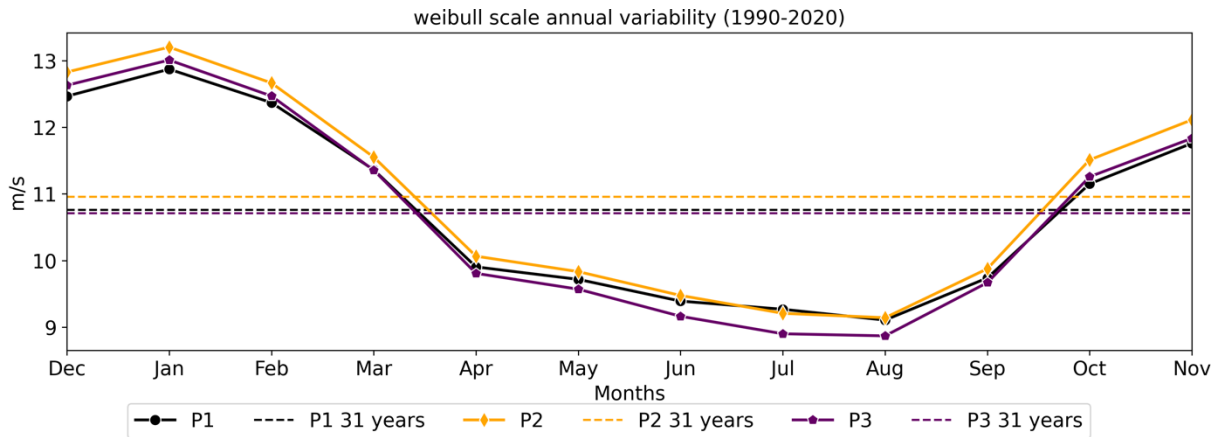


**Figure 35: Same as Figure 33, but for the Ireland region.**

### 4.1.3 Wind extremes analysis

The extreme wind analysis is aimed to characterize the highest wind speeds possible, that can potentially endanger the wind farms in the three regions. In this analysis, the 99<sup>th</sup> percentile (p99) is employed to identify the extreme event that occur 1% of the time. The wind p99 characteristics are computed over a period of 31 years (1990-2020) and every year, as shown in Figure 36 for the Iberia region, Figure 37 for the Ireland region, and Figure 38 for the BeNeLux region. The left panel of each figure illustrates the overall p99, while the right panel illustrates the statistic computed by grouping wind speed every year.

From the overall statistics, it is evident that the extreme wind speed ranges between 16 m/s to 20 m/s for the Iberia region, 21 m/s to 24 m/s for the Ireland region, and 19 m/s to 22 m/s for the BeNeLux region. Among these three, the Ireland region experiences severely extreme winds, BeNeLux experiences moderate extreme winds, while the Iberia region experiences least extreme winds. In all the three regions, the extremity of winds increases with the proximity to the coast.

The 99<sup>th</sup> percentile wind speed values at P1, P2, and P3, are: 18.2 m/s, 18.8 m/s, and 18.9 m/s, respectively for Iberia; 23.4 m/s, 23 m/s, and 23.45 m/s, respectively for Ireland; and 21.8 m/s, 21.85 m/s, and 21.7 m/s, respectively for the BeNeLux regions. These values further strengthen the fact that the Iberia region has considerable spatial disparity, while the remaining two regions exhibit more or less homogeneity in spatial p99 wind speed distribution.

From the yearly time-series plots, the p99 exhibits significant variability across different years. Interestingly, the variability trend is similar in the Ireland and BeNeLux regions, while vastly differed in the Iberia region, which has been observed in the scale parameter interannual variability as well. In the Iberia region, the highest possible wind speeds are observed during 2000 and 2001, with an intensity of 20 m/s, while the 2012 saw least p99 winds at an intensity of 16.6 m/s. Surprisingly, the peak p99 years are not the peak scale parameter year (2013), implying the possibility of an anomalous period of 2000-01.



In the Ireland region, the highest possible winds are observed during 1990, with an intensity of 26 m/s. During the same year, the BeNeLux region also experienced highest winds or 24.5 m/s. In addition, both the regions experienced lowest extreme winds during 2001 and 2010, which are also the lowest years for the scale parameter seen before. Apart from these, during several other years as well the wind extreme does match at these two regions, signifying the influence of large-scale climate teleconnections. Nonetheless, throughout the years, the wind extremes consistently differ by 1 m/s among the three points in the Iberia region, while the difference is marginal at the remaining two regions.

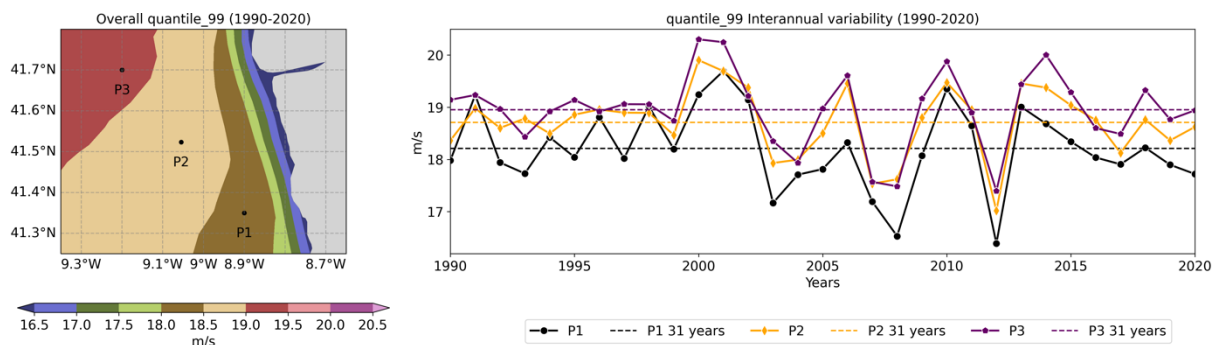


**Figure 36:** Left panel: Surface plots of 99p of 100 m wind speed, estimated during the whole analysis period (1990-2020), over the Iberia region. Right panel: Time-series of 99p of 100 m wind speed computed during each year, at points P1, P2, and P3, shown in the left panel. Horizontal dashed lines represent the overall statistics at the respective points.

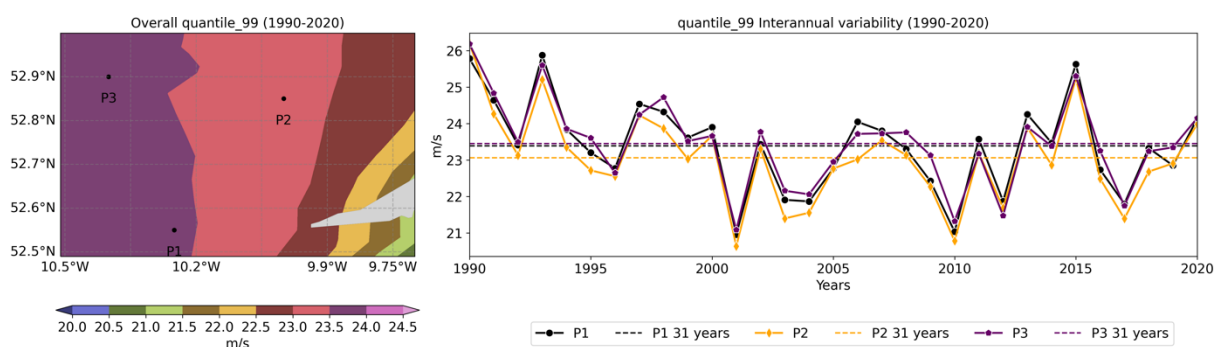


**Figure 37:** Same as Figure 36, but for the Ireland region.

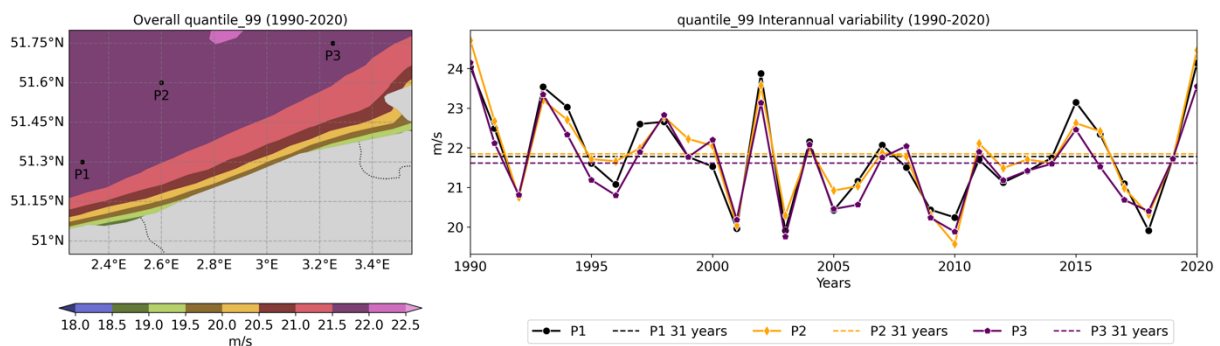


**Figure 38:** Same as Figure 36, but for the BeNeLux region.



## 4.2 Wind power density climate characteristics

In this section, the characteristics of wind power flux or wind power density (WPD), estimated using Equation 30, for 31 years are analysed across the three regions. Since the turbine hub-height wind speed is crucial in wind farm design and planning, the 100 m wind speed is used in estimating the WPD.

**Equation 30** 
$$\text{wind power density (WPD)} = \frac{1}{2}\rho(\text{wind speed})^3$$

The wind power density climate characteristics, in terms of mean, over the Iberia region are presented in this section. The mean statistics are computed across overall, yearly, and monthly time scales.

### 4.2.1 Overall-interannual climate characteristics for 31 years

the WPD mean characteristics are computed over a period of 31 years (1990-2020) and every year, as shown in Figure 39 for the Iberia region, Figure 40 for the Ireland region, and Figure 41 for the BeNeLux region. The left panel of each figure illustrates the overall mean WPD, while the right panel illustrates the mean computed by grouping wind power density every year. From the overall statistics, it is evident that the WPD ranges between 320 W/m<sup>2</sup> to 680 W/m<sup>2</sup> for the Iberia region, 760 W/m<sup>2</sup> to 1310 W/m<sup>2</sup> for the Ireland region, and 640 W/m<sup>2</sup> to 1000 W/m<sup>2</sup> for the BeNeLux region. The absolute increments in the WPD when moving away from the coast are 320 W/m<sup>2</sup>, 550 W/m<sup>2</sup>, and 360 W/m<sup>2</sup> in the Iberia, Ireland, and BeNeLux regions, respectively. If one considers the absolute increments, the Ireland region seems to have the highest spatial disparity. However, the percentage increment is significantly higher in the Iberia region (112%). This analysis strengthens the previous analogy of spatial disparity being higher in the Iberia region, than the remaining two.

To quantitatively assess the spatial disparity, the overall statistics are computed at the three points, which are presented as dashed lines in the right panel. The overall scale parameter values at P1, P2, and P3, are: 510 W/m<sup>2</sup>, 610 W/m<sup>2</sup>, and 660 W/m<sup>2</sup>, respectively for Iberia; 1800, 1600, and 1100, respectively for Ireland; and 940 W/m<sup>2</sup>, 990 W/m<sup>2</sup>, and 940 W/m<sup>2</sup>, respectively for the BeNeLux regions. These values further strengthen the fact that the Iberia region has considerable spatial disparity, while the remaining two regions exhibit more or less homogeneity in spatial WPD distribution.

From the yearly time-series plots, the mean WPD exhibits significant variability across different years. Similar to the wind speed statistics, the variability trend is similar in the Ireland and BeNeLux regions, while vastly differed in the Iberia region. In the Iberia region, the parameter is seen to be lowest at 400 W/m<sup>2</sup> during 2004, 2008, and 2012, while a WPD of 800 W/m<sup>2</sup> is seen during 2010 and 2012. On the contrary, the 2010 is found to be the lowest year for Ireland and BeNeLux regions, with an intensity of 800 W/m<sup>2</sup> and 700 W/m<sup>2</sup>, in the respective regions, while the 1990 is found to be the highest year, with an intensity of 1500 W/m<sup>2</sup> and 1200 W/m<sup>2</sup>, in the respective regions.



Throughout the years, the mean WPD values consistently differ by  $\sim 150 \text{ W/m}^2$  among the three points in the Iberia region. On the other hand, the remaining two regions also experience a difference of  $\sim 100 \text{ W/m}^2$  among the three points, but the percentage difference is still higher at the Iberia region. This is because WPD depends on cube of wind speed, and since the Ireland and BeNeLux regions experience greater winds than Iberia, the absolute difference in the WPD becomes similar. Nonetheless, these observations provide valuable insights into the spatial and temporal variability of the Weibull scale parameter across different regions, which can aid in the design and implementation of wind energy systems.

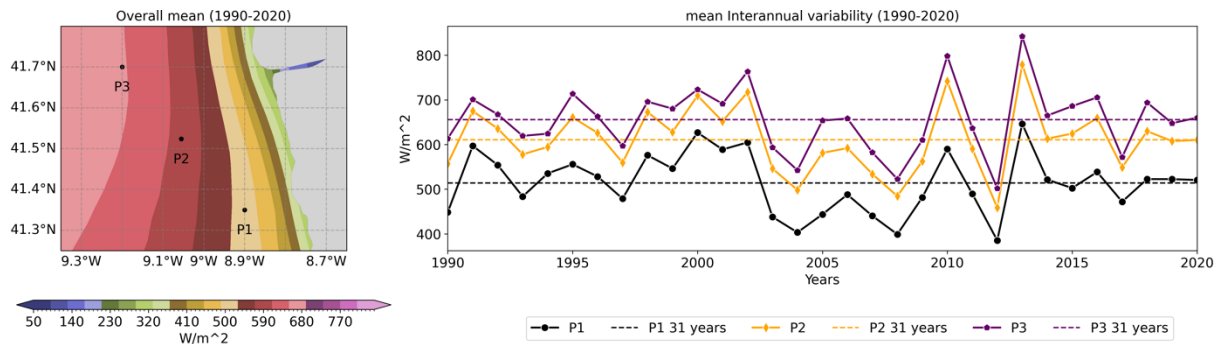


**Figure 39:** Left panel: Surface plots of mean 100 m wind power density, estimated during the whole analysis period (1990-2020), over the Iberia region. Right panel: Time-series of mean 100 m wind power density computed during each year, at points P1, P2, and P3, shown in the left panel. Horizontal dashed lines represent the overall statistics at the respective points.

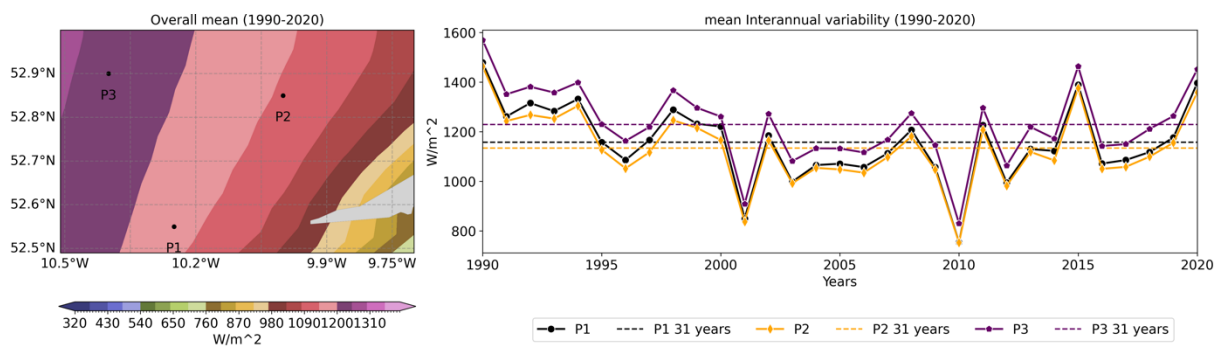


**Figure 40:** Same as Figure 39, but for the Ireland region.

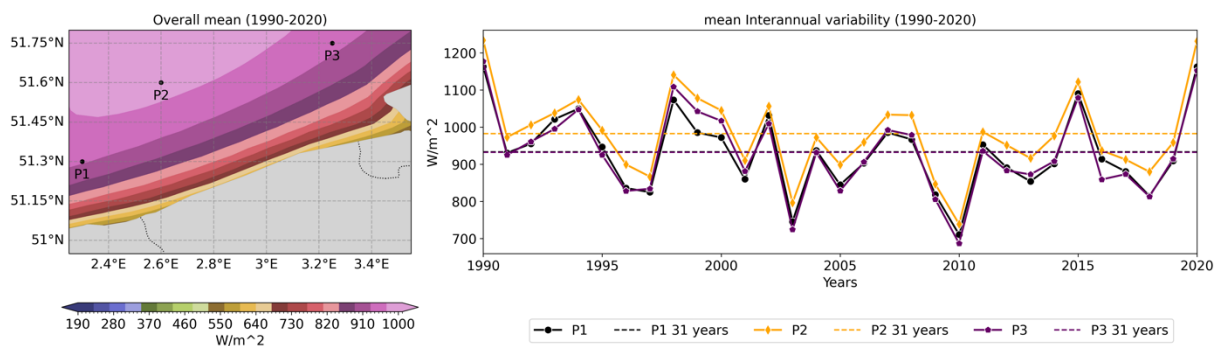


**Figure 41:** Same as Figure 39, but for the Ireland region.



## 4.2.2 Annual-seasonal wind characteristics

To calculate the average WPD, the WPD data is collected from three different points, and then the data for each month is grouped together. The resulting data is presented in Figure 42 for the Iberia region, Figure 43 for the Ireland region, and Figure 44 for the BeNeLux region. Since WPD is a measure derived from wind speed, it follows a similar annual fluctuation pattern as seen in the wind scale parameter. The data in the figures confirms this pattern of annual fluctuation.

However, different regions exhibit unique patterns of fluctuation throughout the year. For instance, Iberia shows a distinct pattern of fluctuation throughout the year, with a peak resource in July followed by a low in September. This pattern is linked to the IPCJ phenomenon. Specifically, in Iberia, July sees the highest WPD values (between 650 W/m<sup>2</sup> and 750 W/m<sup>2</sup> across the three points), and September is the lowest (between 370 W/m<sup>2</sup> and 470 W/m<sup>2</sup>). This marked difference at each point highlights significant spatial variation.

Conversely, both Ireland and BeNeLux display a recurring pattern of fluctuation throughout the year. In Ireland, the average WPD peaks in January (between 1880 W/m<sup>2</sup> and 2040 W/m<sup>2</sup>), gradually decreases to its lowest in July (between 640 W/m<sup>2</sup> and 700 W/m<sup>2</sup>), and then rises again. BeNeLux follows a similar pattern, with the highest mean WPD in January (between 1500 W/m<sup>2</sup> and 1600 W/m<sup>2</sup>), decreasing to its lowest in July (~550 W/m<sup>2</sup>) before rising.

When analyzing the data seasonally as Winter (Dec, Jan, Feb), Spring (Mar, Apr, May), Summer (Jun, Jul, Aug), and Autumn (Sep, Oct, Nov), further insights into seasonal variability emerge. Across all regions, the highest mean WPD occurs in winter, primarily due to European Windstorms, while the lowest mean WPD is observed in summer in the Ireland and BeNeLux regions, consistent with the climatology over the North Sea. However, Iberia deviates from this pattern with a secondary peak in summer, which is attributed to the IPCJ phenomenon.

It is notable that during the winter months, the mean WPD in both Ireland and BeNeLux is significantly above the overall mean, benefiting wind power generation. Yet, the decline in mean WPD during summer is more pronounced than the overall average. This pattern of annual fluctuation is crucial for the planning and design of wind farms. In contrast, the Iberia region exhibits a relatively stable mean WPD throughout the year, with the exception of July and September, indicating its potential for consistent wind power generation.



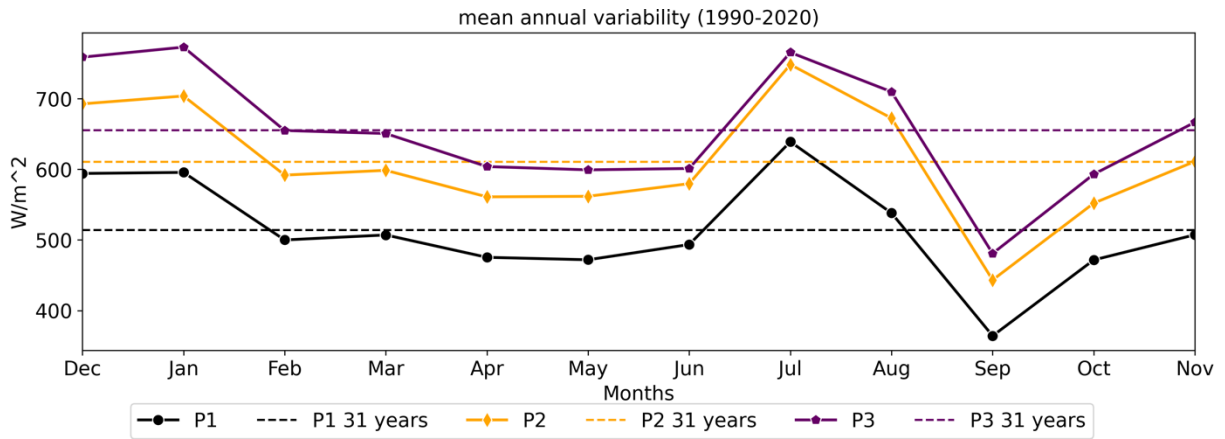


**Figure 42: Time-series of 100 m wind power density computed during each month, at points P1, P2, and P3, over the Iberia region. Horizontal dashed lines represent the overall statistics at the respective points.**

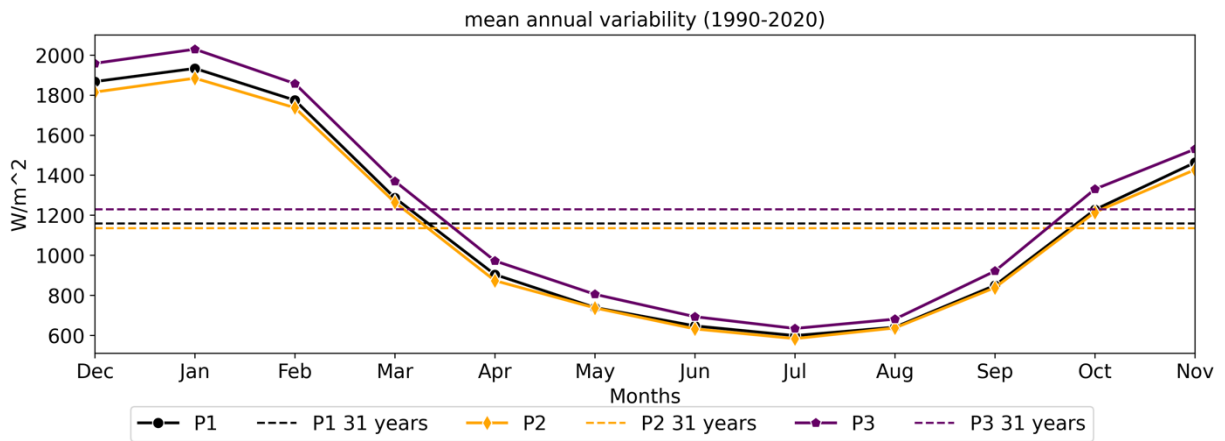


**Figure 43: Same as Figure 42, but for the Ireland region.**

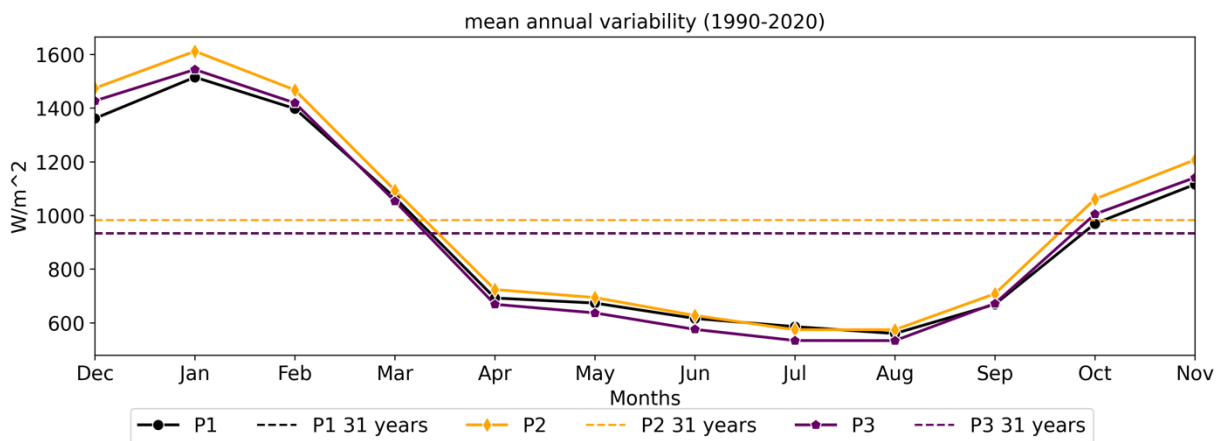


**Figure 44: Same as Figure 42, but for the BeNeLux region.**



## 5 High-resolution solar resource dataset

For the solar resource assessment as well, the CERRA 3-hourly data is adopted. It is well known that the surface air temperature and the shortwave solar radiation flux at the surface are the main contributors to solar energy. However, the surface air wind speed is also known to play a major role in enhancing the solar panel output. Thus, in this report, the meteorological variables, namely 10 m wind speed, 2m air temperature (t2m), and downward shortwave radiation flux at the surface (SWDOWN) are extracted from the CERRA reanalysis data. For reference, Figure 45 illustrates the annual mean wind speed at 10 m level, averaged over 31 years during 1990 to 2020. The figure clearly illustrates the diversity in wind speed magnitude, ranging from 2 m/s to 10 m/s. Within this figure, the regions of interest are represented by red dashed rectangles over the Iberia coast, Ireland coast, and BeNeLux (Belgium, Netherlands, and Luxemburg) coasts. Over these locations, the wind speeds are around 6 m/s, 10 m/s, and 8 m/s, respectively.

Similarly, Figure 46 illustrates the annual mean surface air temperature, averaged over 31 years from 1990 to 2020. The temperature decreases with latitude, which is expected due to the Earth's curvature. However, a peculiar observation is that the temperatures at Ireland and Netherlands coasts are relatively warmer compared to the areas on the same latitude, which is attributed to the Gulf Stream. Over the interested regions, the mean temperatures are seen to be around 15 °C (Iberia) and 10 °C (Ireland and BeNeLux).

Figure 47 illustrates the annual mean downward shortwave radiation flux at the surface, averaged over 31 years from 1990 to 2020. Over the interested regions, the mean radiation is seen to be around 15 W/m<sup>2</sup> (Iberia), 125 W/m<sup>2</sup> Ireland, and 100 W/m<sup>2</sup> (BeNeLux).

Further analysis is strictly restricted to the three interested regions, namely, Iberia, Ireland, and BeNeLux, which are presented in the following sections.



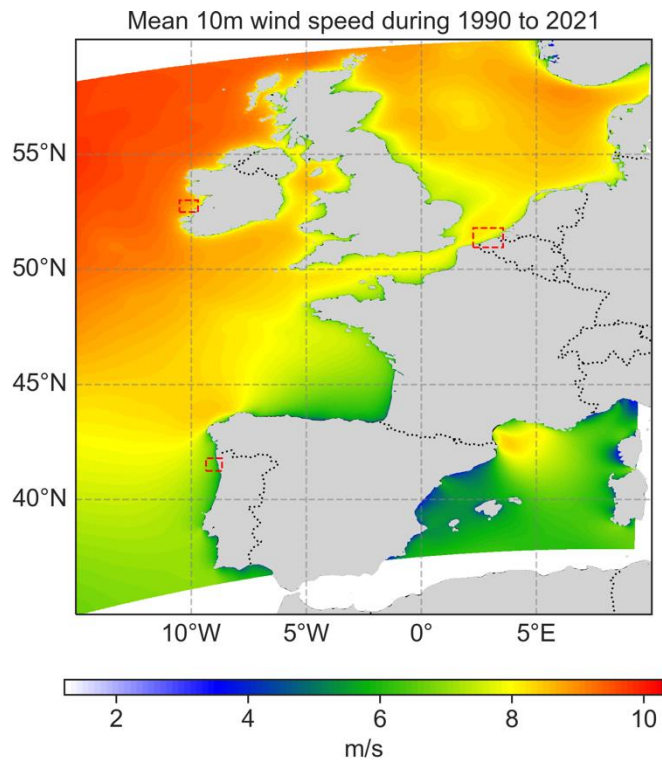


**Figure 45: Spatial illustration of 10 m wind speed from CERRA reanalysis, averaged over 31 years, during 1990 to 2021. The red dashed boxes represent regions of interest for further analysis, at Iberia, Ireland, and BeNeLux (combination of Belgium, Netherlands, and Luxemburg countries) locations.**

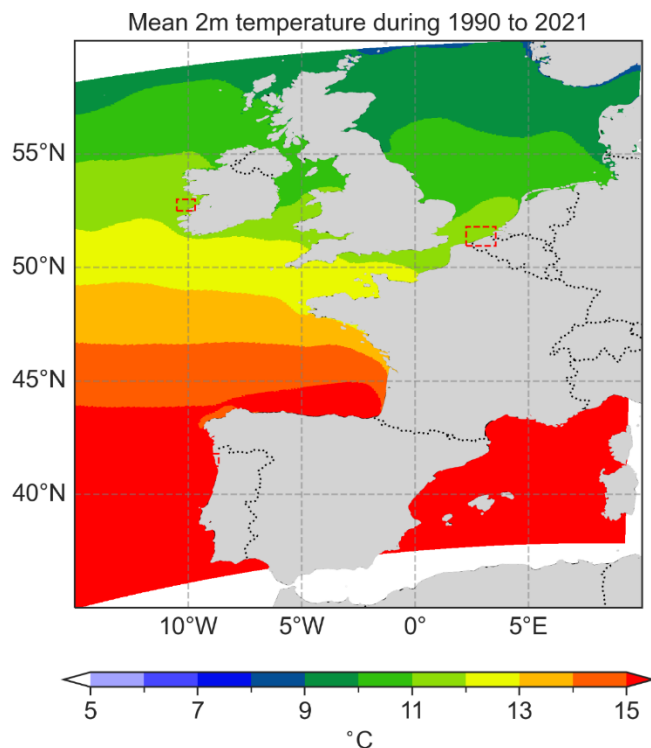


**Figure 46: Spatial illustration of 2 m air temperature from CERRA reanalysis, averaged over 31 years, during 1990 to 2021. The red dashed boxes represent regions of interest for further**





analysis, at Iberia, Ireland, and BeNeLux (combination of Belgium, Netherlands, and Luxemburg countries) locations.

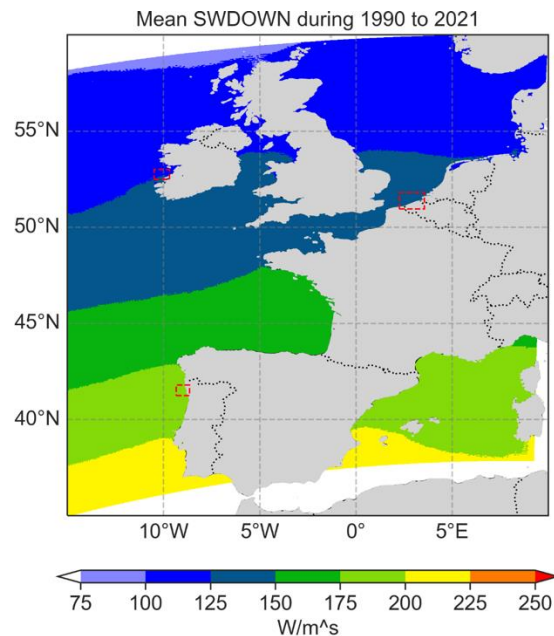


**Figure 47: Spatial illustration of downward shortwave radiation flux at the surface from CERRA reanalysis, averaged over 31 years, during 1990 to 2021. The red dashed boxes represent regions of interest for further analysis, at Iberia, Ireland, and BeNeLux (combination of Belgium, Netherlands, and Luxemburg countries) locations.**

## 6 Solar resource assessment

### 6.1 Surface air temperature climate characteristics

This section reports the climate characteristics of surface air temperature. The mean statistics are computed across overall, yearly, and monthly time scales. Since the temperature is measured in °C, which is an interval scale, computing the coefficient of variation does not have any physical sense. On the other hand, the extremity in surface air temperature is of paramount importance since high temperatures significantly reduce solar PV efficiency. Thus, the 99<sup>th</sup> percentile is used in extreme event analysis. The p99 is computed on overall and yearly time scales.

#### 6.1.1 Overall-interannual characteristics for 31 years

the t2m mean characteristics are computed over a period of 31 years (1990-2020) and every year, as shown in Figure 48 for the Iberia region, Figure 49 for the Ireland region, and Figure 50 for the BeNeLux region. The left panel of each figure illustrates the overall mean WPD, while the right panel illustrates the mean computed by grouping wind power density every year at three points (P1, P2, and P3).

In Iberia, the overall mean t2m ranges between 15°C near the shore and 15.8°C far offshore. The t2m shows a monotonically increasing trend with distance from the

coast. The yearly time-series plot exhibits significant variability, with the lowest value of 14.7°C observed during 1991 and the highest value of 16.25°C during 1997. The mean temperature values at the three points consistently differ by 0.25°C throughout the years, suggesting marginal spatial disparity.

Similarly, in Ireland, the left panel indicates an overall mean t2m ranging between 11.2°C near the shore and 11.8°C far offshore. The yearly time-series plot shows significant variability, with the lowest values of ~11,1°C observed during 1993, 1995, and 2010, and the highest value of 12.3°C during 2007. The differences between mean temperature values at the three points are insignificant, suggesting marginal spatial disparity.

In BeNeLux, the left panel displays an overall mean t2m ranging between 11.1°C near the shore and 11.5°C far offshore, indicating marginal spatial disparity. The yearly time-series plot exhibits significant variability, with the lowest value of 9.5°C observed during 1996, and the highest value of 12.5°C during 2014. The difference between mean temperature values at the three points is marginal.

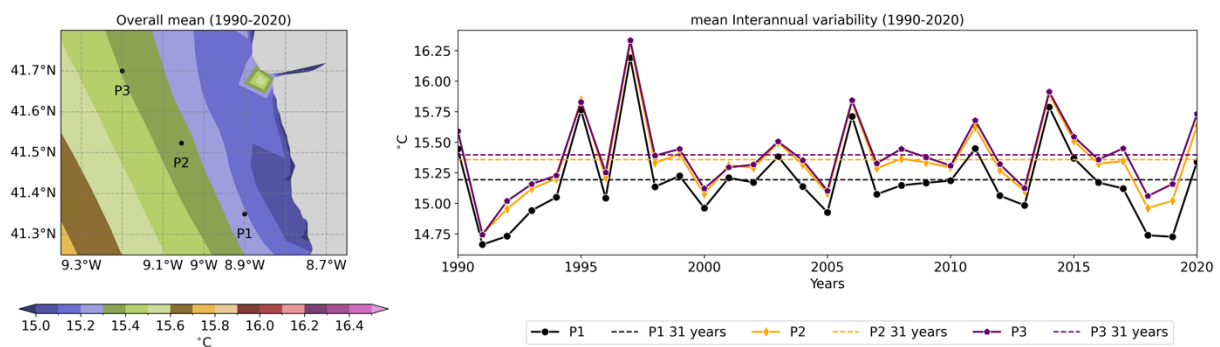


**Figure 48: Left panel: Surface plots of mean 2m temperature, estimated during the whole analysis period (1990-2020), over the Iberia region. Right panel: Time-series of 2 m temperature mean computed during each year, at points P1, P2, and P3, shown in the left panel. Horizontal dashed lines represent the overall statistics at the respective points.**

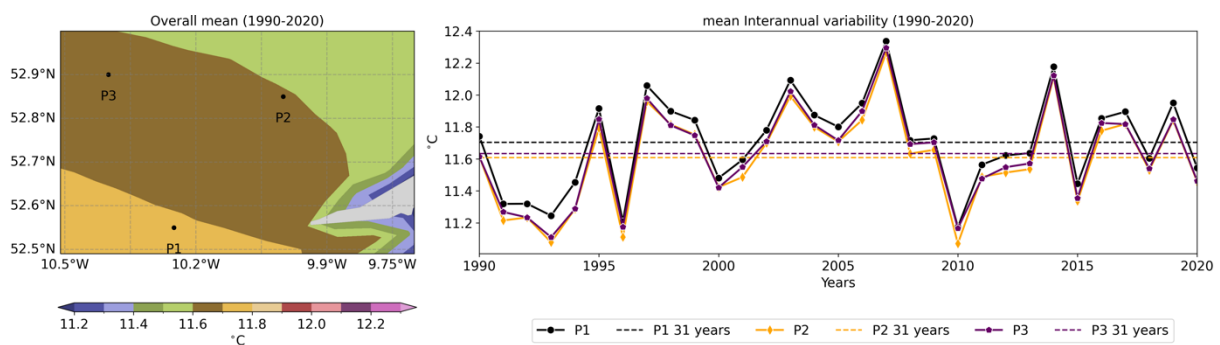


**Figure 49: Same as Figure 48, but for the Ireland region.**



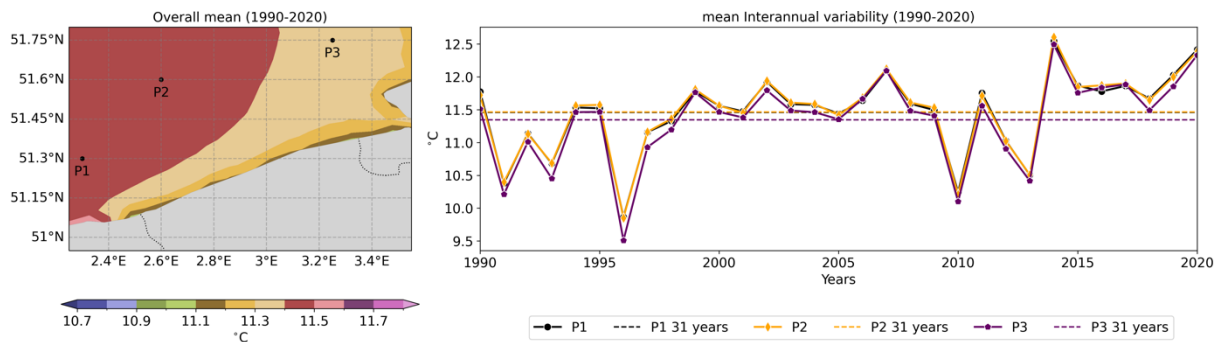


**Figure 50: Same as Figure 48, but for the BeNeLux region.**

## 6.1.2 Annual-seasonal characteristics

Across each month, the t2m is grouped and analyzed for annual variability. In Iberia (Figure 51), the highest t2m values of  $\sim 18^{\circ}\text{C}$  are observed during August, while the lowest values of  $\sim 12.5^{\circ}\text{C}$  are observed during February. Seasonally, Summer exhibits the highest mean values ( $\sim 17.5^{\circ}\text{C}$ ), and Winter shows the lowest mean values ( $\sim 12.5^{\circ}\text{C}$ ). The temperature differences among the three points are very small, around  $0.25^{\circ}\text{C}$ , even on the annual scale, suggesting marginal spatial disparity.

Similarly, in Ireland (Figure 52), the parameter exhibits annual variability across the months, with the highest values of  $\sim 15.5^{\circ}\text{C}$  observed during August and the lowest values of  $\sim 8.8^{\circ}\text{C}$  observed during February. Seasonally, Summer exhibits the highest mean values ( $\sim 14^{\circ}\text{C}$ ), while Winter shows the lowest mean values ( $\sim 9^{\circ}\text{C}$ ). The temperature differences among the three points are insignificant, suggesting marginal spatial disparity.

In BeNeLux (Figure 53), the parameter exhibits annual variability across the months, with the highest values of  $\sim 18^{\circ}\text{C}$  observed during August and the lowest values of  $\sim 6^{\circ}\text{C}$  observed during February. Seasonally, Summer exhibits the highest mean values ( $\sim 16^{\circ}\text{C}$ ), while Winter shows the lowest mean values ( $\sim 7^{\circ}\text{C}$ ). During Winter months, the temperature difference among the three points is higher, close to  $0.5^{\circ}\text{C}$ , while during Summer, the difference is  $\sim 0.2^{\circ}\text{C}$ , and during the remaining seasons, the difference is insignificant, suggesting dynamic variability depending on the season.

Overall, the analysis indicates that while there are variations in t2m across regions and seasons, the spatial disparity remains marginal in Iberia and Ireland, whereas it's more pronounced in BeNeLux, especially during Winter months. Interestingly, the seasonal mean temperatures in the BeNeLux region are much higher than the Ireland region, though they are on the same latitude.

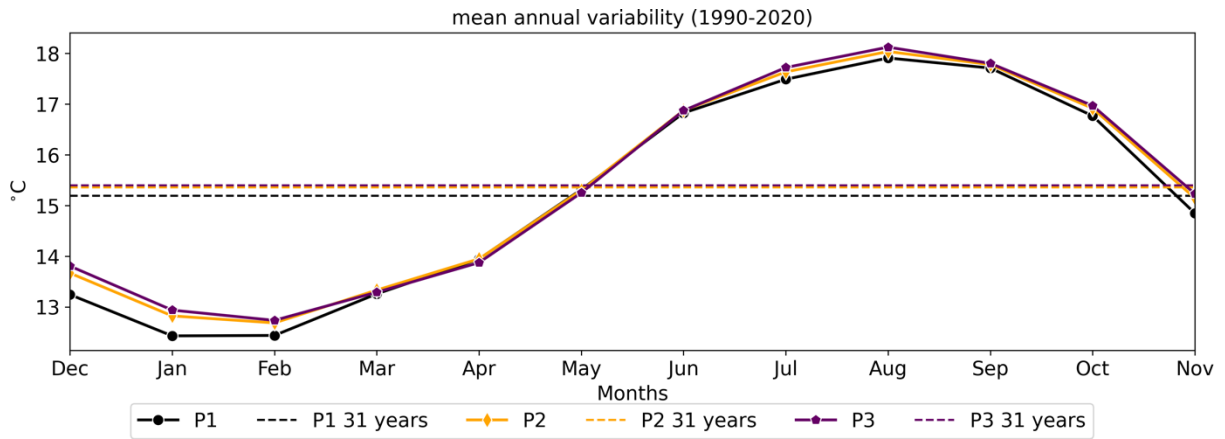


**Figure 51:** Time-series of 2 m temperature mean computed during each month, at points P1, P2, and P3, over the Iberia region. Horizontal dashed lines represent the overall statistics at the respective points.

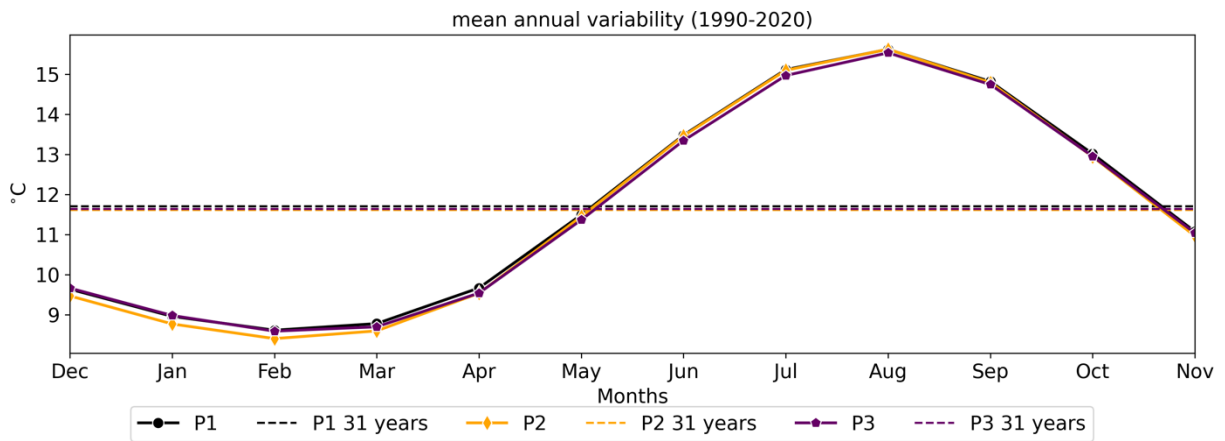


**Figure 52:** Same as Figure 51, but for the Ireland region.

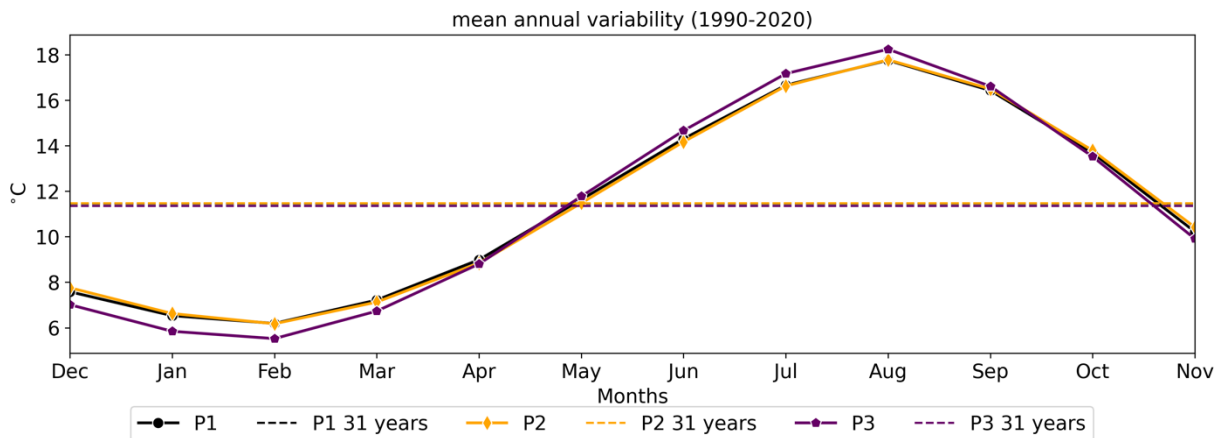


**Figure 53:** Same as Figure 54, but for the Ireland region.

### 6.1.3 Heat extremes analysis

The t2m p99 characteristics are computed over a period of 31 years (1990-2020) and every year, as shown in Figure 54 for the Iberia region, Figure 55 for the Ireland



region, and Figure 56 for the BeNeLux region. The left panel of each figure illustrates the overall statistic, while the right panel illustrates the statistic computed by grouping t2m every year at three points (P1, P2, and P3).

From the overall statistics, it is evident that the extreme temperature ranges between 20°C to 25°C for the Iberia region, 17°C to 19°C for the Ireland region, and 19°C to 23°C for the BeNeLux region. Among these three, the Iberia region experiences severely extreme temperatures, BeNeLux experiences moderate extremes, while the Ireland region experiences the least extreme temperatures. In all three regions, the extremity of temperature decreases with the proximity to the coast, and is very strong near the coast.

The 99<sup>th</sup> percentile temperature values at P1, P2, and P3, are: 20.7°C, 20.2°C, and 20.2°C, respectively for Iberia; 17.2°C, 17.3°C, and 17.1°C, respectively for Ireland; and 19.8°C, 19.8°C, and 20.5°C, respectively for the BeNeLux regions. In the Iberia and Ireland coasts, the temperature extremes exhibit homogeneous spatial distribution, while the BeNeLux shows considerable spatial variability.

From the yearly time-series plots, the p99 exhibits significant variability across different years and regions. In the Iberia region, the highest possible temperature was observed during 2006, with an intensity of 22°C, while 2019 saw the lowest p99 temperature at an intensity of 19.2°C. In the Ireland region, the highest possible temperature was observed in 1995, with an intensity of 19.8°C, while the lowest p99 was observed in 2010, at 15.7°C.

On the contrary, the BeNeLux region experienced the highest temperatures in 2020, with an intensity of 22.3°C, while the lowest was observed at 17.8°C. Interestingly, none of the annual variability patterns match among the regions, signifying the influence of local scale weather conditions on temperature extremity.

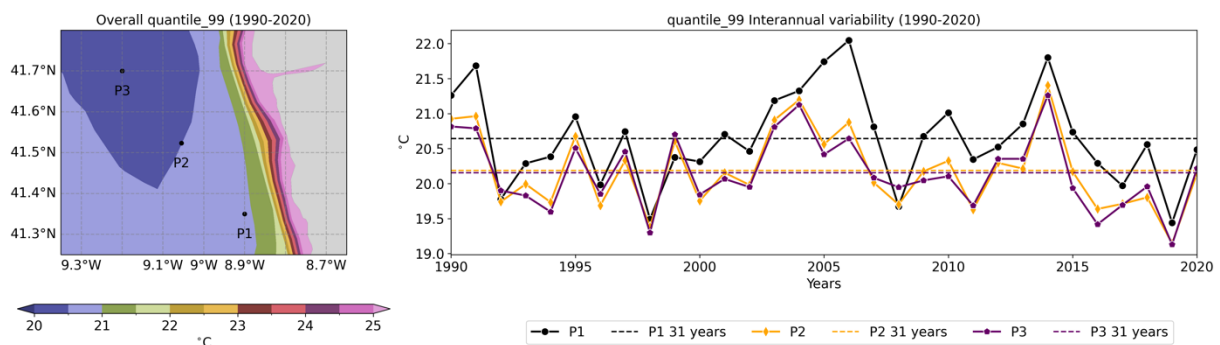


**Figure 54: Left panel: Surface plots of 99p of 2 m temperature, estimated during the whole analysis period (1990-2020), over the Iberia region. Right panel: Time-series of 99p of 2m temperature computed during each year, at points P1, P2, and P3, shown in the left panel. Horizontal dashed lines represent the overall statistics at the respective points.**



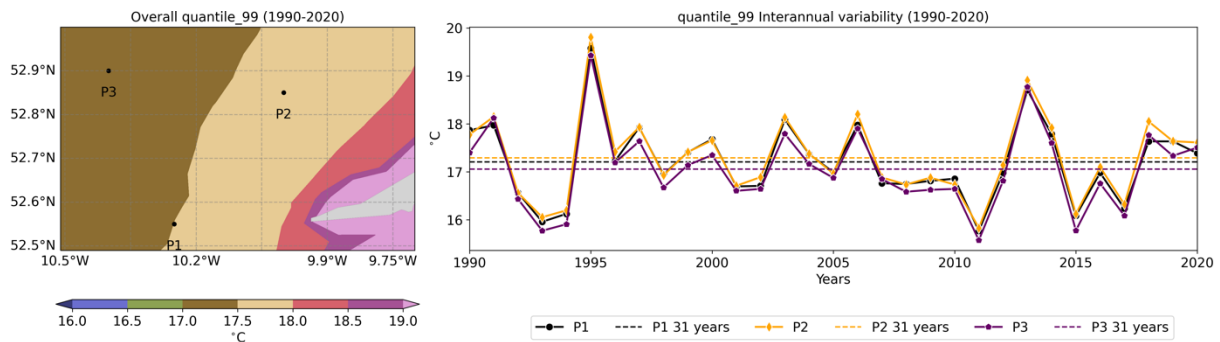


Figure 55: Same as Figure 54, but for the Ireland region.

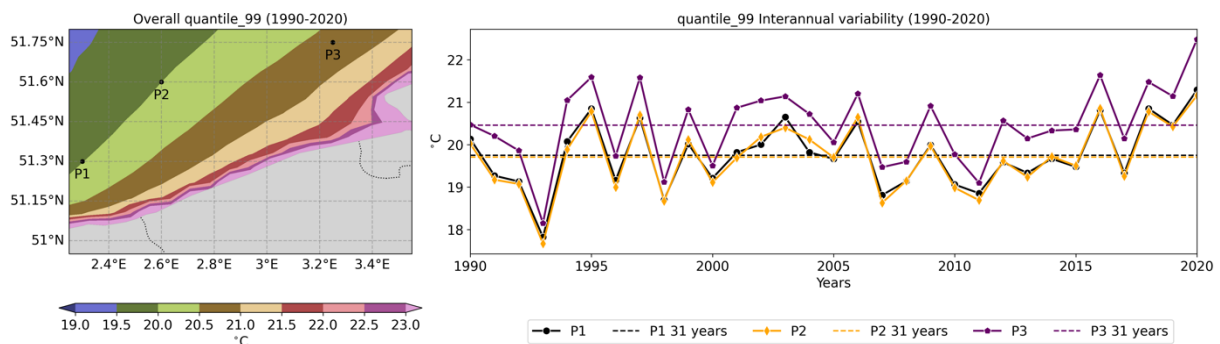


Figure 56: Same as Figure 54, but for the BeNeLux region.

## 6.2 Surface solar radiation flux climate characteristics

In this section, the climate characteristics of SWDOWN are analyzed using mean. Since SWDOWN becomes zero during night time, the estimation of coefficient of variance does not give any information, which becomes too large. On the other hand, the extremity of solar radiation flux does not have any implication on the efficiency of PV cell, which makes it meaningless in estimating.

### 6.2.1 Overall-interannual characteristics for 31 years

The mean characteristics of solar radiation flux have been analyzed across the regions of Iberia (Figure 57), Ireland (Figure 58), and BeNeLux (Figure 59) over the period spanning from 1990 to 2020. The left panel of each figure illustrates the overall mean SWDOWN, while the right panel illustrates the mean computed by grouping SWDOWN every year at three points (P1, P2, and P3).

Across all regions, the overall mean solar flux exhibits marginal spatial patterns, such that the flux ranges between 180 W/m<sup>2</sup> to 186 W/m<sup>2</sup> in Iberia, 118 W/m<sup>2</sup> to 128 W/m<sup>2</sup> in Ireland, and 130 W/m<sup>2</sup> to 136 W/m<sup>2</sup> in BeNeLux regions, respectively.

When examining the yearly variations, significant variability is observed in the mean flux values. In Iberia, the annual mean flux values range between 175 W/m<sup>2</sup> to 192 W/m<sup>2</sup>, with considerable fluctuations noted over the years. Similarly, Ireland shows considerable variability around the overall mean values, ranging between 115 W/m<sup>2</sup> to 134 W/m<sup>2</sup>. BeNeLux, on the other hand, exhibits marginal variations



around the overall mean values, with the annual mean flux ranging between 125  $W/m^2$  to 150  $W/m^2$ .

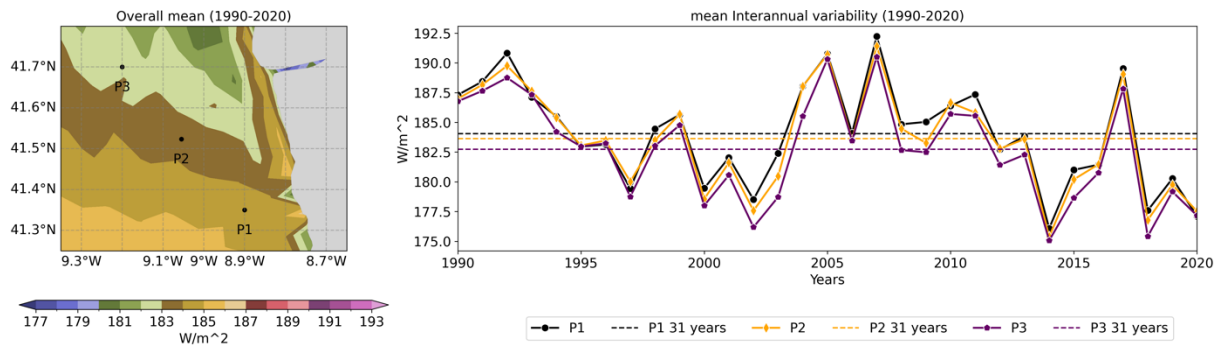


**Figure 57:** Left panel: Surface plots of mean SWDOWN, estimated during the whole analysis period (1990-2020), over the Iberia region. Right panel: Time-series of SWDOWN mean computed during each year, at points P1, P2, and P3, shown in the left panel. Horizontal dashed lines represent the overall statistics at the respective points.

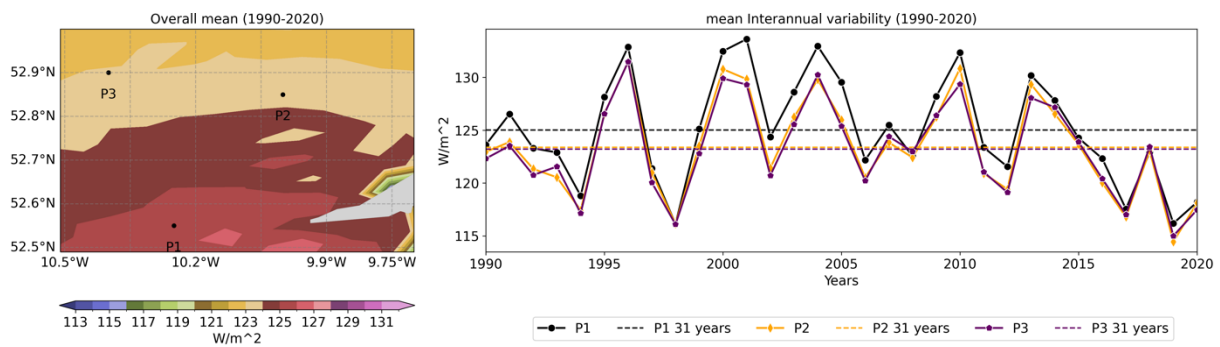


**Figure 58:** Same as Figure 57, but for the Ireland region.

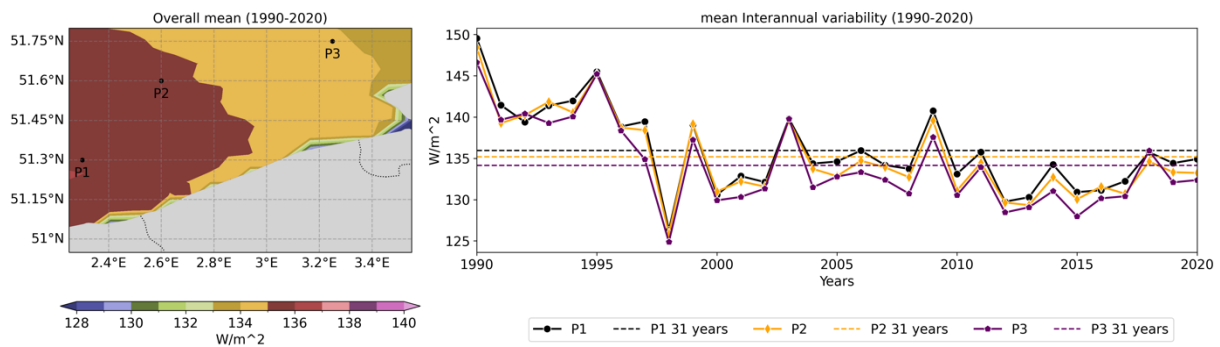


**Figure 59:** Same as Figure 57, but for the BeNeLux region.

## 6.2.2 Annual-seasonal characteristics

Monthly and seasonal variability in solar flux has been analyzed across the regions of Iberia, Ireland, and BeNeLux. The mean is computed across each month by grouping the SWDOWN during the respective month, extracted at the three points, and is presented in Figure 60 for Iberia, Figure 61 for Ireland, and Figure 62 for BeNeLux.



Across all regions, monthly analysis reveals significant variability in solar flux. For instance, in Iberia, the highest values of  $\sim 300 \text{ W/m}^2$  are observed during July, while the least values of  $60 \text{ W/m}^2$  are observed during December. Similarly, in Ireland and BeNeLux, the highest values of  $250 \text{ W/m}^2$  are observed during June, while the lowest values of  $30 \text{ W/m}^2$  are observed during December. Irrespective of the intensity, a sinusoidal annual variability is observed in the three regions,

Seasonally, similar patterns are observed across the regions. Summer months consistently exhibit the highest mean flux values, while winter months display the least values. Furthermore, a peculiar observation at all locations is that the surface air temperature is seen highest during August, while the solar flux is during July, indicating a lag in response between temperature and solar radiation flux.

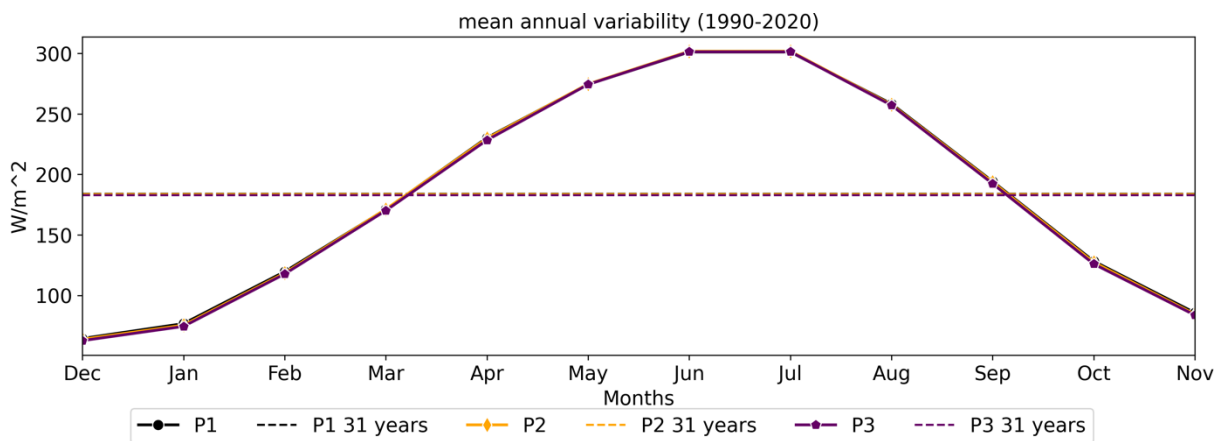


**Figure 60: Time-series of SWDOWN computed during each month, at points P1, P2, and P3, over the Iberia region. Horizontal dashed lines represent the overall statistics at the respective points.**

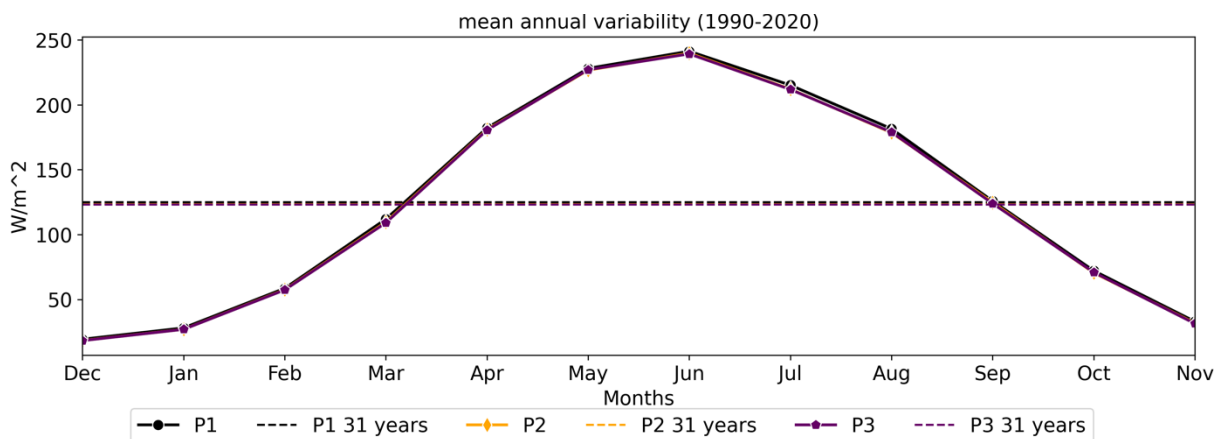


**Figure 61: Same as Figure 60, but for the Ireland region.**





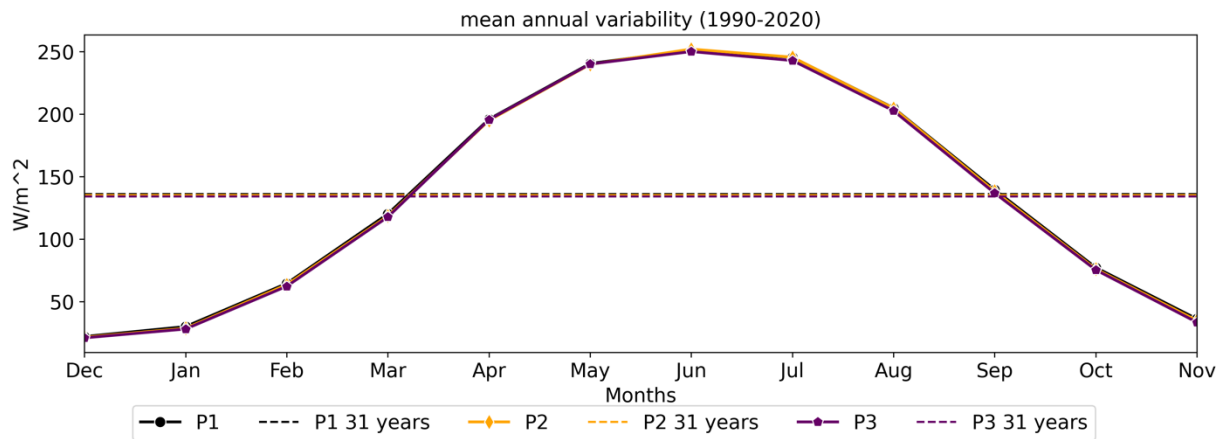


Figure 62: Same as Figure 60, but for the BeNeLux region.

### 6.3 Surface wind climate characteristics

The present section aims to provide climate characteristics of 10 m surface wind resources across three regions: Iberia, Ireland, and BeNeLux. As mentioned earlier during the wind resource assessment, in cases with skewed data, the application of the Weibull distribution is more suitable, which is characterized by its slope and scale parameters, as shown in Equation 29. The Weibull scale statistics are computed across overall, yearly, and monthly time scales. Since the surface air wind speed only contributes to 10-15% of the overall performance, the variability statistic (shape) is not assessed due to its insignificance on solar resources.

#### 6.3.1 Overall-interannual characteristics for 31 years

The Weibull scale characteristics are computed over a period of 31 years (1990-2020) and every year, as shown in Figure 63 for the Iberia region, Figure 64 for the Ireland region, and Figure 65 for the BeNeLux region. The left panel of each figure illustrates the overall Weibull scale parameter, while the right panel illustrates the Weibull scale parameter computed by grouping wind speed every year.

From the overall statistics, it is evident that the wind speed ranges between 5 m/s to 8 m/s for the Iberia region, 7.5 m/s to 10.5 m/s for the Ireland region, and 7.5 m/s to 9.3 m/s for the BeNeLux region. Among these three, the Iberia region exhibits a difference of 3 m/s in the scale parameter when moving parallelly away from the coast, indicating that the spatial disparity is considerable in this region. Though the Ireland region also shows a 3 m/s difference in wind speed, it is due to the presence of a spit, which increases surface roughness and decreases wind speed. On the other hand, the BeNeLux exhibits a difference of 1 m/s when moving from near shore to far shore, indicating a marginal spatial disparity.

To quantitatively assess the spatial disparity, three random points, P1, P2, and P3, are chosen from each region, and their overall statistics are presented as dashed lines in the right panel. The overall scale parameter values at P1, P2, and P3, are: 6.9 m/s, 7.5 m/s, and 7.7 m/s, respectively for Iberia; 9.8 m/s, 9.8 m/s, and 10.2 m/s, respectively for Ireland; and 9.1 m/s, 9.3 m/s, and 8.9 m/s, respectively for the



BeNeLux regions. These values further strengthen the fact that the Iberia region has considerable spatial disparity, while the remaining two regions exhibit more or less homogeneity in spatial wind speed distribution.

From the yearly time-series plots, the scale parameter exhibits significant variability across different years. Interestingly, the variability trend is relatively similar in the Ireland and BeNeLux regions, but the similarity is much lesser than that of the 100 m wind speed. On the other hand, the time series is vastly different in the Iberia region, where the parameter is seen to be lowest at 6.3 m/s during 2004, 2008, and 2012, while the highest value of 8.7 m/s is seen during 2013. On the contrary, the parameter is seen lowest during 2010, reaching 8.6 m/s over Ireland and 8.3 m/s over the BeNeLux. Across these two regions, the parameter is commonly highest during 1990, 2015, and 2020 years, while several years differently exhibit a maximum in both regions. This suggests that the large-scale climate teleconnections responsible for the wind maxima in the Ireland region are also responsible for the BeNeLux region, but the same cannot be inferred for the Iberia region. Apart from these, the Ireland and BeNeLux regions also exhibit differences during some years, like 2001 and 2003, during which the wind scale parameter is observed to be different, suggesting that the local climate characteristics also play a role in surface wind characteristics.

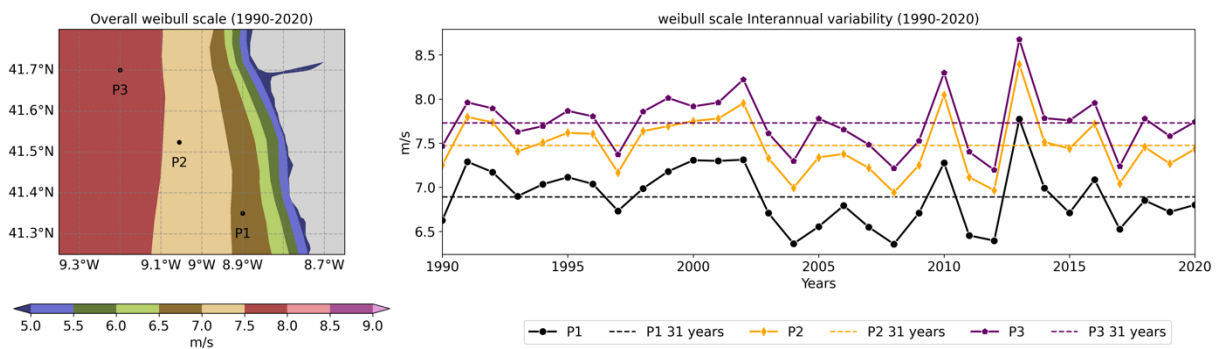


**Figure 63:** Left panel: Surface plots of Weibull scale parameter of 10 m wind speed, estimated during the whole analysis period (1990-2020), over the Iberia region. Right panel: Time-series of 100 m wind Weibull scale parameter computed during each year, at points P1, P2, and P3, shown in the left panel. Horizontal dashed lines represent the overall statistics at the respective points.

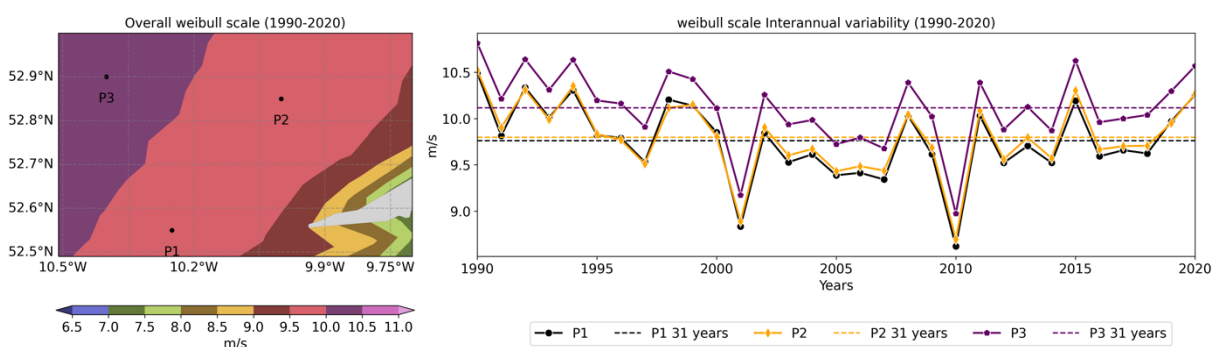


**Figure 64:** Same as Figure 63, but for Ireland region.



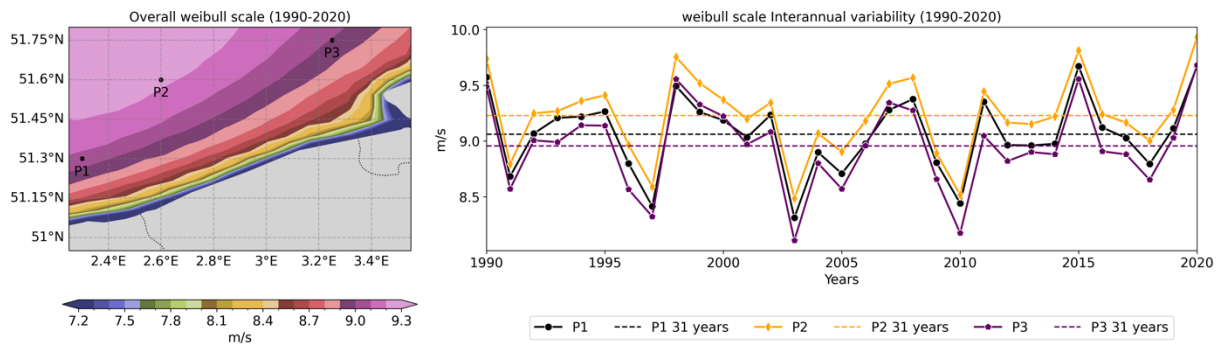


**Figure 65: Same as Figure 63, but for BeNeLux region.**

### 6.3.2 Annual-seasonal characteristics

The Weibull scale statistics are computed across each month by grouping the wind speed during the respective month, extracted at the three points, and are presented in Figure 66 for the Iberia region, Figure 67 for the Ireland region, and Figure 68 for the BeNeLux region. The annual variability in the three regions is identical to that of the 100 m wind speed climatology, which is obvious. Among the three regions, Iberia exhibits an entirely different annual variability across the months, while the remaining two regions exhibit a generic cyclic annual variability. The same has been seen earlier. However, an interesting observation is that the scale parameter is not highest during July in the Iberia region, unlike the 100 m variability, but rather January. A possible explanation is that the jet strength of the IPCJ decreases with height and becomes insignificant at the 10 m (surface) level, which makes the July scale parameter lesser. On the other hand, the occurrence of the European Windstorms during January makes the scale parameter higher.

Nonetheless, the scale parameter in the Iberia region is seen highest during January (ranging between ~7.5 m/s to 8.5 m/s among the three points), and least during September (ranging between 5.8 m/s to 6.6 m/s among the three points). Another interesting characteristic is that the scale parameter consistently differs by ~0.8 m/s among the three points, indicating a significant spatial disparity.

In the Ireland region, the parameter is seen highest during January (ranging between 11.9 m/s to 12.2 m/s), gradually decreasing to the minimum during July (ranging between 8 m/s to 8.3 m/s), and then increasing. A similar annual variability is observed in the BeNeLux region as well. The parameter is seen highest during January (ranging between 11 m/s to 11.3 m/s), gradually decreasing to the minimum during August (ranging between 8.5 m/s to 8.7 m/s), and then increasing.

Grouping the scale statistics seasonally as Winter (Dec, Jan, Feb), Spring (Mar, Apr, May), Summer (Jun, Jul, Aug), and Autumn (Sep, Oct, Nov) gives more insights regarding seasonal variability. In all regions, the scale parameter is seen highest during winter, which is mainly attributed to the European Windstorms. On the contrary, the scale parameter is observed to be minimum during summer in the Ireland and BeNeLux regions, which has been the climatology over the North Sea.



However, the Iberia region stands out as the outlier to have a maximum scale parameter during summer, which is again attributed to the occurrence of IPCJ.

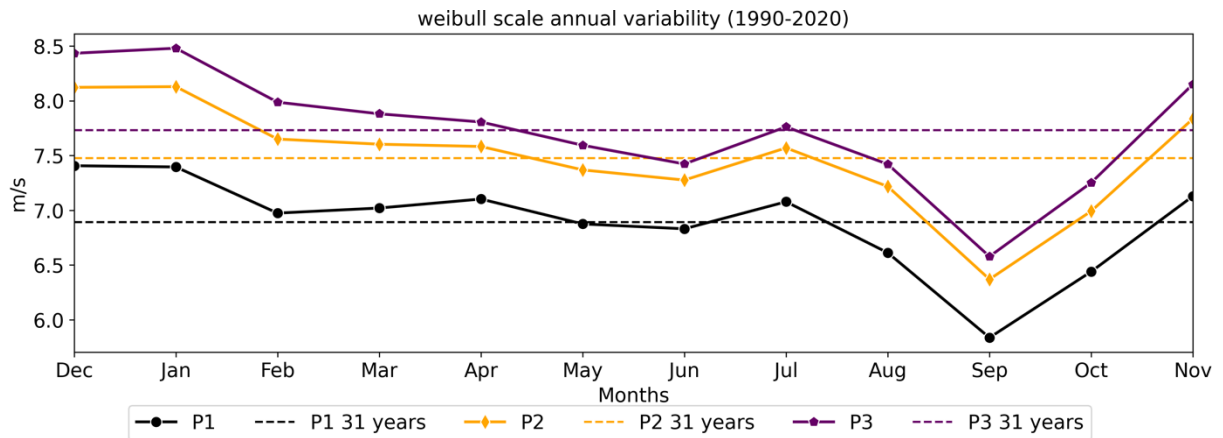


Figure 66: Time-series of 10 m wind Weibull scale parameter computed during each month, at points P1, P2, and P3, over the Iberia region. Horizontal dashed lines represent the overall statistics at the respective points.

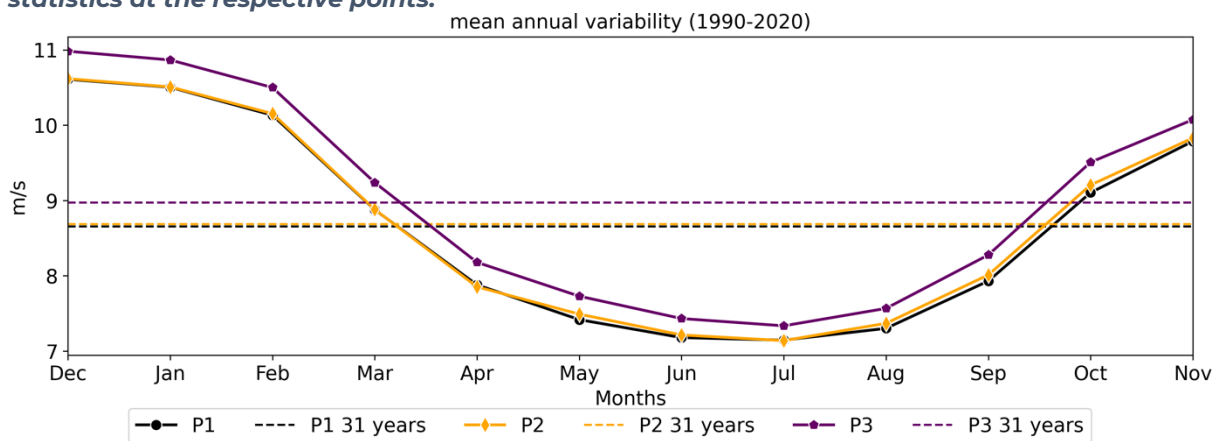


Figure 67: Same as Figure 66, but for the Ireland region.

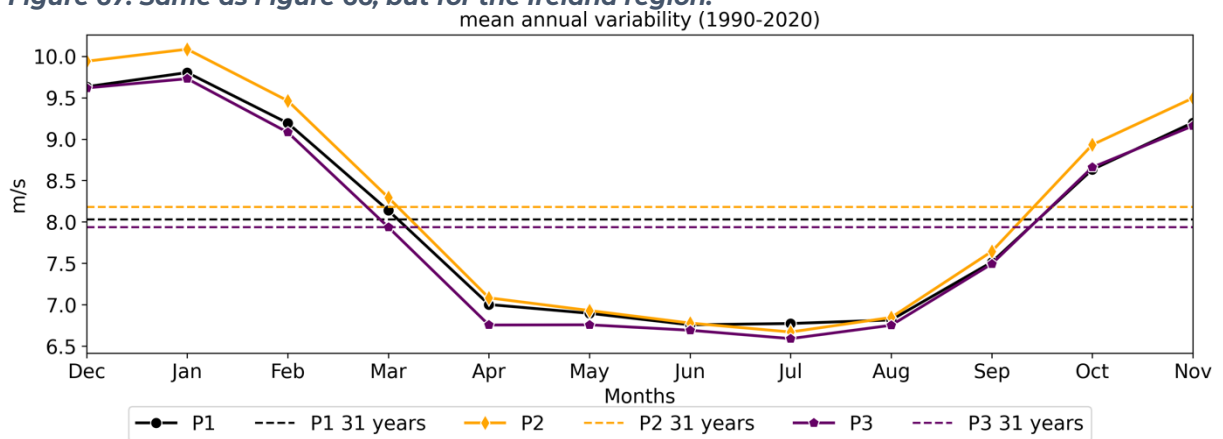
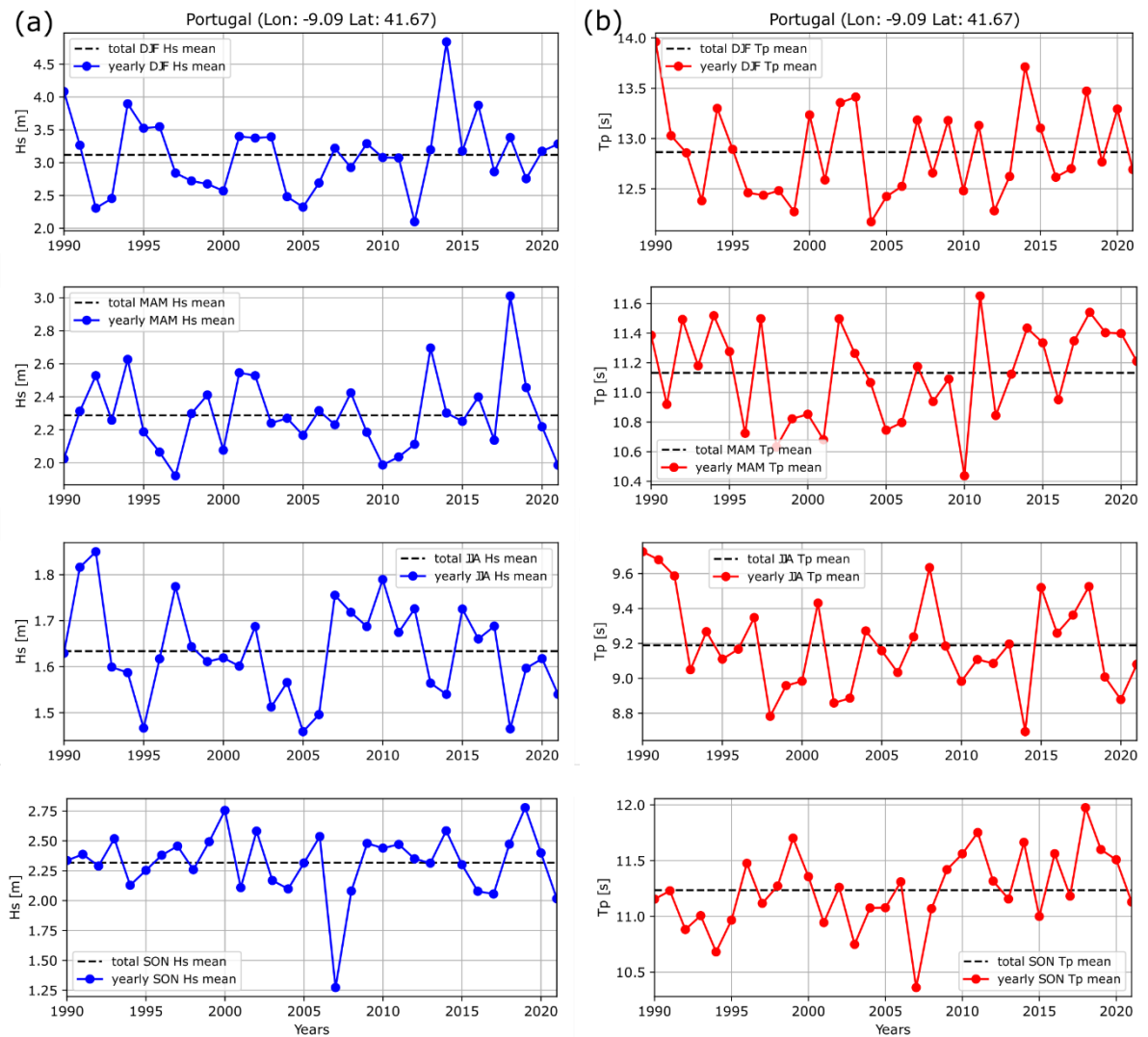


Figure 68: Same as Figure 66, but for the BeNeLux region.



# Annex A: Seasonal mean wave conditions at specific locations

The time series of seasonal mean values for  $H_s$  and  $T_p$  presented below, are aimed to provide an idea of the variation range compared to the 32-years mean.



**Figure 69: (a)  $H_s$  and (b)  $T_p$  yearly mean seasonal values compared to the 32-years mean. Location: Portugal.**



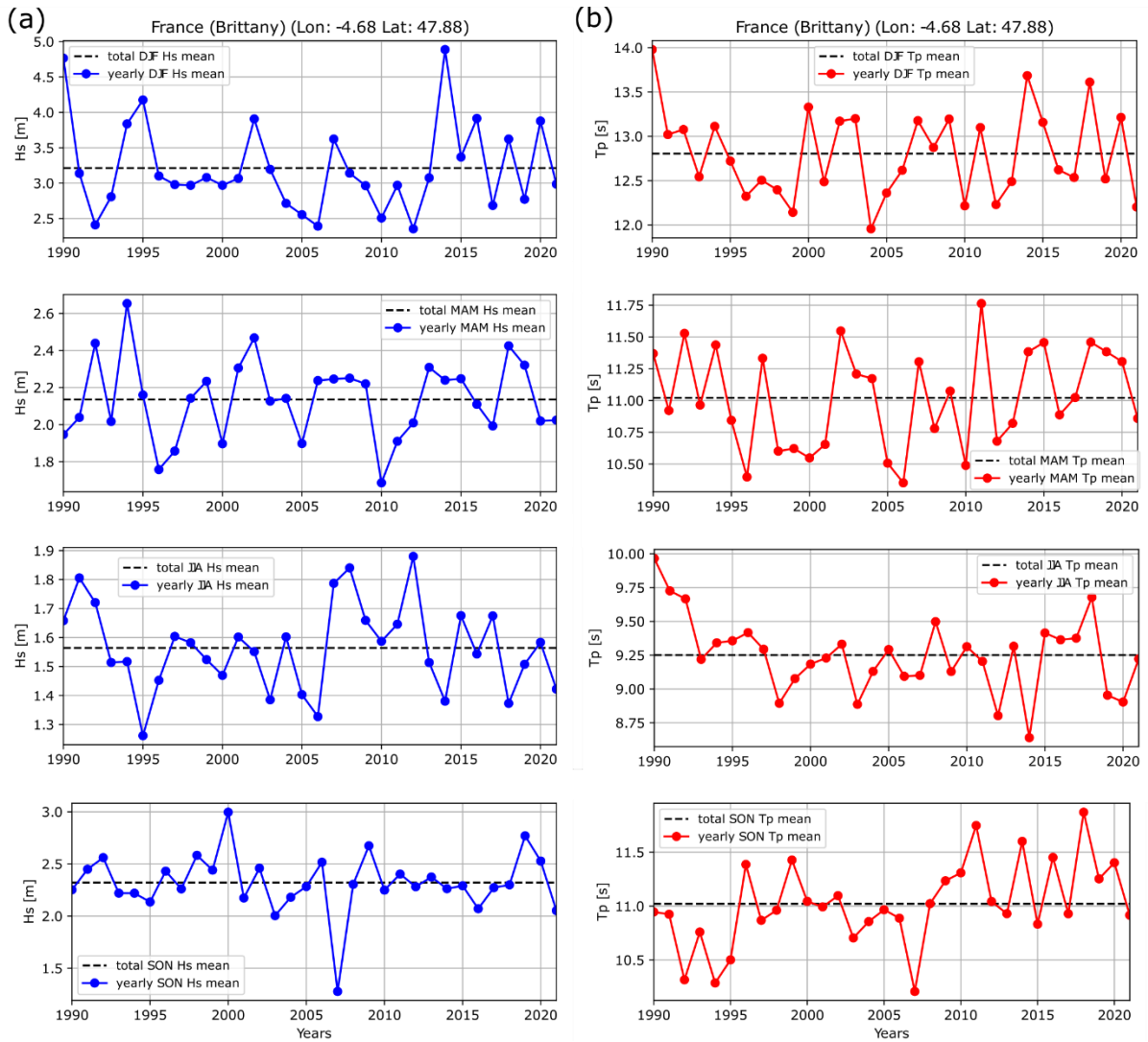


**Figure 70: (a)  $H_s$  and (b)  $T_p$  yearly mean seasonal values compared to the 32-year mean. Location: Brittany (France).**



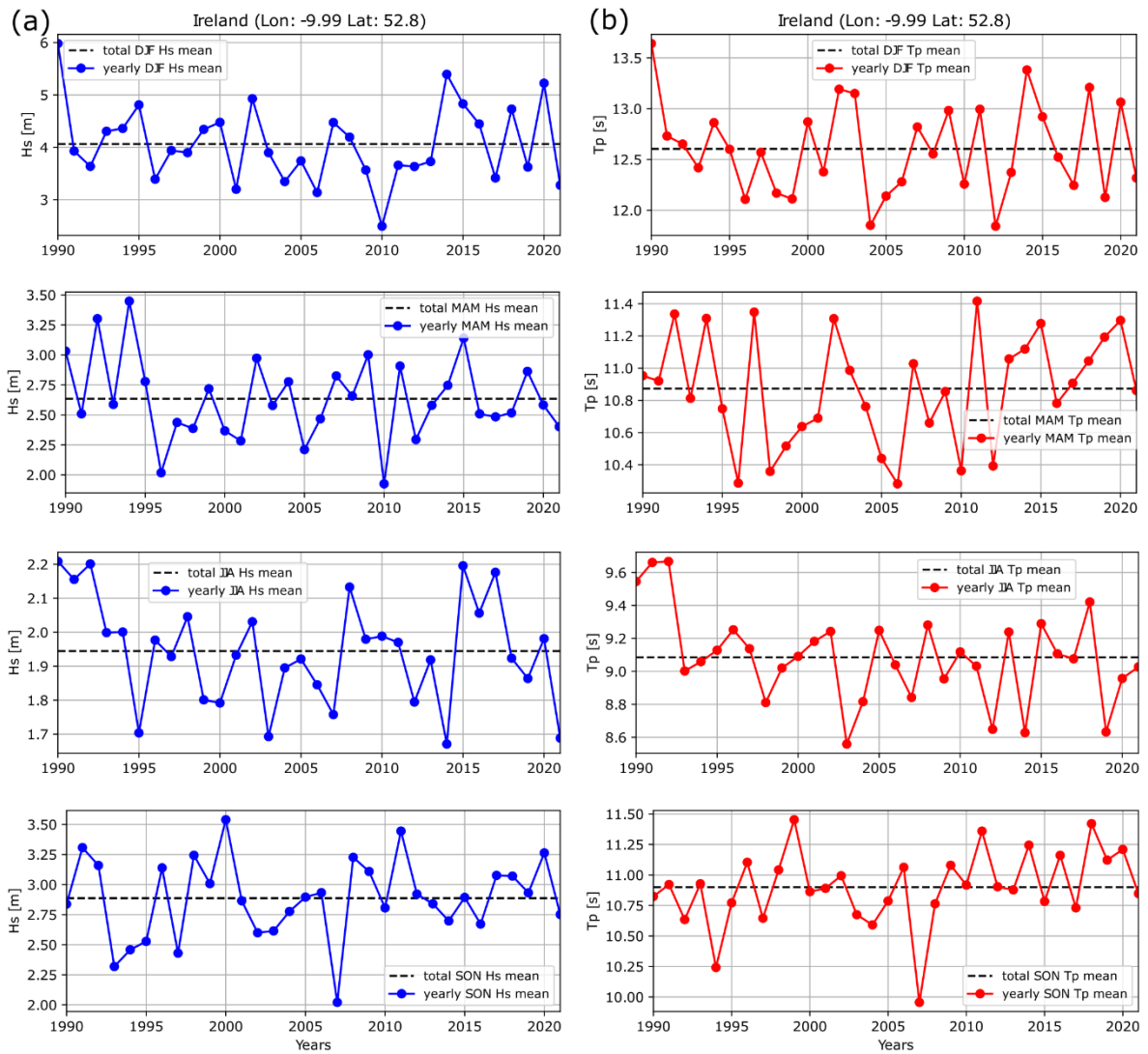


**Figure 71: (a)  $H_s$  and (b)  $T_p$  yearly mean seasonal values compared to the 32-years mean. Location: Ireland.**



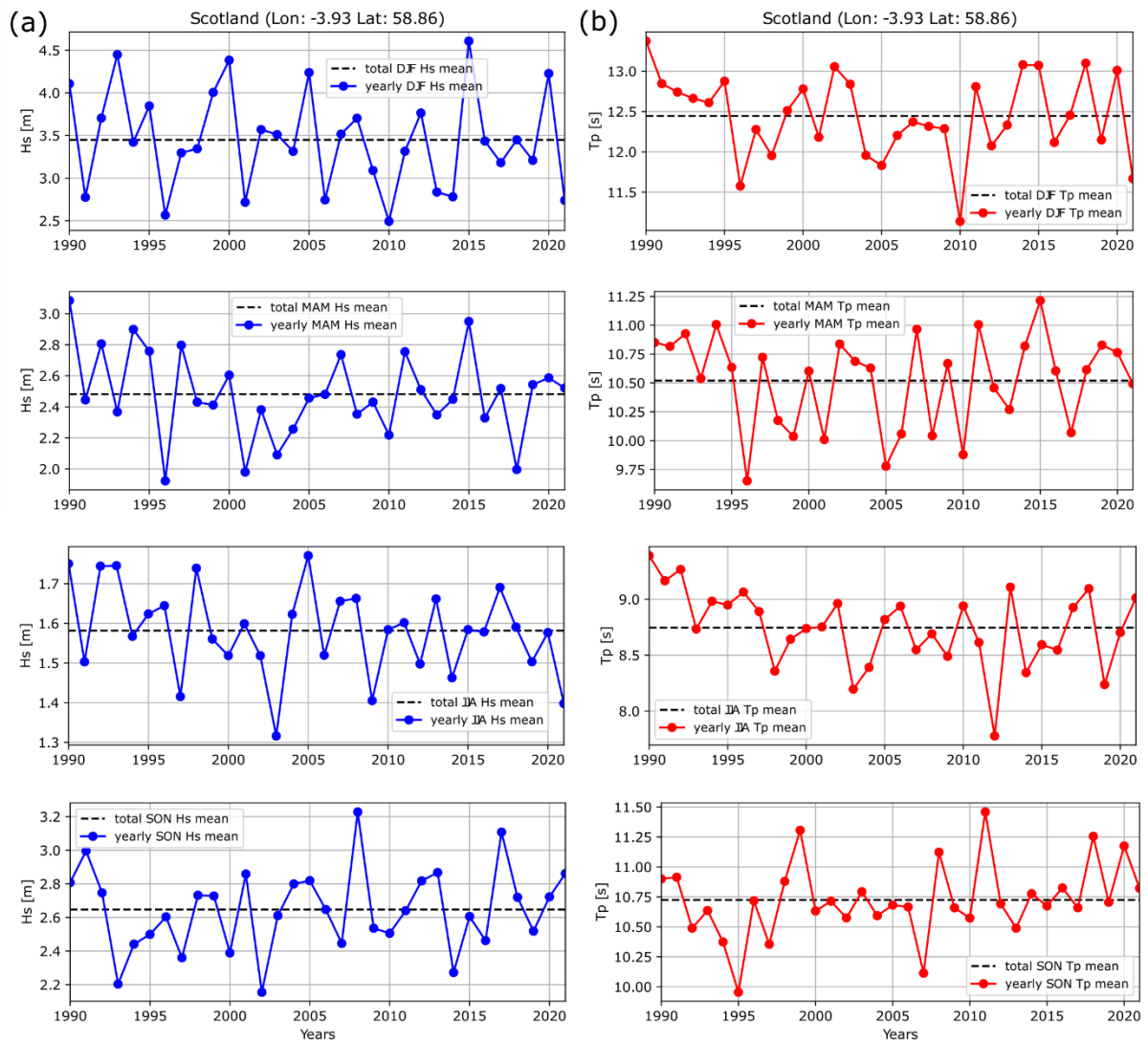


**Figure 72: (a)  $H_s$  and (b)  $T_p$  yearly mean seasonal values compared to the 32-years mean. Location: Scotland.**





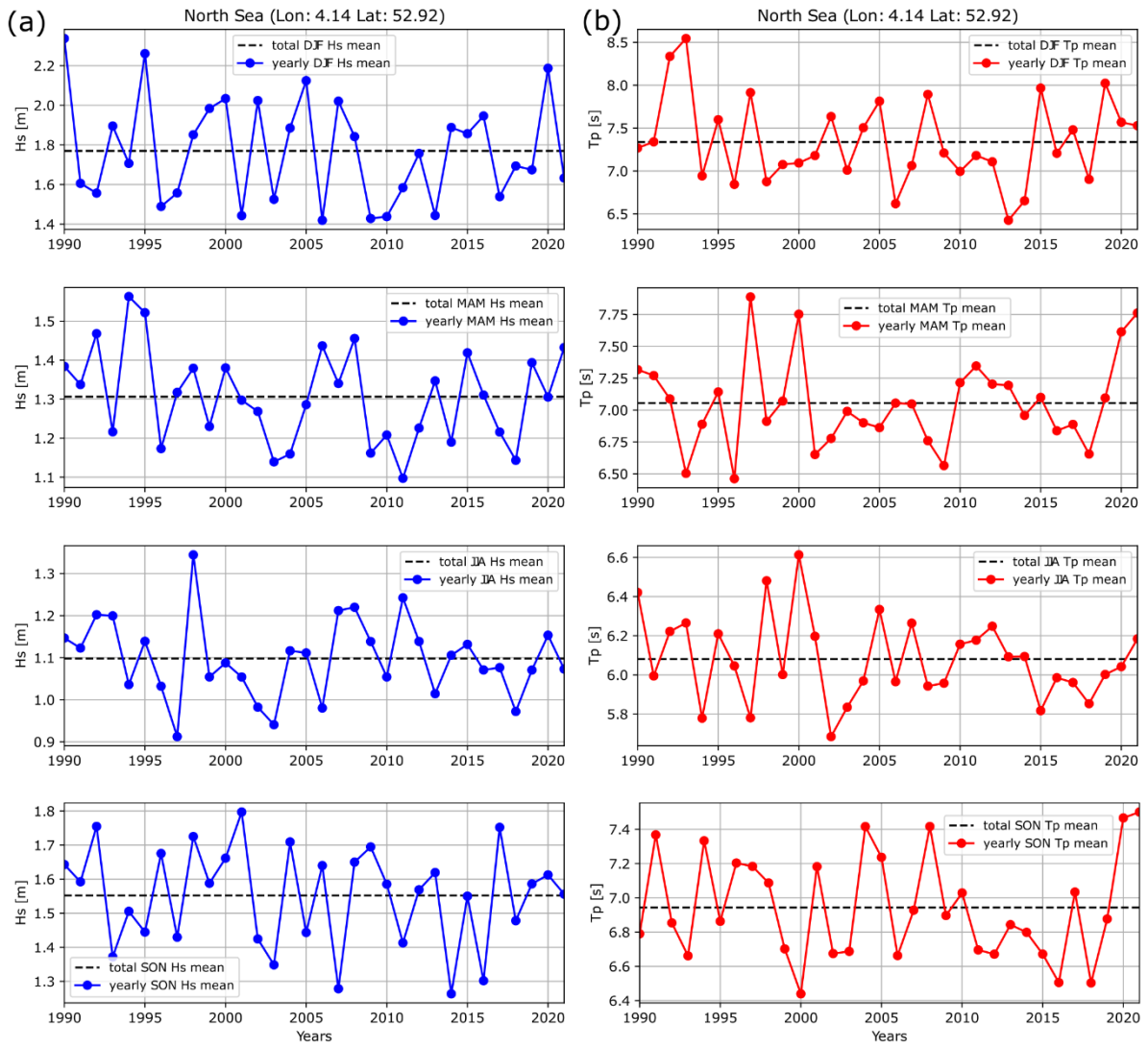


**Figure 73: (a)  $H_s$  and (b)  $T_p$  yearly mean seasonal values compared to the 32-years mean. Location: North Sea.**



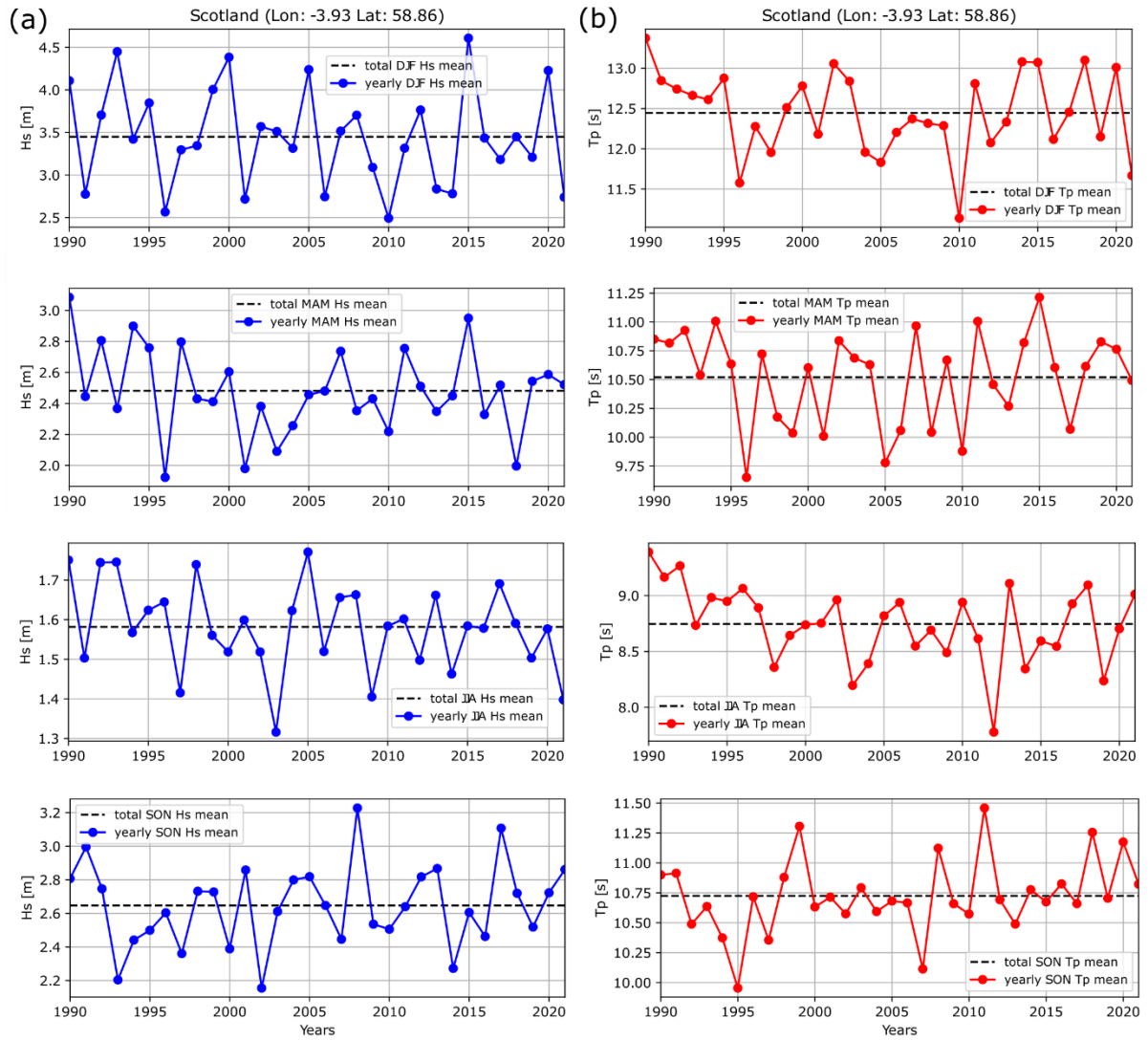


**Figure 74: (a)  $H_s$  and (b)  $T_p$  yearly mean seasonal values compared to the 32-years mean. Location: Scotland.**



# Annex B: Seasonal mean wave conditions at specific locations

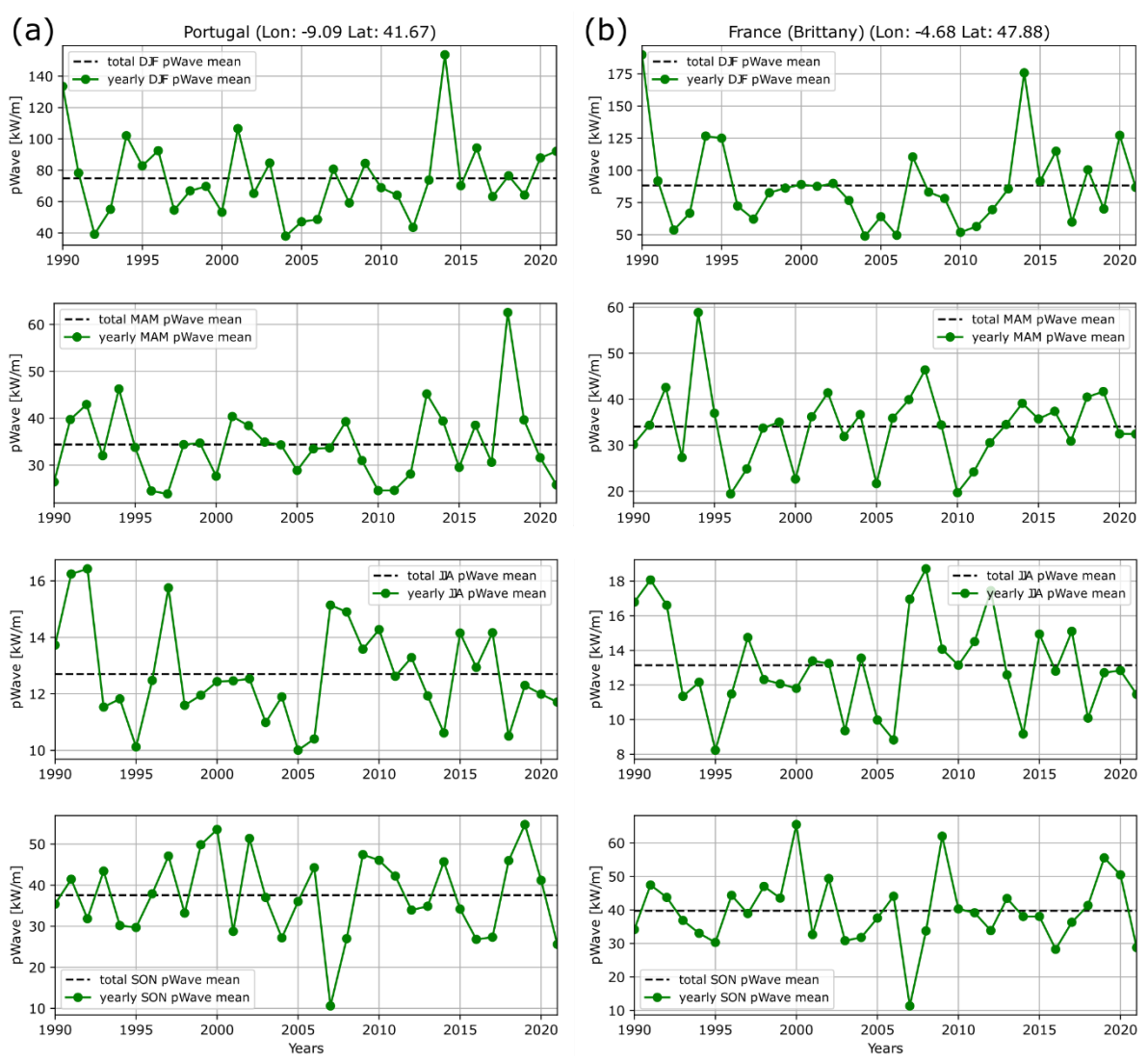


**Figure 75: Seasonal 32-year mean (dashed black lines) and yearly seasonal mean in (a) Portugal and (b) Brittany (France).**



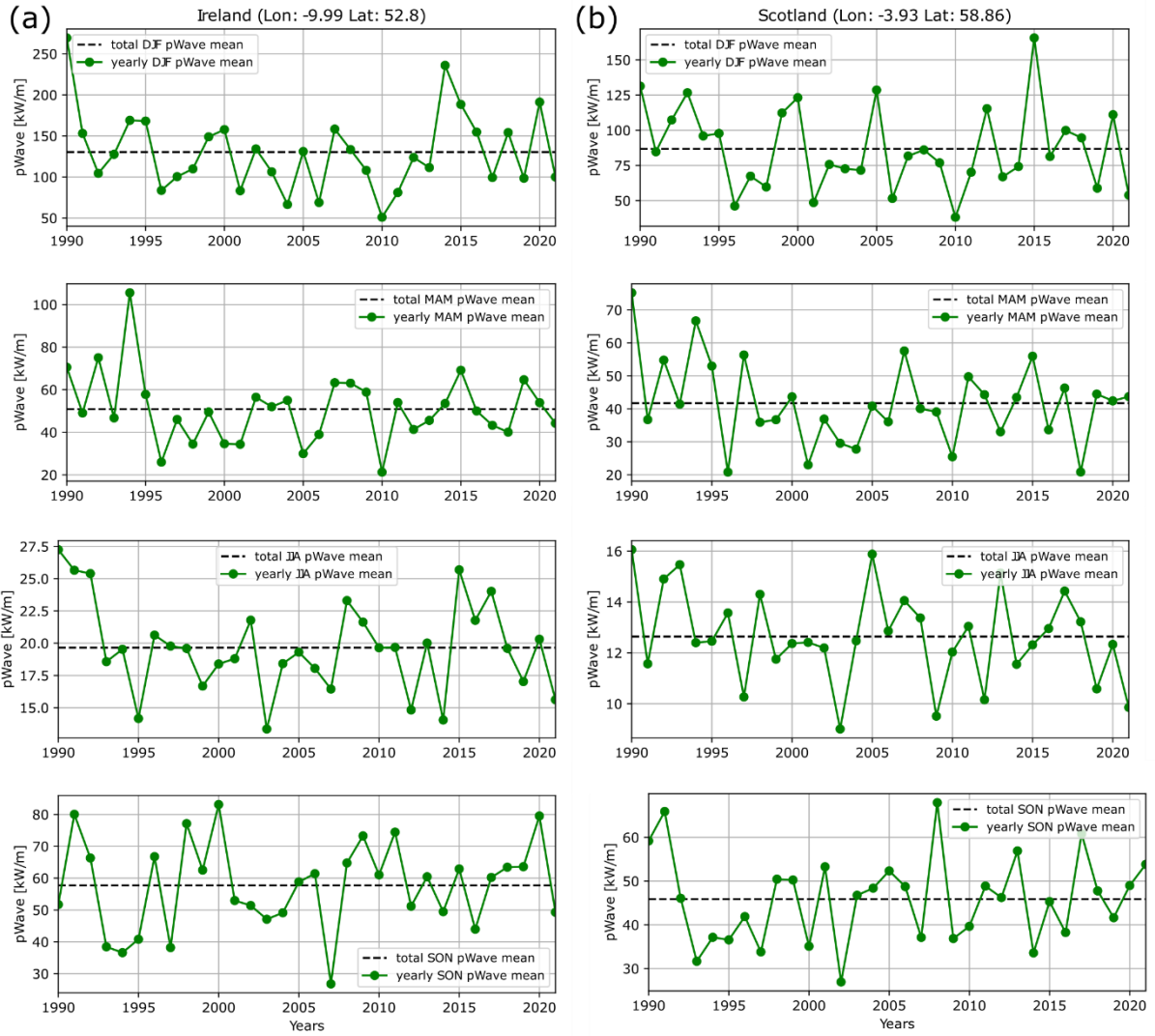


**Figure 76: Seasonal 32-year mean (dashed black lines) and yearly seasonal mean in (a) Ireland and (b) Scotland.**



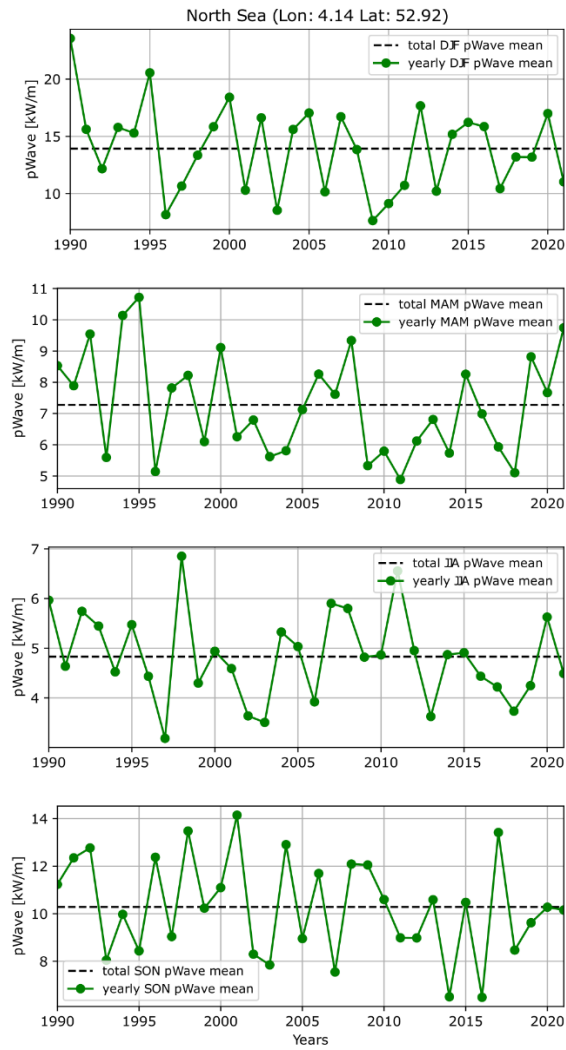


**Figure 77: Seasonal 32-year mean (dashed black lines) and yearly seasonal mean in Dutch waters (North Sea).**

